EFFECT OF PLANT ROOT INTRUSION ON THE WATER BALANCE OF LANDFILL COVER SYSTEMS

By

Linda Leeann Williams

Thesis
Submitted to the Faculty of the
Graduate School of Vanderbilt University
in partial fulfillment of the requirements
for the degree of

MASTER OF SCIENCE
in
Environmental Engineering

May, 2005

Nashville, Tennessee

Approved:
Florence Sanchez
James H. Clarke

ACKNOWLEDGEMENTS

This research project was made possible with funds provided by the Consortium for Risk Evaluation with Stakeholder Participation (CRESP) II through the U.S. Department of Energy Grant DE FG 01-03EW15336. Additional entities appreciated are Vanderbilt University School of Engineering and the U.S. Salinity Laboratory. For patient and constant advisement, I would like to thank Dr. Florence Sanchez. Finally, for support both financial and emotional, I thank my parents.

TABLE OF CONTENTS

Page

Appendix Page

LIST OF TABLES

LIST OF FIGURES

LIST OF ABBREVIATIONS

ACAP	Alternative Cover Assessment Project
ALCD	Alternative Landfill Cover Demonstration
CCL	Compacted Clay Layer
DOE	Department of Energy
EPA	Environmental Protection Agency
ET	Evapotranspiration
GCL	Geosynthetic Clay Layer
HLW	High Level Waste
LLW	Low Level Waste
NRC	Nuclear Regulatory Commission
RCRA	Resource Conservation and Recovery Act
TRU	Transuranic Waste
UMT	Uranium Mill Tailings

CHAPTER I

INTRODUCTION

Background

Radioactivity is a natural and spontaneous process by which the unstable atoms of an element emit or radiate excess energy in the form of particles or waves. These emissions are collectively called ionizing radiations. Depending on how the nucleus loses this excess energy, either a lower energy atom of the same form will result, or a completely different nucleus and atom can be formed.

Radioactivity was discovered just before the turn of the twentieth century, and the following decades were spent in development of nuclear technology by both government and private industry. The largest consumption of radioactive materials was by production of nuclear power and nuclear weaponry (Blackman 2001).

The shadow of international tensions in the early twentieth century motivated the race to develop nuclear weapons. During World War II, the United States established a uranium enrichment site at Oak Ridge, a plutonium production site at Hanford, and a nuclear weapon development site at Los Alamos (U.S. Department of Energy 1997).

Civilian consumption of radioactive materials was largely from nuclear power production, although the private industry was contracted to process uranium for the government sites (U.S. Department of Energy 1997).

During the first decades of development, the wastes from the production and processing of radioactive materials were of low priority. It was thought that future technological innovations would provide a solution (Blackman 2001). The volume of waste under U.S. DOE jurisdiction was thirty-six million m^3 as of 1997, with sixty-eight percent (~24 million m^3) attributed to weapons and thirty-two percent (~12 million m^3) from non-weapons sources (U.S. Department of Energy 1997).

The decaying process of radioactive materials has potentially harmful effects on humans, which were seen in the first scientists working with radioactive materials and later, in the aftermath of the atomic bombs dropped in Japan. Radioactive wastes are also potentially harmful to those exposed (Blackman 2001).

Protection from radioactive materials comes only from isolation or shielding until stability of the material is attained. Current designs for waste isolation systems include a design life of hundreds to thousands of years.

Disposal and isolation methods of radioactive wastes have evolved with time. Before 1970, disposal of high level wastes (HLW) on the ocean floor was common. HLW, defined as spent nuclear fuel from civilian and government sources, is now being stored in tanks and in buried drums at numerous DOE facilities while awaiting disposal by deep burial in a geological repository (Blackman 2001; U.S. Department of Energy 1997). Transuranic (TRU) waste was buried in shallow trenches prior to 1970. Currently, TRU waste is being stored in drums and boxes while awaiting disposal at the Waste Isolation Pilot Plant (WIPP) (Blackman 2001; U.S. Department of Energy 1997).

While wastes with more activity and longer lives await a more permanent disposal, shallow burial is still a common disposal method for low level wastes (LLW) and uranium mill tailings (UMT). Many of the UMT burial sites are close to residential areas, and so an effective isolation system is imperative. The burial sites are essentially landfills which make use of a cover to isolate and protect the buried radioactive wastes (Blackman 2001).

The landfill covers may be compromised by poor maintenance, weathering, or intrusion of humans, animals and vegetation. Evidences of all these compromises have been seen at DOE UMT disposal sites within ten years, and in some cases only a year after site closure (U.S. DOE 1990a; U.S. DOE 1990b; U.S. DOE 1992; U.S. DOE 1993).

Plant intrusion is a prime concern for closed disposal sites, and has been documented within a year after a site closure (U.S. DOE 1990a). The roots of unintended vegetative growth can increase the hydraulic conductivity of a landfill cover by two orders of magnitude (Waugh and Smith 1997). The volume of infiltrating water reaching the waste may be greatly increased by a more porous soil. Water balance in landfill system is therefore a key component to landfill cover management. "To determine the water balance in a landfill is the first step in designing and managing landfills (Bengtsson et al. 1994)."

Research Objectives

The overall objective of this research project was to evaluate the performance of landfill cover systems in the event of plant root intrusion. The specific objectives for this study were to:

1. Determine the effect of root intrusion and the resulting increase in the saturated hydraulic conductivity on the unsaturated water movement in cover systems;
2. Investigate the effect of low infiltration rate versus large infiltration rate on the water balance of cover systems with and without plant intrusion;
3. Compare how plant intrusion affects the water balance for different cover designs; and,
4. Determine whether, in the event of plant intrusion, the plant should be eliminated or left in place.

HYDRUS-1D, a finite element software model for water flow and solute transport, was used as an evaluation tool.

Thesis Structure

Chapter 2 is a literature review of the components, designs, and potential failure modes of engineered isolation containment systems, and discusses different water transport models. Chapter 3 is a description and a parametric sensitivity analysis of HYDRUS-1D, the hydrologic software used for the study. Chapter 4 presents an evaluation of plant growth effects using the Burrell, Pennsylvania, uranium mill tailings site as a case study. Chapter 5 is a comparison of the water balance and effects of plant growth for different landfill cover designs. Conclusions and recommendations are in Chapter 6.

CHAPTER II

LITERATURE REVIEW

Contaminant Isolation Systems

Waste containment systems are designed to isolate the waste until it has decayed or biodegraded. Figure 1 shows the components of a typical contaminant isolation system and possible interactions with the surrounding environment.

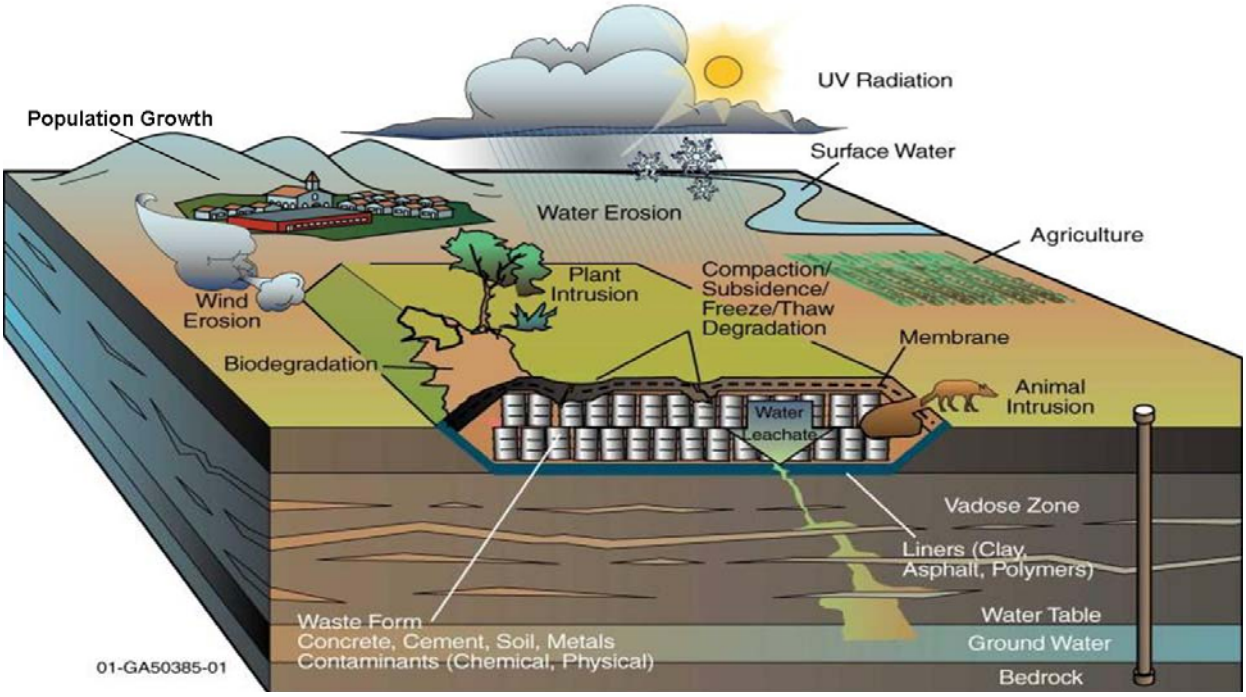

Figure 1. Containment Isolation System (INEEL 2001).

Radioactive waste may be in various forms: cemented or concreted, stored in drums or boxes, soils, or loose contaminated debris.

A low permeable liner of clay, asphalt, or a geosynthetic polymer may be placed below the waste layer. The liner prevents leachate from seeping through to the groundwater.

A leachate recovery system may be above the bottom liner as an additional precaution against groundwater contamination.

The waste is isolated from the surface by a cover system comprised of earth and sometimes of geosynthetic materials.

The contaminant isolation system is placed in the natural environment, and it is subject to physical, chemical, and biological interactions.

Physical factors include climatic influences such as temperature changes, precipitation, and wind patterns. Chemical interactions can occur by UV radiation exposure or other chemical reactions either in the waste layer or in the containment system. Biological effects on the containment system include the proximity of human, animal, or plant life.

Cover Systems

Landfill covers over buried waste are designed to protect against physical, chemical and biological factors. Specifically, the landfill cover should prevent contaminant from entering the environment, protect humans from exposure to the contaminants, and minimize water infiltration to the waste.

Components

Landfill cover designs typically include multiple layers, each with a specific function. The layers needed in a design are dependent on the type of waste and the climate region of the landfill site. Figure 2 shows the components typically found in a landfill cover.

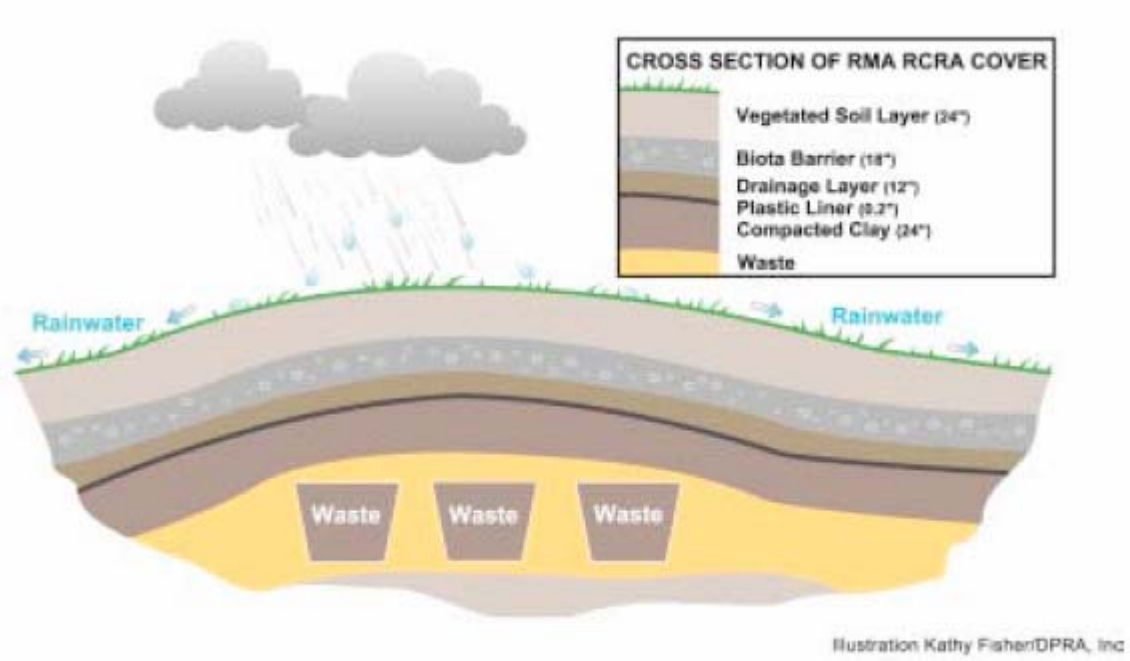

Figure 2. Typical layers of a landfill cover (Interstate Technology & Regulatory Council 2003).

The uppermost layer can be a vegetated soil layer or a layer composed of riprap. A vegetated soil layer usually is uncompacted, native topsoil. The vegetation on a landfill cover reduces the soil water by evapotranspiration and helps prevent erosion of the landfill cover. A riprap layer, composed of rocks, cobbles or gravel, is an alternative to vegetation on the top of the landfill cover. The riprap aids in preventing erosion, although it allows infiltration of water (Suter et al. 1993).

The biointrusion layer (biota barrier) lies below the topsoil layer. The rock or gravel layer is meant to discourage burrowing animals from reaching the waste layer. The biointrusion layer may also be designed to inhibit deep-rooting plants. A landfill cover may be designed with the biointrusion layer on the surface instead of subsurface (Smith et al. 1997; Suter et al. 1993).

The drainage layer is designed with a large hydraulic conductivity ($Ks \geq 10^{-2}$ cm/sec) (U.S. Environmental Protection Agency 1983b) to encourage water transport off and away from the barrier layer. A coarse material such as sand or cobbles can be used to achieve the large hydraulic conductivity. The drainage layer also serves to protect the physical integrity of the barrier layer below (Caldwell and Reith 1993).

The barrier layer, also called the infiltration layer, is intended to retard and reduce the flow of water to the waste layer below. The barrier layer may be a compacted clay or a geosynthetic material. The compacted clay layer or compacted soil layer (CSL) has a designed maximum infiltration rate of 10^{-7} cm/sec (U.S. Environmental Protection Agency 1983b). The compacted clay layer is simple to construct and easy to implement (Caldwell and Reith 1993). The geosynthetic clay is composed of bentonite clay. The bentonite clay is less susceptible to cracking than clay because it has high capacity for swelling and shrinking and is able to 'heal' itself after a freeze-thaw cycle or after drying. A study by Shan and Daniel revealed that no change in hydraulic conductivity of geosynthetic clay was evident after three freeze-thaw cycles (Daniel 1994). The geosynthetic clay can have a design hydraulic conductivity of $5x10^{-9}$ cm/sec (Dwyer et al. 2000a).

As additional barrier, a geomembrane layer may be used. The geomembrane is a low permeability layer placed below the compacted barrier layer. The geomembrane may be made of high density polyethylene (HPDE), polyvinyl chloride (PVC) or other type of polymer (Qian et al. 2002).

RCRA Cover Designs

Specifications regarding landfill covers are regulated by the Resource Conservation and Recovery Act (RCRA) in Title 40 of the Code of Federal Regulations, as mandated by the Environmental Protection Agency (EPA). These cover designs include one or more of the component layers discussed previously.

The RCRA subtitle C landfill cover is designed for hazardous waste, and is often used for low level radioactive waste. Figure 3 shows a schematic of the RCRA Subtitle C cover design. The top layer of the cover is 60 cm of native soil for vegetation growth. Below this layer is a 30 cm drainage layer of sand or synthetic material with a minimum hydraulic conductivity of 10^{-2} cm/sec. A geomembrane layer is below the drainage layer. At the bottom of the cover is the barrier layer comprised of 60 cm of native soil compacted to a maximum hydraulic conductivity of 10^{-7} cm/sec (U.S. Environmental Protection Agency 1983b).

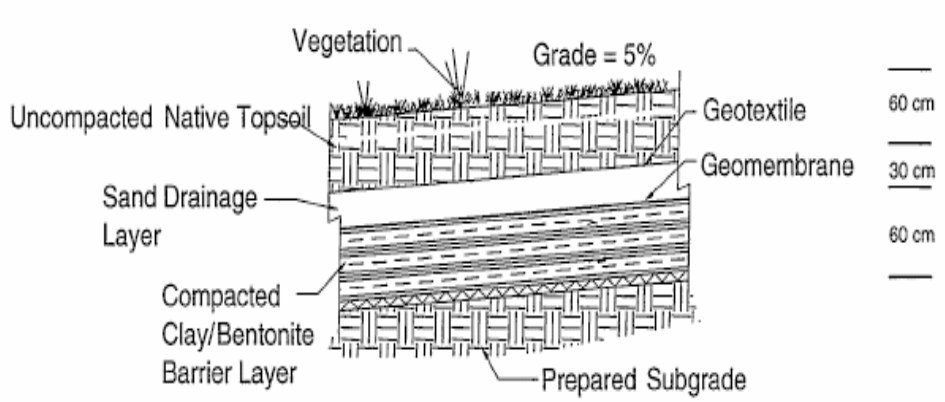

Figure 3. RCRA subtitle 'C' as shown by (Dwyer et al. 2000b).

The RCRA Subtitle D landfill cover is designed for municipal solid wastes. Figure 4 shows a sketch of a RCRA Subtitle D cover design. The upper fifteen centimeters is the erosion layer with plant growth for erosion prevention. The lower 45 cm of the cover is a compacted barrier layer of native soil, designed with a maximum 10^{-5} cm/sec hydraulic conductivity. The total depth above the waste layer is sixty centimeters (U.S. Environmental Protection Agency 1983a).

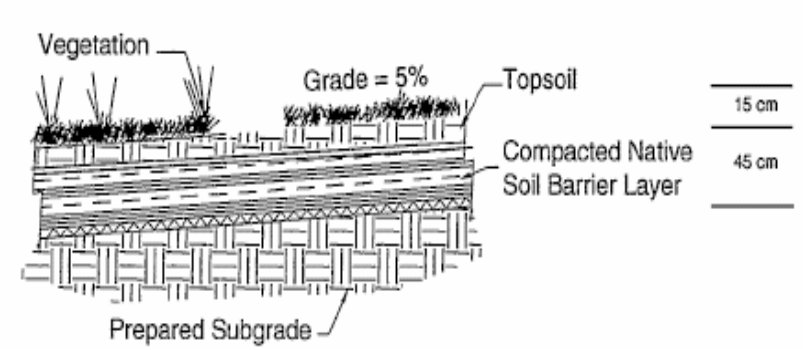

Figure 4. RCRA's subtitle 'D' Landfill cover as shown by (Dwyer et al. 2000a).

Alternative Covers

Alternative cover designs are being explored in landfill cover performance studies (Albright et al. 2002; Dwyer et al. 2000a). Alternative covers may be complex designs with geosynthetic materials, or simple designs such as the Evapotranspiration Cover.

An Evapotranspiration Cover generally consists of a thick monolith layer of native soil. The fifteen-centimeter erosion layer shown in Figure 5 is the layer designed for vegetation. Plant growth is expected and encouraged to aid evapotranspiration (Dwyer et al. 2000a). With no clear distinction in the erosion layer and the underlying evapotranspiration layer, plants may root much deeper than fifteen cm. The design depth of the evapotranspiration layer should be great enough to hold infiltrated water until removed by plant roots and evaporation (Albright et al. 2002). The Evapotranspiration cover may be compacted, but has no specific designed maximum hydraulic conductivity.

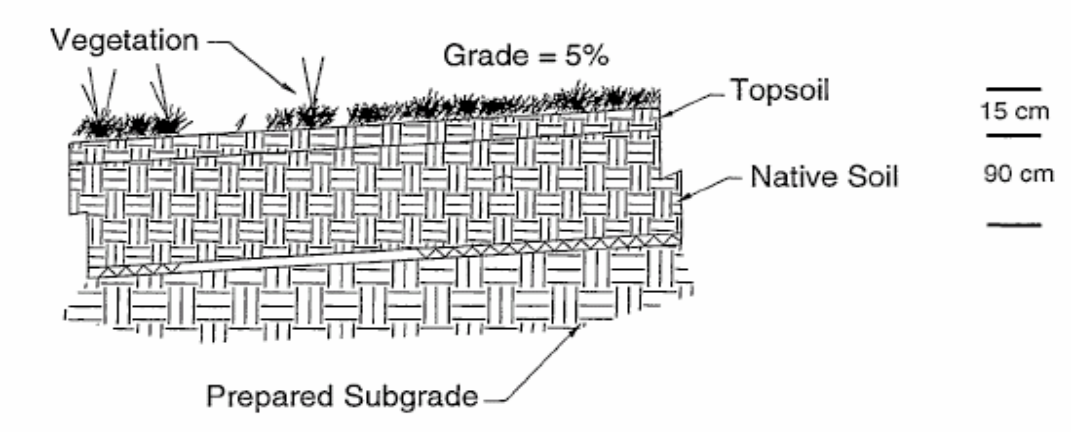

Figure 5. Evapotranspiration layer as shown by (Dwyer et al. 2000a).

Cover failure modes

Engineered landfill covers are not invincible. In fact, "all waste encapsulation schemes will ultimately fail (Caldwell and Reith 1993)." The definition of failure here is that an aspect of the engineered barrier is not performing as designed, in other words, a "non-compliance" of the design. A non-compliance does not necessarily have immediate harmful effects, but

compounded non-compliances may create a path to a major failure. For risk assessment and development of maintenance and repair strategies, it is essential to understand the modes and probabilities of failure. Two major categories of failures are caused by biological and physical effects.

Biological Failure Modes

Biointrusion of the engineered cover is difficult to eliminate. Animals and plants entering the landfill area create a perpetual cycle. Vegetation entices animals, and as animal population increases, more vegetation seeds are transported to the location by the animals. Human intrusion can be also very destructive. Hazardous waste in an abandoned landfill may be disturbed by man's development and construction (Landeen 1994).

Animal Intrusion

Animals do not obey regulations placed by humans, and so often are a threat to engineered containment systems. Small burrowing mammals are of greatest concern; the animals' movement through the cover can compromise its design.

Burrows throughout the cap can increase the hydraulic conductivity of the soil, allowing water to infiltrate more quickly and more deeply. The burrows can create passages for air and thereby dry out the soils (Landeen 1994).

Animals can also burrow into the hazardous material. For example, the woodchuck will burrow up to 1.5 meters, the ground squirrel and pocket mouse burrow to 1.4 meters. If the animals did come into contact with the buried waste, they would then be able to contaminate themselves and transport the waste to the surface and wherever they traveled above ground.

One solution to prevent burrowing animals is to keep the landfill cover mowed and clear of deep vegetation. Suter et al. (Suter II et al. 1993) pointed out that earthworms, capable of burrowing two meters deep, are not deterred by mowed grass aboveground. The cavities in the soil created by earthworms can produce the same results as the burrows of animals. In addition, the movement of the earthworms encourages plant rooting.

Additionally, animals can also be capable of transporting seeds to the cover by their fur or through their excrement. The plant growth resulting from the seed transport is likely to be deep-rooting vegetation not intended for the cover design.

Plant Intrusion

Plants as a vegetative cover are an important component of the landfill cover design. As discussed previously, the purpose of intentionally planning for plant growth is to control erosion and to reduce the water flux by taking up water in the soil through their roots, thereby aiding transpiration.

There are also negative effects of plant growth. Of major concern is the possibility that the roots could actually penetrate through to the buried waste. This could result in the roots' transporting contaminants to the surface, where undesirable contact could occur. Grasses can reach rooting depths of up to eight meters; deciduous trees have a mean rooting depth of 3.3 meters but can root to depths of 30 meters (Suter II et al. 1993). These depths are enough to penetrate through any landfill design.

The effects of plant roots extend beyond contaminant uptake and transport. Root growth can change the soil dynamic, and root decay leaves open cavities within the soil profile. Studies by Waugh and Smith (Waugh and Smith 1997) show that unintended plant root growth can increase the hydraulic conductivity of a soil by two orders of magnitude.

An increase in the hydraulic conductivity would cause the cover to no longer meet the design criteria. This could mean that the design time of the cover would be compromised, or that more water would infiltrate through the cover, reaching the waste.

Uprooted plants on a landfill cover would result in a large hole, possibly exposing the waste but definitely allowing easier access to the waste by animals, plants, or water. Alternately, the roots' uptake of water could dry out soils with high water content potential, such as clay, and then the soil could crack, also resulting in an increase of hydraulic conductivity (Suter et al. 1993).

Human Intrusion

Although it is human regulation that protects landfills, humans are not protected absolutely. Memory is short, and sites are difficult to maintain indefinitely. Both the EPA and the United States Nuclear Regulatory Commission (NRC) have said that it is unlikely that active control of disposal sites will be possible after a maximum of one hundred years (Caldwell and Reith 1993).

A case study related to the topic of negligence is the Love Canal saga. In the late seventies, detrimental health effects in Love Canal were attributed to hazardous waste burial. A

school was built directly on a landfill used by chemical manufacturers, and children were exposed to the toxic wastes. After the area was evacuated and leveled, a fence was erected around the area. Fewer than thirty years after the evacuation, new home construction has begun on the site. This case shows that protected sites are not even effective deterrents to human population (Kostelnik et al. 2004).

Physical Failure Modes

Physical failure modes occur within the landfill cover as a result of natural or climatic effects such as freezing and thawing cycles, intermittent wetting/drying by precipitation events, and erosion.

Freezing and thawing cycles can increase the hydraulic conductivity of a soil. A study by Miller and Lee (Miller and Lee 1999) revealed that in a simulated cover, the water movement through the bottom increased by an order of magnitude after three freeze-thaw cycles.

A wet soil shrinks as it dries, and a great water loss can result in cracking. Successive shrink/swell cycles increase the magnitude of the cracks, continually increasing the porosity of the soil. Clay materials are particularly susceptible to cracking. Prevention of cracking can be achieved by covering the barrier layer to keep the moisture content of the soil at an acceptable level (Suter et al. 1993).

The top soil layer protects the underlying layers of a landfill cover. Erosion lessens this protection by allowing physical and biological factors to more easily degrade the other layers. Daniel (Daniel 1994) states that soil erosion on a cover is almost inevitable.

Evaluation of Long Term Performance of Landfill Covers

The design life of a containment isolation system is based on the type of waste to be isolated. A design life of 200 to 1000 years is considered "long-term (Caldwell and Reith 1993)."

Factors compromising landfill covers have been documented after only a few years (U.S. DOE 1990a; U.S. DOE 1990b; U.S. DOE 1992; U.S. DOE 1993; Waugh 1999), suggesting that design regulations should be reconsidered. In addition to the RCRA design requirements which include a minimum thickness and a maximum hydraulic conductivity for the cover, Ho et al (Ho

et al. 2004) indicated that site-specific information such as climate, soil, and vegetation should also be considered.

Many disposal sites have closed only recently and so long-term evaluations are not available. Continued monitoring is imperative at disposal sites (Kumthekar et al. 2002; Waugh 1999) as a preventive measure and to evaluate future improvements to landfill cover design.

Computational evaluations of long-term landfill performances have been developed (Ho et al. 2004; Leoni et al. 2004). Results from such models revealed that potential failures occur in the clay layer by wet-dry cycles and water percolation through the cover, resulting in elevated concentration of contaminants in groundwater.

Landfills and Water Balance

In a landfill, water content comes from the waste itself, from the landfill soil cover, and by precipitation (Bengtsson et al. 1994). The water content in contact with the waste should be minimal to prevent hazardous contaminants from leaching. The resulting leachate could eventually flow into the groundwater, thereby contaminating it (Bengtsson et al. 1994; Johnson et al. 1998). The water balance in the landfill cover is also a very important issue. Part of the landfill cover design is to limit the water reaching the waste and thus protecting against leaching and groundwater contamination (Khire et al. 1997). However, a compacted clay barrier layer would crack if the residual moisture content were not maintained (Suter et al. 1993). The ideal balance allows the barrier layer to retain effective moisture content while limiting the flux through to the buried waste.

A study on a municipal solid waste incinerator (MSWI) bottom ash landfill showed that discharge through the landfill and landfill cover after a precipitation event was rapid and in large proportion to the precipitation volume (Johnson et al. 1998). A single precipitation event in the winter resulted in more than 90% of the water volume discharging through the bottom of the landfill within days (50% transported in less than 4 days), while precipitation events in the summer months resulted in less discharge (between 9 and 40%). This was attributed to increased evaporation during the summer (due to the warmer temperature) and increased transpiration from plant growth. Preferential flow paths through the landfill can also account for some volume of water not discharged through the bottom of the landfill (Johnson et al. 1998; Ludwig et al. 2000).

However, even with preferential flow, evaporation, and transpiration in periods with little precipitation, Johnson et al (Johnson et al. 1998) observed that the discharge through the landfill was never zero. According to Johnson et al (Johnson et al. 1998), the landfill acted as a reservoir for water that was held within the landfill by perched water tables with a residence time of approximately three years.

Groundwater contamination from leaching is expected more in humid areas than in arid areas, but an arid site study found that "considerable quantities of leachate" were present (Al-Yaqout and Hamoda 2003). This was attributed to rising groundwater levels and to the liquid wastes disposed at the site.

Plant Intrusion and Water Balance in Cover Systems

Plants are "largely responsible for the water removal from the landfill cover (Albright et al. 2002)," and therefore have a major influence on the landfill water balance. While plant root water uptake is a design consideration of landfill covers, unintended plant growth may be detrimental rather than beneficial.

As discussed in the section on plant intrusion, studies have shown that plants increase the saturated hydraulic conductivity Ks. The increased Ks then allows more water infiltration, which would be able to contact the buried waste (Waugh and Smith 1997). If the roots grow deep enough seeking more water, they may penetrate the waste layer and transport the contaminants up through the landfill cover.

One solution to control plant growth on a landfill is to use pesticides (Waugh and Smith 1997). Although this solution would prevent further plant growth, it does not fix the damage already created by plant root growth. In fact, it may worsen the problem by allowing the cavities formerly occupied by roots to become a drainage system for water. If the plants are allowed to live, they will continue to take up water and possibly remedy their own destruction.

The objectives of this research are therefore to determine the effects of plant intrusion on the water balance of landfill cover systems and determine the best remedy (i.e., eliminate the tree or leave it in place) in the event of plant growth on a landfill cover. A water transport modeling software with plant root water uptake capabilities was the tool chosen to reach these objectives.

Water Flow Models

Two principal types of water transport modeling software exist: those that solve the Richards' equation and those that solve the water balance (Albright et al. 2002). Table 1 shows some water transport modeling software and the type of model used.

Table 1. Comparison of Water Balance Modeling Software.

Model name	Water retention method	Water retention function used
EPIC	Water balance	
HELP	Water balance	
TOUGH-2	Richards' equation	
MACRO	Richards' equation	
UNSAT-H	Richards' equation	van Genuchten, Brooks and Corey
HYDRUS	Richards' equation	van Genuchten, Brooks and Corey
LEACHM	Richards' equation	Campbell

Water Balance Models

Water balance models, or storage-routing models, calculate the water retention curve parameters based on user input. Generally, the required input points are field capacity, wilting point, and saturated water content, and the calculated values are drainable porosity (saturated water content minus field capacity) and water-holding capacity (field capacity minus wilting point) (Albright et al. 2002).

Richards' Equation Based Models

Modeling software solving Richards' equation uses one of several water content functions to solve for the water retention curve (Albright et al. 2002). Richards' equation is

$$\frac{\partial \theta}{\partial t} = -\frac{\partial J}{\partial x} + S \qquad [1]$$

where θ is the volumetric water content, t is time, J is flux, x is the spatial coordinate, and S is the sink term. Table 2 lists the parameters in the following water retention functions.

The van Genuchten function for water content θ is

$$\theta(h) = \theta_r + \frac{\theta_s - \theta_r}{\left[1 + (\alpha h)^n\right]^m} \quad [2]$$

(Šimunek et al. 1998)

The Brooks and Corey function for water content is

$$\theta_e = \frac{\theta - \theta_r}{\theta_s - \theta_r} \quad [3]$$

The Campbell function for water content is

$$\theta = \theta_s \left(\frac{h}{h_a}\right)^{-1/b} \quad [4]$$

(Albright et al. 2002)

Table 2. Water Retention Function Parameters

Parameter	Description	Units
Θ	Water content	(-)
J	Flux	(L/T)
h	Pressure head	(L)
x	Profile depth	(L)
Θr	Residual water content	(-)
Θs	Saturated water content	(-)
α	Parameter in van Genuchten	(L^{-1})
n	Parameter in van Genuchten	(-)

Available Software

The water transport software models listed in Table 1 have been included in various studies comparing the appropriateness of water transport models (Albright et al. 2002; Johnson et al. 2001; Khire et al. 1997; Scanlon et al. 2002). At the end of the chapter, Table 3 gives a summary of the software models discussed.

EPIC

The EPIC (Erosion-Productivity Impact Calculator) modeling software was developed in the early 1980s as an agricultural tool and solves for water retention by the water balance. It contains extensive plant and other agricultural considerations and accepts precipitation input. Albright et al (Albright et al. 2002) found that the EPIC software under-predicted drainage, and that the HELP software was superior to EPIC for landfill cover simulations. EPIC is a DOS-operating program in the public domain, and more information may be found at the website http://www.brc.tamus.edu/epic/index.html.

HELP

The Hydrologic Evaluation of Landfill Performance, or HELP, was developed by the U.S. Army Engineers Waterways Experiment Station. The HELP model solves the water balance by the storage routing method (2005; Albright et al. 2002). Input information required by HELP includes daily weather information, and HELP considers plant growth and water uptake. HELP is the only model specifically designed for landfill cover evaluation, but it is limited by its solving method. Model comparisons generally find that HELP, as a water balance model, is not as accurate as models based on Richards' equation (Khire et al. 1997; Scanlon et al. 2002). Albright found that HELP, like EPIC, under predicted drainage from the landfill cap (Albright et al. 2002). HELP is a DOS-operating program and may be downloaded at the website http://www.wes.army.mil/el/elmodels/index.html#landfill.

TOUGH-2

Transport Of Unsaturated Groundwater and Heat, or TOUGH-2, is a finite-difference model solving Richards' equation for multi-dimensional transport. TOUGH-2 was designed for use in nuclear waste isolation studies and variably saturated water transport (Pruess et al. 1999). TOUGH-2 does not have any plant growth considerations, although it allows evapotranspiration

input data. TOUGH-2 was used in the evaluation of Yucca Mountain and has been used in alternative landfill cover evaluations (Albright et al. 2002; Dwyer et al. 2000a). TOUGH-2 may be purchased by contacting the Energy Science and Technology Software Center (ESTSC). (http://www.osti.gov/estsc/order.htm)

MACRO

MACRO is based on Richards' equation and includes an additional term to account for preferential flow though macro pore and micro pore water movement (Johnson et al. 2001). MACRO may be used to model saturated or unsaturated media. MACRO can account for plant water uptake and calculates solute transport as well as water transport. Johnson compared MACRO with HYDRUS, and found that preferential flow was significant and should be included in a model. MACRO may be downloaded at the website http://www.mv.slu.se/bgf/Macrohtm/Macro5_0/download5_0.htm.

UNSAT-H

UNSAT-H, developed at Pacific Northwest Laboratory (PNL), solves Richards' equation for one-dimensional flow in unsaturated media by the finite difference method (2005). UNSAT-H accounts for plant transpiration, and allows user input about the soil media properties. A study by Khire (Khire et al. 1997) found that UNSAT-H was more accurate than the water balance solver HELP. Albright et al (Albright et al. 2002) found that UNSAT-H under-predicted drainage, but that the model was physically realistic. UNSAT-H is comparable to HYDRUS, and so if a two-dimensional model is required, Albright et al suggest HYDRUS-2D. UNSAT-H may be downloaded at the website http://hydrology.pnl.gov/resources/unsath/unsath.asp.

HYDRUS-1D

HYDRUS-1D is a finite element solution to Richards' equation for one-dimensional flow in variably saturated media. The HYDRUS-1D software includes plant growth and plant root water uptake options. In addition to the modeling of water flux, HYDRUS can simulate contaminant transport through the media and contaminant root uptake. A soil catalogue is contained within the software, but user input data of soil hydraulic properties is also allowed (Šimunek et al. 1998). HYDRUS-1D is a DOS-operating program and may be downloaded at the website http://www.pc-progress.cz/Fr_Hydrus.htm.

HYDRUS-2D

HYDRUS-2D includes all the function of HYDRUS-1D and includes the modeling software SWMS_2D for two-dimensional water movement. The two-dimensional solution is useful when lateral flow modeling is required. Albright (Albright et al. 2002) found that the predictions of HYDRUS-2D were physically realistic, but that drainage was under-predicted. HYDRUS-2D may be purchased, or a demo version may be downloaded, at the website http://www.pc-progress.cz/Fr_Hydrus.htm.

LEACHM

The Leaching Estimation And CHemistry Model, LEACHM, is a one-dimensional transport model solving Richards' equation with a finite difference approach (2005). The code was created for use in agricultural applications and solves only for unsaturated media. Although it was developed for agricultural use, it is limited by its lack of plant considerations and does not account for water runoff (Albright et al. 2002). LEACHM does account for chemical transport in addition to water flow. A 2002 survey of users did not find any use of LEACHM in landfill cover modeling (Albright et al. 2002). LEACHM, a DOS-operating program, may be downloaded at the website http://www.scieng.flinders.edu.au/cpes/people/hutson_j/leachweb.html.

Table 3. Water Transport Model Summary.

Model name	**Plant Growth**	**Solute Transport**	**Variably saturated media**
EPIC	Yes	No	
HELP	No	Yes	Yes
TOUGH-2	No	Yes	No
MACRO	Yes	Yes	Yes
UNSAT-H	Yes	No	No
HYDRUS	Yes	Yes	Yes
LEACHM	Yes	Yes	no

CHAPTER 3

HYDRUS-1D AND PARAMETRIC SENSITIVITY ANALYSIS

Introduction

HYDRUS-1D is a finite element model that has the capability to model one dimensional water flow and solute transport for variably saturated media. The software allows for up to ten different soil layers and contains a catalogue of soil parameters. A catalogue of plant growth and water uptake parameters is also a part of the HYDRUS-1D software. HYDRUS-1D is now available in the public domain. The HYDRUS-1D software was chosen as a tool for this research project.

Governing Equations

Details of the equations solved by HYDRUS-1D are in APPENDIX A.

HYDRUS-1D is based on Richards' equation for unsaturated flow. Richards' equation for one-dimensional flow contains two dependent variables, pressure head h and water content θ (Warrick 2002). The form of the equation used by HYDRUS-1D (Šimunek et al. 1998) is coupled with a sink term S:

$$\frac{\partial \theta}{\partial t} = \frac{\partial}{\partial x}\left[K\left(\frac{\partial h}{\partial x} + \cos\alpha \right) \right] - S \qquad [5]$$

where α is the angle between flow direction and vertical axis and x is the vertical gradient. HYDRUS-1D solves for water content using the van Genuchten (van Genuchten 1980) equation when the pressure head is negative:

$$\theta(h) = \begin{cases} \theta_r + \dfrac{\theta_s - \theta_r}{\left[1 + \left| \alpha h \right|^n \right]^m} & h < 0 \\ \theta_s & h \geq 0 \end{cases} \qquad [6]$$

where θ is the water content, θ_r is the residual water content, and θ_s is the saturated water content, and l and m are empirical constants.

The hydraulic conductivity is solved as a function of water content in HYDRUS-1D using the method of Mualem (Mualem 1976):

$$K(h) = K_s S_e^l \left[1 - \left(1 - S_e^{1/m} \right)^m \right]^2 \quad [7]$$

where Ks is the saturated hydraulic conductivity and the effective water content Se is given by

$$S_e = \frac{\theta - \theta_r}{\theta_s - \theta_r} \quad [8]$$

The sink term S in Equation [5] accounts for root water uptake by transpiration.

$$S(h) = \alpha(h) S_p \quad [9]$$

where

$$S_p = \frac{1}{L_R} T_p \quad [10]$$

$$L_R(t) = L_m f_r(t) \quad [11]$$

$$f_r(t) = \frac{L_0}{L_0 + (L_m - L_0) e^{-rt}} \quad [12]$$

The function α(h) is described in APPENDIX A. S_p is the potential root water uptake rate (Feddes et al. 1978). L_R is the depth of the root zone, L_m is the maximum rooting depth and $f_r(t)$ is the root growth coefficient given by the Verhulst-Pearl logistical growth equation in Equation [12]. L_0 is the initial rooting depth, and r is the growth rate (Šimunek and Suarez 1993).

Table 4. HYDRUS-1D user input (Šimunek et al. 1998).

Geometry Input	
Number of Soil Materials	
L	Depth of Soil Profile [L]
α	Slope [-]
Time Information	
Final Time [T]	
Number of Time-Variable Inputs	
Soil Water Retention Parameters	
θ_r	Residual soil water content [-]
θ_s	Saturated soil water content [-]
α	Parameter α in the soil water retention function [L^{-1}]
n	Parameter n in the soil water retention function [-]
K_s	Saturated hydraulic conductivity [LT^{-1}]
Root Growth Parameters	
L_0	Initial root depth [L]
L_m	Final (maximum) root depth [L]
t_0	Initial root growth time [T]
t	Harvest time [T]
Root Water Uptake Parameters	
h_1	Value of the pressure head below which roots start to extract water from the soil [L]
h_2	Value of the pressure head below which roots extract water at the maximum possible rate [L]
h_3	Value of the limiting pressure head below which roots cannot longer extract water at the maximum rate [L]
h_4	Value of the pressure head below which root water uptake ceases (usually taken at the wilting point) [L]
T_p	Potential transpiration rate [LT^{-1}]
Time Variable Input Data	
Time	Time for which a data record is provided [T]
Precip	Precipitation rate [LT^{-1}] (in absolute value)
Evap	Potential evaporation rate [LT^{-1}] (in absolute value)
Trans	Potential transpiration rate [LT^{-1}] (in absolute value)
hCritA	Absolute value of the minimum allowed pressure head at the soil surface [L]
FluxTop	Time-dependent flux at the soil surface boundary [L/T]
hTop	Time-dependent pressure head at the soil surface boundary [L]
KodTop	Set equal to -1 (+1) when flux (pressure head) is specified as the soil surface boundary condition

Sensitivity Analysis

A sensitivity analysis of the parameters of HYDRUS-1D was conducted to examine how changes in the value of a parameter vary the simulation output. Small changes in a parameter resulting in relatively large output changes are indicative of a parameter's sensitivity. The objectives of the sensitivity analysis were to find the parameters of greater importance in a water flow simulation in the vadose zone, and to determine the effect of plant growth on the water balance. The parameters considered were saturated hydraulic conductivity Ks, saturated water content θs, residual water content θr, initial water content θi, and plant root growth.

Scenario Description

The scenario designed for the sensitivity analysis represented a compacted soil landfill layer above a waste layer. A single soil type of clay with a depth of 10 cm was considered. The values for clay's soil water retention parameters are contained in the HYDRUS-1D catalogue (Table 5).

Two precipitation cases, representing a landfill in A) a humid region and in B) an arid region, were considered. Precipitation Case A representing a humid region was subjected to a constant precipitation rate of 0.5 cm/day. A precipitation rate of 0.5 cm/day corresponds approximately to 180 cm per year (72 inches per year), which is typical in humid environments. Precipitation Case B, the arid site, was simulated by a constant precipitation rate of 0.05 cm/day, which translates into 18 cm (7 inches) of rainfall per year (NCDC 2005). Figure 6 shows the schematic of the scenario.

One additional scenario was considered for evaluation of saturated hydraulic conductivity effects using a clay soil with a depth of 60 cm (the clay depth in a RCRA C landfill cover). For this case, only the 0.5 cm/day precipitation was evaluated.

Table 5. Soil water retention parameters for clay (Carsel and Parrish 1988; Šimunek et al. 1998).

Θr, residual water content (-)	Θs, saturated water content (-)	α (1/cm)	n (-)	Ks, saturated hydraulic conductivity (cm/day)
0.068	0.38	0.008	1.09	4.8

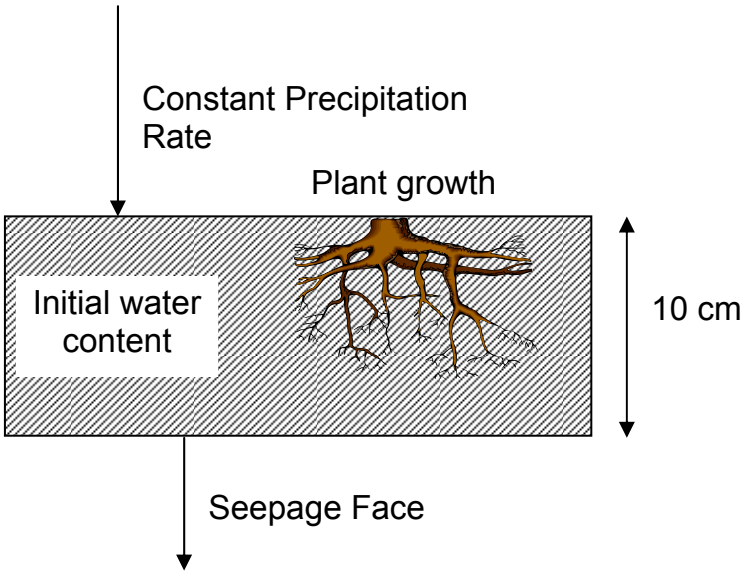

Figure 6. Scenario for Sensitivity Analysis

Model Setup

The van Genuchten-Mualem soil hydraulic model (See Equations [6], [7]) with the air-entry value of -2 cm option was selected within HYDRUS-1D. For the simulations involving root water uptake, the Feddes equation was selected (See Equation [10]).

The upper boundary condition for the simulations was a constant flux. The lower boundary condition was selected as seepage face, which is recommended for lysimeter representation (Šimunek et al. 1998).

The simulations in this study were conservative, as runoff and evaporation processes were not considered. The amount of water infiltrating the top of the landfill cover was assumed equal to the precipitation values.

For each 10-cm soil depth case, the simulations were run for 10 days (Precipitation Case A) or 100 days (Precipitation Case B). The maximum and minimum time steps and iteration criteria varied for the simulations, and are listed, along with the remaining input parameters for HYDRUS-1D, in APPENDIX B.

For the case using 60-cm soil depth, the simulations were evaluated for thirty days.

Parameters considered

The parameters varied were (i) the saturated hydraulic conductivity Ks, (ii) the saturated water content θs, (iii) the residual water content θr, (iii) the initial water content θi, and (iv) plant root growth. Table 6 presents the range of values used for each of these parameters. Since the saturated hydraulic conductivity Ks is the parameter most likely to be affected during plant intrusion, the value for this parameter was increased by two orders of magnitude and evaluated as another baseline case. A third baseline case simulated the compacted state of clay by decreasing the hydraulic conductivity by two orders of magnitude.

Table 6. Parameter Values for Sensitivity Analysis.

	Ks (cm/day)			Water content (-)			Plant growth	
	#1	#2	#3	θ_S	θ_r	θ_{ini}	Root depth (cm)	PET[3] (cm/day)
Baseline	4.8	0.048	480	0.380	0.068	0.2	0	0
- 25%	3.6	0.036	360	0.285	0.051	0.15	5[1]	0.5[1]
+ 25%	6	0.06	600	0.475	0.085	0.25	10[2]	3[2]

(1) Grass growth (2) Tree growth (3) Potential Evapotranspiration Rate

Results

The results are presented as a comparison of the total amount of water infiltrating through the soil after ten days for the humid site simulation and after 100 days for the arid site simulation.

The change in cumulative bottom flux was calculated as:

$$\Delta F = \frac{F_{Test} - F_{Baseline}}{F_{Baseline}} X\,100 \qquad [13]$$

where ΔF is the percentage change in the result value of the cumulative bottom flux, F_{Test} is the result value for using the test parameter value, and $F_{Baseline}$ is the result value for using the baseline parameter value.

The ΔF values for the 25% changes of each parameter are presented in tables and graphs for both the humid and arid site.

In addition, bar graphs comparing the amount of water are presented for each variable of the sensitivity analysis.

Precipitation Case A: 0.5 cm/day

Saturated Hydraulic Conductivity Considerations

Simulations were run for all variables listed in Table 6 using a 10-cm soil depth, but for the 60-cm soil depth only the Ks case # 1 were simulated.

For the 10-cm clay soil simulations, 25% changes in the saturated hydraulic conductivity Ks had very little effect on the water flux through the clay layer. When the Ks was on the order of 10^{-2} cm/day (10^{-7} cm/sec), no change in water flux was seen for the variations of Ks (Figure 7 A, Table 7). Only a 0.01 % change was noted when Ks was in the 10^{0} cm/day range (Table 7), and the results from the third case when Ks~10^{2} cm/day were also small. [N.B. The values from the third Ks test were inconsistent, as the increased and decreased Ks both resulted in greater water flux than did the baseline. This issue requires further study.]

Figure 7 A compares not only the 25% variations of Ks values, but also the three cases of Ks which vary by two orders of magnitude. The resulting fluxes for these Ks values were similar; the percent change from Ks = 4.8 to K s= 0.48 cm/day was 0.13%, and only 0.03% change between Ks= 4.8 and Ks = 480 cm/day (Table 8). The clay soil is often difficult to model using the van Genuchten method, because the hydraulic conductivity decreases sharply near saturation (Simunek 2004). In these cases, the water flux through the cover increased sharply for all values of Ks. As seen in Figure 7 B, by day 10 the clay soil was saturated for all Ks cases, which may account for the similarities in the amount of water flux.

For the 60-cm soil depth simulations, the percent changes of flux are presented in Table 9 at 21.24 days, and the flux through the cover as a function of time is shown in Figure 8. At 21.24 days, the 25% decrease in Ks resulted in a 42.2% change in water flux through the cover, and the 25% increase in Ks resulted in a 28.9% change in water flux (Table 9, Figure 8 B).

This simulation revealed that the saturated hydraulic conductivity does have a significant effect on water flux. The larger, 60-cm soil depth in this simulation illustrated the sensitivity of the Ks parameter as the soil approached saturated conditions.

Table 7. Effect of 25% variations of Ks on Water Flux

	Variable Change	Ks #1 cm/day	ΔF, %	Ks #2 cm/day	ΔF, %	Ks #3 cm/day	ΔF, %
T =10 days	- 25%	0.036	0.00	3.6	0.01	360	0.01
	+ 25%	0.060	0.00	6.0	0.01	600	0.03

Table 8. Effect of orders of magnitude variations of Ks on Water Flux

	Variable Change	Ks, cm/day	ΔF, %
T =10 days	10^{-2}	.048	0.13
	10^{2}	480	0.03

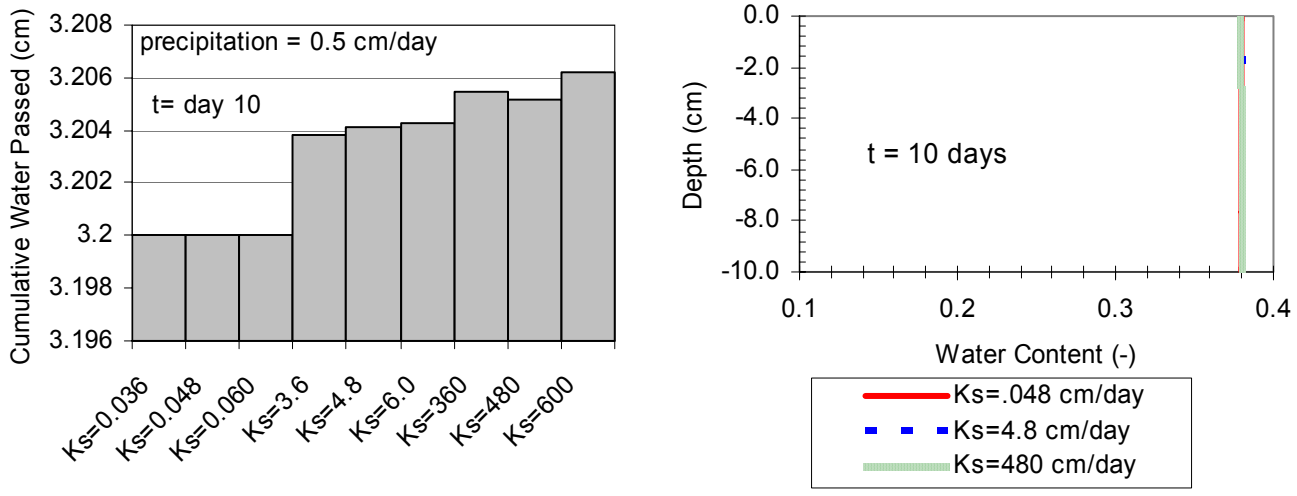

A. B.

Figure 7. Ks variations. A) Cumulative Water Flux after 10 days and B) Water Content at 10 days.

Table 9. Effect of 25% variations of Ks on Water Flux

	Variable Change	Ks, cm/day	ΔF, %
T =10 days	-25%	3.6	42.2
	+25%	6.0	28.9

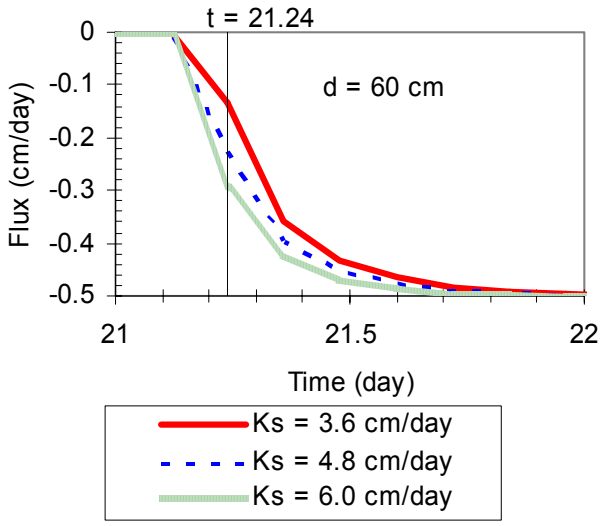

A.

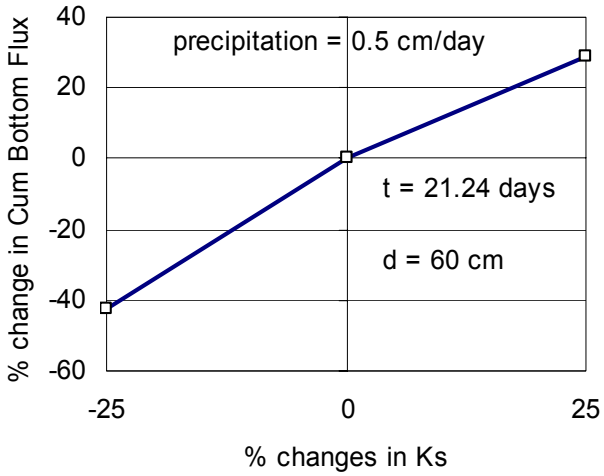

B.

Figure 8. Ks variations. A) Flux through the cover as a function of time and B) Change in Flux at 21.24 days.

Saturated water content considerations

The saturated water content θs is a parameter determining the effective water content, which in turn is used in solving hydraulic conductivity (Equations [7], [8]). This analysis revealed that θs is a sensitive parameter; the change in water flux was about 23% for the 25% decreased θs and about 42% for the 25 % increased θs (Table 10). Figure 9 A and B demonstrate the relationship of the water flux and the saturated water content.

Table 10. Effect of 25% variations of θs on Water Flux

	Variable Change	Water content θs	ΔF, %
T =10 days	- 25%	0.285	22.85
	+ 25%	0.475	42.06

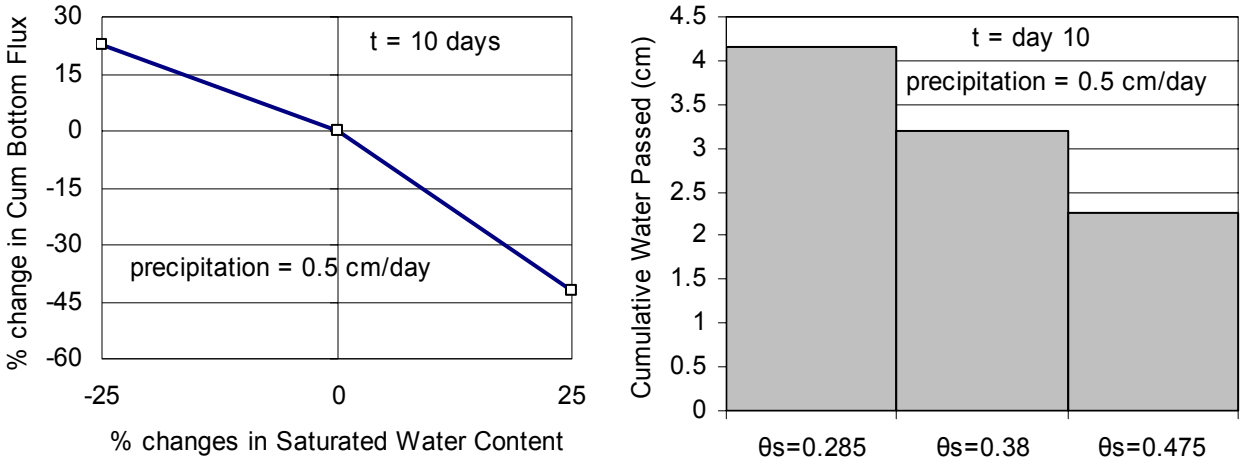

A. B.

Figure 9. θs variations. A) Change in Flux and B) Cumulative Water Flux after 10 days.

Residual water content considerations

Variations of 25% in the residual water content had very little effect on the water flux through the cover; the percent change in F was only 0.01 for the 25% variations of θr (Table 11). The residual water content would be expected to be influential in dry conditions, but as seen in Figure 7 B, the clay soil is saturated.

Table 11. Effect of 25% variations of θr on Water Flux.

	Variable Change	Water content θr	ΔF, %
T =10 days	- 25%	0.051	0.01
	+ 25%	0.085	0.01

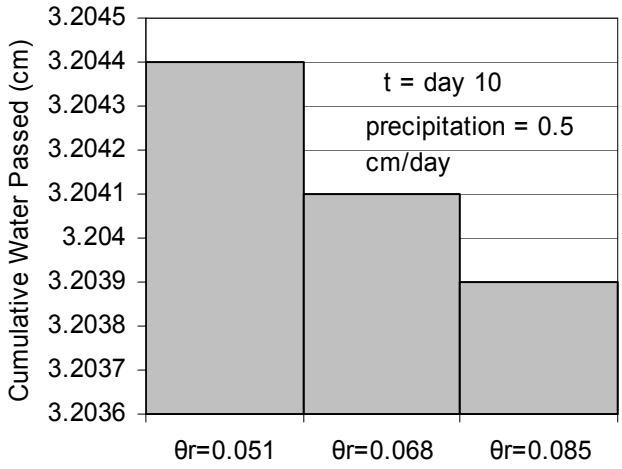

Figure 10. θr variations. Cumulative Water Flux after 10 days.

Initial Moisture Content considerations

The initial moisture content was a sensitive parameter in this analysis. The changes in water flux were 18.5% for the -25% θ change and 15.5% for +25% change (Table 12). Figure 11 shows the relationship between water flux and initial water content. The moisture content in the soil changes as a function of time and depending on precipitation, evaporation, and other processes affecting the soil. The initial moisture content is influential only at the beginning of the simulation; long-term simulations would decrease the effect of initial water content on water flux.

Table 12. Effect of 25% variations of θi on Water Flux.

	Variable Change	Water content θ_i	ΔF, %
T =10 days	- 25%	0.15	18.49
	+ 25%	0.25	13.50

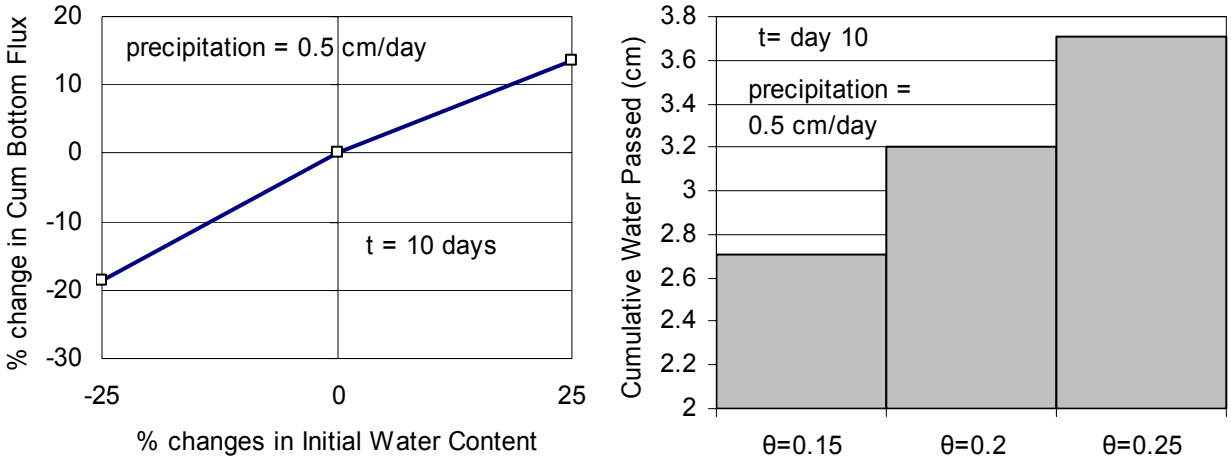

A. B.

Figure 11. θi variations. A) Change in Flux and B) Cumulative Water Flux after 10 days.

Plant Considerations

The plant growth and root water uptake processes were significant influences on the water flux. The plants' roots provided an alternative path for the water, by transporting it upward instead of down through the soil cover. As seen in Figure 12, the presence of the plants reduced the water flux to negligible amounts. Table 13 shows that the presence of the plants reduced the water flux by essentially 100%.

Table 13. Effect of Plants on Water Flux

	Variable Change	Root Depth, cm	PET[3], cm/day	ΔF, %
T = 10 days	Grass	5[1]	0.5[1]	100.00
	Tree	10[2]	3[2]	100.00

(1) Grass growth (2) Tree growth (3) Potential Evapotranspiration Rate

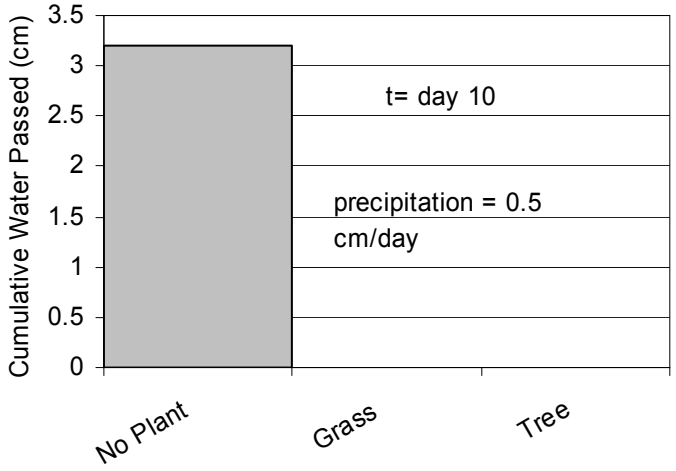

Figure 12. Plant variations. Cumulative Water Flux after 10 days.

Precipitation Case B: 0.05 cm/day

Saturated Hydraulic Conductivity Considerations

Here, as in the Precipitation Case A, the saturated hydraulic conductivity had very little effect on the flux F through the 10-cm soil layer. All the variations resulted in 0.01 % or less change in the flux, with the exception of Ks case #3 when Ks=600 cm/day, where the ΔF= 0.3 % (Table 14). In comparison with a 25% Ks change, however, even the 0.3% change was very small. Table 15 gives the values for the percent change in water flux when the Ks varied by orders of magnitudes. For a change of two orders of magnitude of Ks, the water flux changed by 0.2 % or less. These values indicate an insignificant influence of Ks, and as discussed in the section on Ks effects for Precipitation Case A, the clay material may be a factor in this outcome.

Table 14. Effect of 25% variation of Ks on Water Flux

	Variable Change	Ks #1 cm/day	ΔF, %	Ks #2 cm/day	ΔF, %	Ks #3 cm/day	ΔF, %
T = 100 days	- 25%	0.036	0.00	3.6	0.01	360	0.01
	+ 25%	0.060	0.00	6.0	0.00	600	0.30

Table 15. Effect of orders of magnitude variation of Ks on Water Flux

	Variable Change	Ks, cm/day	ΔF, %
T =10 days	10^{-2}	.048	0.16
	10^{2}	480	0.20

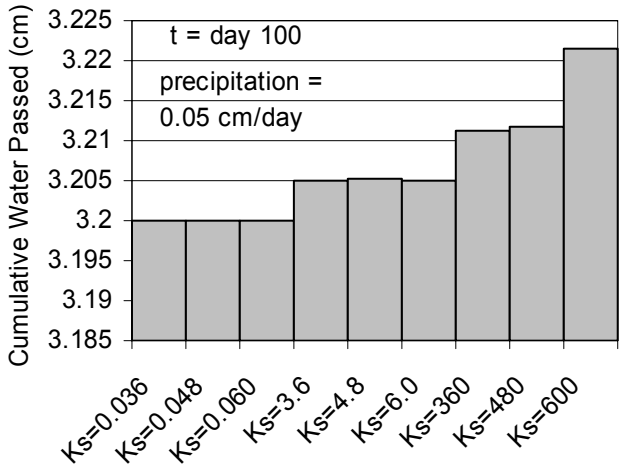

Figure 13. Ks variations. The Cumulative Water Flux after 100 days.

Saturated water content considerations

The saturated water content had a significant influence on the flux; the 25 % changes in θs resulted in about a 30 % as seen in Table 16 and Figure 14 A. These results were consistent with those in Precipitation Case A.

Table 16. Effects of 25% variations of θs on Flux

	Variable Change	Water content θs	ΔF, %
T =100 days	- 25%	0.285	29.59
	+ 25%	0.475	29.59

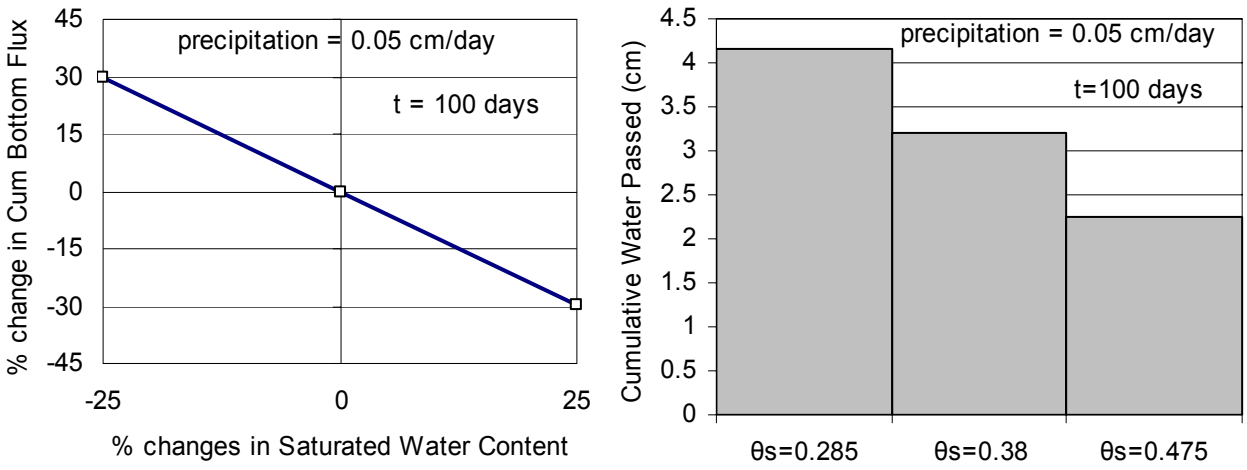

A. B.

Figure 14. θs variations. A) Change in Flux and B) Cumulative Water Flux after 100 days.

Residual water content considerations

The residual water content here, as with the humid Precipitation Case A, had very little influence on the water flux. While there was a change in flux as the θr varied (Figure 15), the actual change was only a negligible 0.01 % for the 25 % variations (Table 17).

Table 17. Effect of 25% variations of θr on Flux.

	Variable Change	Water content θr	ΔF, %
T =100 days	- 25%	0.285	0.01
	+ 25%	0.475	0.01

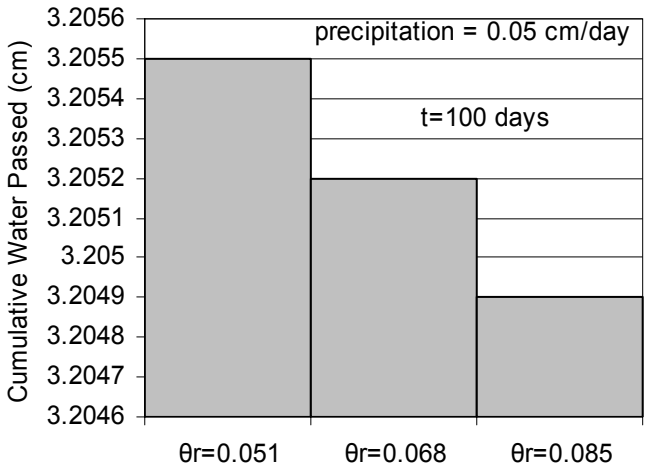

Figure 15. θr variations. Cumulative Water Flux after 100 days.

Initial Moisture Content considerations

The initial moisture content was a parameter influencing the water flux. For 25% changes in the initial moisture content, the change in water flux was 15.6% (Table 18, Figure 16). As discussed in the results for Precipitation Case A, the effect of the initial moisture content expires for long-term simulations

Table 18. Effect of 25% variations of θi on Water Flux

	Variable Change	θ_i	ΔF, %
T =100 days	- 25%	0.285	15.60
	+ 25%	0.475	15.60

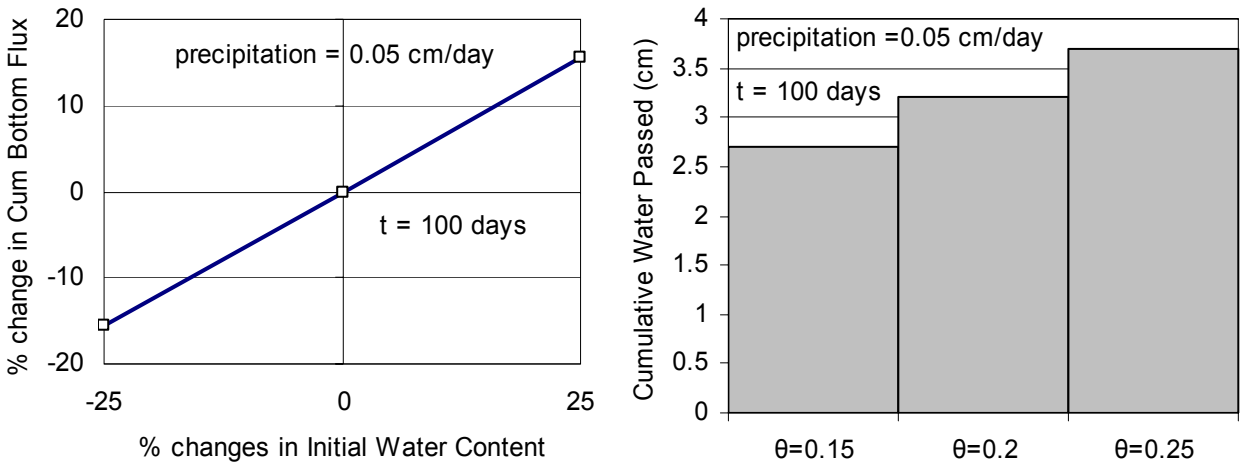

A. B.

Figure 16. θi variations. A) Change in Flux and B) Cumulative Water Flux after 100 days.

Plant growth consideration

As seen in Precipitation Case A, the plants reduced the water flux through the cover by 100% (Table 19), or to negligible amounts (Figure 17).

Table 19. Effect of Plants on Water Flux.

	Root Depth, cm	PET[3], cm/day	ΔF, %
T = 100 days	5[1]	0.5[1]	100.00
	10[2]	3[2]	100.00

(1) Grass growth (2) Tree growth (3) Potential Evapotranspiration Rate

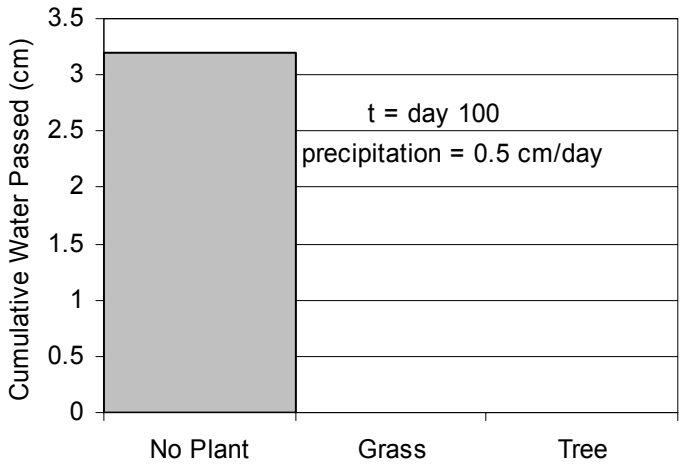

Figure 17. Plant variations. Cumulative Water Flux after 100 days.

Conclusions

The sensitivity analysis revealed that the significant water retention parameters were the saturated water content and the initial water content. However, the effect of the initial water content is limited, and would be less significant with simulation time as the soil water reaches equilibrium. The saturated hydraulic conductivity was also a sensitive parameter in water balance calculations; however, small depths of soil did not reveal much variation of water flux. The change in water flux rate through the clay was sharp as saturated conditions were approached.

The plant root growth and root water uptake processes were significant influences on the water flux. Since evaporation and runoff processes were not considered in these analyses, root water uptake was the only alternative path for the water in the soil. Both the grass and the tree were able to essentially eliminate flux through the soil layer.

CHAPTER IV

BURRELL SITE CASE STUDY

Introduction

The DOE site at Burrell, Pennsylvania, has a 4-acre uranium mill tailings (UMT) landfill containing 86,000 tons of contaminated material. The site was closed in 1987, and unintended vegetation was found within three years of closure. Waugh and Smith (Waugh and Smith 1997) performed a study of the effects of root intrusion at the site, and concluded that plant growth on a soil cover can increase the saturated hydraulic conductivity Ks of a compacted soil layer (CSL) by two orders of magnitude. The recommended solution for unintended vegetation is to eliminate the plants by using herbicide (Waugh and Smith 1997); however, even if existing vegetation is eliminated, the detrimental effects on the landfill cover will remain.

Objectives

This intent of this study was to evaluate the effects of plant growth on water transport through the cover. This study will compare the water movement through a landfill cover (i) as designed with no vegetation growth, (ii) after establishment of vegetation, and (iii) after vegetation has been eliminated.

Simulation Considerations

HYDRUS-1D was used as the modeling tool for simulating water transport through the Burrell UMT landfill cover. Three scenarios were considered; two considering only water transport processes, but with different soil hydraulic properties, and one with root growth and root water uptake. The Burrell UMT site, while in a humid location, will be simulated in a humid environment and in an arid environment.

Cover design and material properties

The landfill cap design at Burrell is shown in Figure 18. The uppermost layer is a 30-cm riprap layer, the middle layer is a 30-cm drainage layer, and the compacted soil layer above the

residual radioactive material is 90-cm thick. The landfill cover design at Burrell was simulated using three soil layers in HYDRUS-1D. The riprap layer was represented by a coarse sand layer, the drainage layer was represented by the sand soil, and the compacted soil layer used the soil hydraulic properties from the Burrell study measurements. Table 20 lists the soil water retention parameters used for each layer.

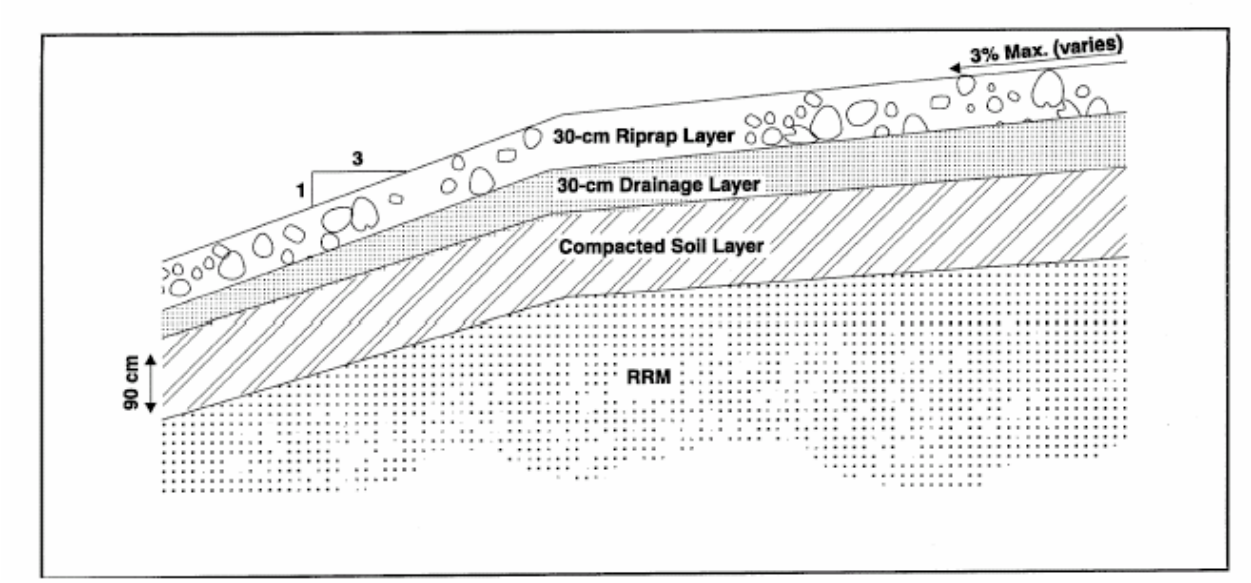

Figure 18. Burrell Cover (Waugh and Smith 1997).

Table 20. Burrell Study Compacted Soil Layer Properties (Šimunek et al. 1998; Waugh and Smith 1997).

Site name	Θs (-)	Θr (-)	n (-)	α (cm-1)	Ks, cm/day (cm/sec)
Riprap	0.43	0.045	2.68	0.145	1400 ($1.6x10^{-2}$)
Drainage	0.43	0.045	2.68	0.145	700 ($8x10^{-3}$)
CSL Design	0.364	0.10	1.524	0.0001	0.00864 ($1x10^{-7}$)
Degraded	0.364	0.10	1.524	0.0001	2.592 ($3x10^{-5}$)

Scenarios evaluated

Three scenarios were evaluated: Scenario 1 assumed that the cover performed as designed over the entire period of the evaluation. Scenarios 2 and 3 assumed that the cover had tree growth with a root depth of 90 cm, which resulted in an increase of the saturated hydraulic conductivity of the compacted soil layer to $3x10^{-5}$ cm/sec, as found in the Burrell study (Waugh and Smith 1997). Scenario 2 considered that the tree had been eliminated, and Scenario 3 considered that the tree had been allowed to remain.

Two precipitation conditions were considered to capture the impact of extreme precipitation events: (A) a constant precipitation rate of 0.5 cm/day to represent the generic case of a humid climate region, (B) a constant precipitation rate of 0.05 cm/day to represent the generic case of an arid climate region.

Model set up

The van Genuchten-Mualem soil hydraulic model with the air-entry value of -2 cm option (See Equations [6], [7] in Chapter 3) was selected within HYDRUS-1D. For the simulations involving root water uptake, the Feddes equation was selected (See Equations [10] in Chapter 3). The deciduous fruit tree was selected as a generic tree representation, and the parameters for this tree, contained in the HYDRUS-1D catalogue, are given in APPENDIX C.

The upper boundary condition for Precipitation cases A and B was a constant flux. The lower boundary condition applied to the scenario was the seepage face, which is the recommended lysimeter representation (Šimunek et al. 1998). The initial water content in the compacted soil layer was selected to be uniform at 20 %, which was consistent with the results of the Burrell study (Waugh and Smith 1997).

The period of evaluation was specified as 100 years, or 36500 days.

The simulations in this study were conservative, as runoff and evaporation processes were not considered. The amount of water infiltrating the top of the landfill cover was assumed equal to the precipitation values. Additionally, the graded slope of the cover designs were not considered in the simulations.

The remaining details of the simulations' input parameters in HYDRUS-1D are included in APPENDIX C.

Results and Discussion

The results of the simulations are presented as the water content in the landfill covers, the flux through the bottom of the landfill cover, and cumulative water passed after 100 years.

The water content profiles, at 1 month, 1 year and 100 years, compare each of the three scenarios.

The flux through the bottom of the landfill cover is presented as a function of time. The flux is presented as a negative value, as the geometry of the cover is positive upward and negative with cover depth. The cumulative water passed through the bottom of the cover is compared for each cover in each scenario.

The liquid to solid (LS) ratio is an indication of the amount of water that is expected to contact the waste material over the estimated time period. The L/S ratio here was calculated using Equation [14].

$$LS\left[\frac{\mathrm{V}}{\mathrm{M}}\right] = \frac{\text{amount infiltrated at time t } [\mathrm{L}]}{\rho_{fill}\left[\frac{\mathrm{M}}{\mathrm{V}}\right]\cdot \mathrm{H}_{fill}[\mathrm{L}]} \qquad [14]$$

The value used for the density of the waste ρ was 1.46 g/cm^3, and the depth of the waste H was 180 cm, as specified for the Burrell site UMT landfill (Waugh 1997).

Precipitation Case A.

Figure 19 shows a comparison of the soil moisture content in the landfill cover for the three scenarios. After one month (Figure 19 A) the degraded compacted clay layer in Scenario 2 was already saturated (θs = 0.364). Within the first year, both Scenarios 1 and 2 showed a saturated compacted clay layer, and the upper layers (θs = 0.43) of Scenario 1 were also saturated (Figure 19 B). No significant change was exhibited in the soil water content from one to one hundred years (Figure 19 B,C). Scenario 3, with root water uptake considerations, reduced the water content by about 10 % in the soil at 100 years. No definite change is seen at the root depth level for Scenario 3, so it is assumed that the water uptake occurs in the upper layer(s), preventing water transport to the lower layer(s).

The degraded landfill cover in Scenario 2 reached an equilibrium flux rate (0.5 cm/day) through the cover before day 10, and in Scenario 1 by day 100 (Figure 20 A). The flux through the cover of Scenario 3 was negligible for the 100 year simulation (Figure 20 A, B). After 100

years, the amount of water transported through the cover was essentially the same for Scenarios 1 and 2, and approximately equal to the amount of precipitation that had infiltrated the top of the cover (Figure 20 B), greater than $1x10^4$ cm.

The LS ratio shown in Figure 21 was reduced by more than 6 orders of magnitude when a tree is available for water uptake. At after 100 years, the LS was on the order of 100 L/kg for Scenarios 1 and 2, and was negligible for Scenario 3. LS ratio values of less than 2 L/kg have been observed after 10 years, and it is thought that it may take 1000 years for a reduced-infiltration landfill to reach a LS ratio of 1 L/kg (Hjelmar et al. 2001; Johnson et al. 1998).

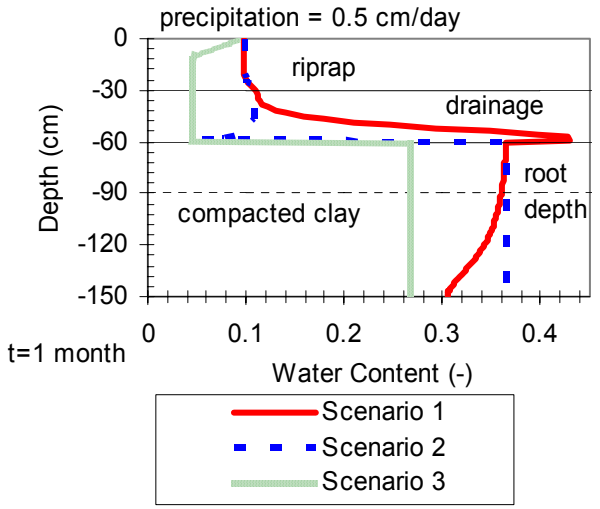

A.

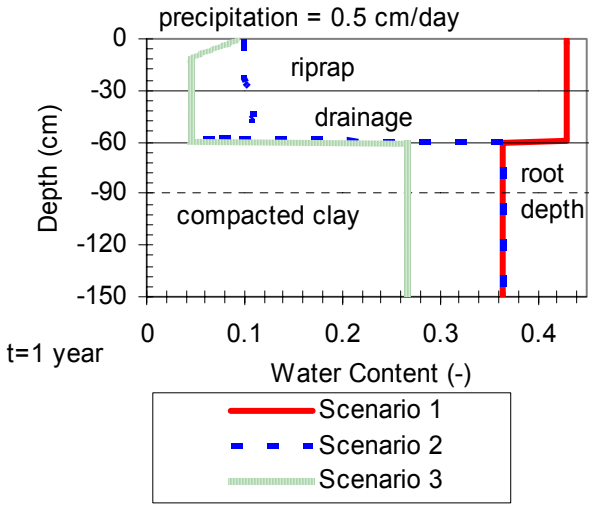

B.

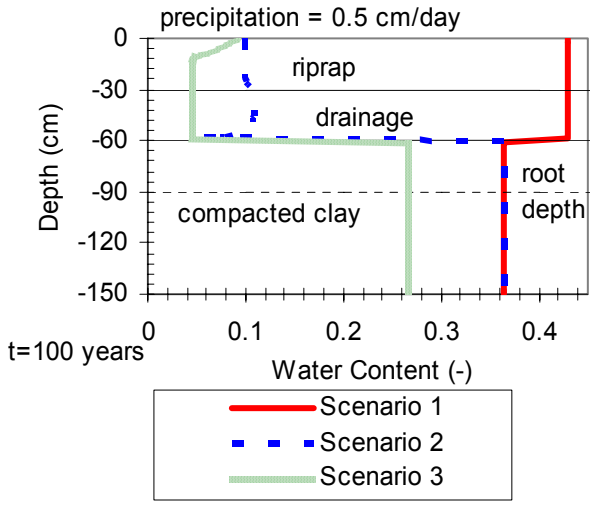

C.

Figure 19. Soil water content for the three Scenarios at A) 1 month, B) 1 year, and C) 100 years.

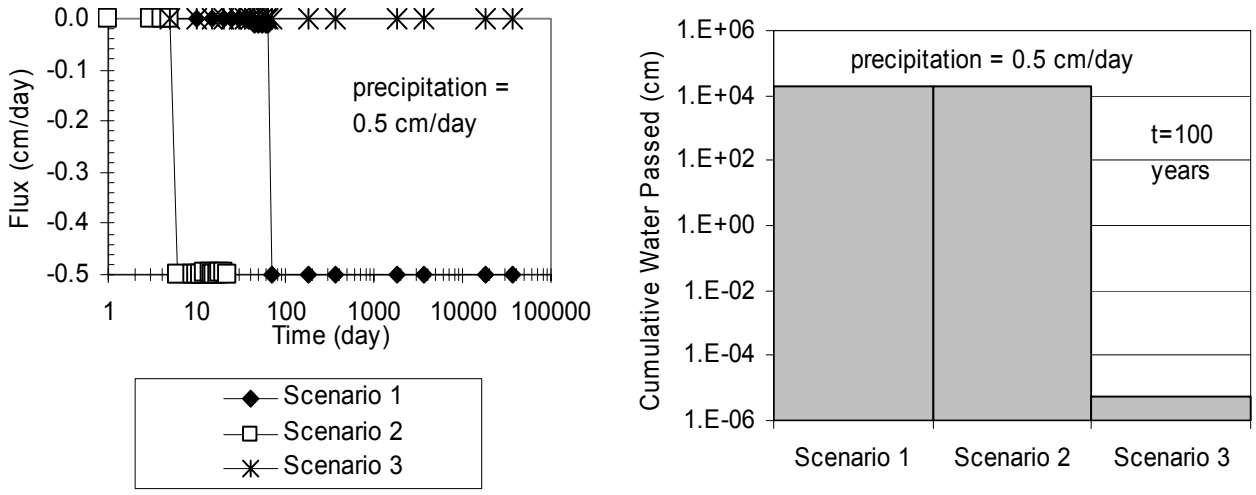

A. B.

Figure 20. The Flux of Water through the bottom of the soil profile A) as a function of time and B) after 100 years.

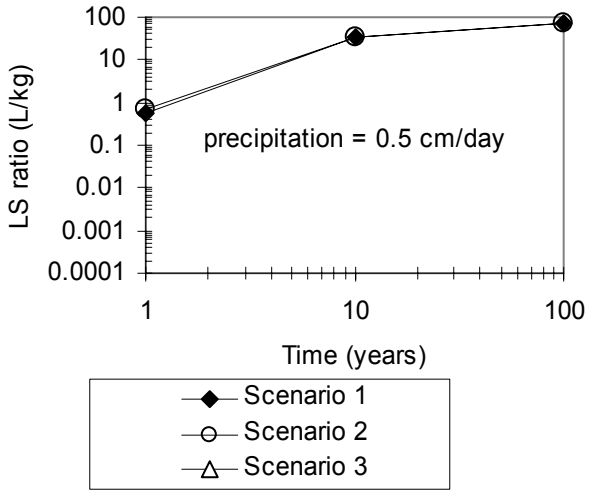

Figure 21. LS ratio as a function of time for the three Scenarios.

Precipitation Case B.

The soil moisture content profiles (Figure 22) for Precipitation Case B (0.05 cm/day) are given for times 1 month, 1 year, and 100 years. After one month (Figure 22 A), none of the three scenarios exhibited saturated conditions (clay $\theta s = 0.364$, upper layers $\theta s = 0.43$), as compared with Precipitation Case A (0.5 cm/day), where the degraded clay layer in Scenario 2 was already saturated (Figure 19 A). By the first year, however, the clay layer in both Scenarios 1 and 2 are saturated, although the upper layers of Scenario 1 are not yet saturated (Figure 22 B). After 100 years, the soil moisture content profile for Precipitation Case B looks identical to Precipitation Case A at 1 or 100 years (Figure 19 B, C, Figure 22 C).

Figure 23 A shows the flux rate through the bottom of the soil covers. The degraded Scenario 2 quickly reaches equilibrium with the influx rate (0.05 cm/day), while the flux rate for Scenario 1 takes about three years to reach equilibrium. The flux through the cover of Scenario 3 is negligible for the 100 year simulation (Figure 23A, B). After 100 years, the amount of water transported through the cover is on the order of 1000 cm for Scenarios 1 and 2 (Figure 23 B).

The LS ratio shown in Figure 24 is reduced by more than 6 orders of magnitude when a tree is available for water uptake. At after 100 years, the LS was on the order of 10 L/kg for Scenarios 1 and 2, and was negligible for Scenario 3.

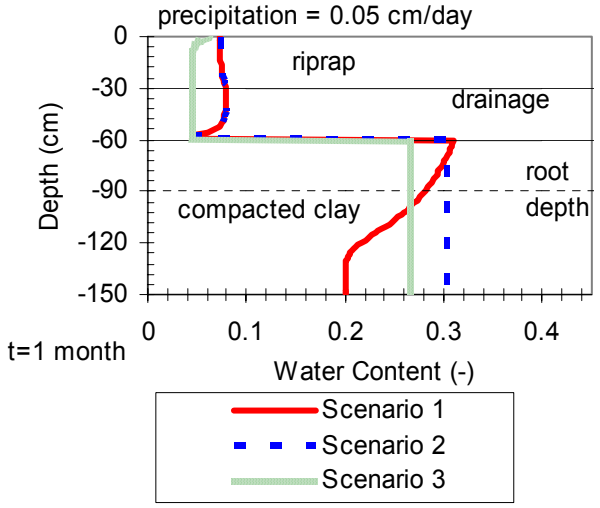

A.

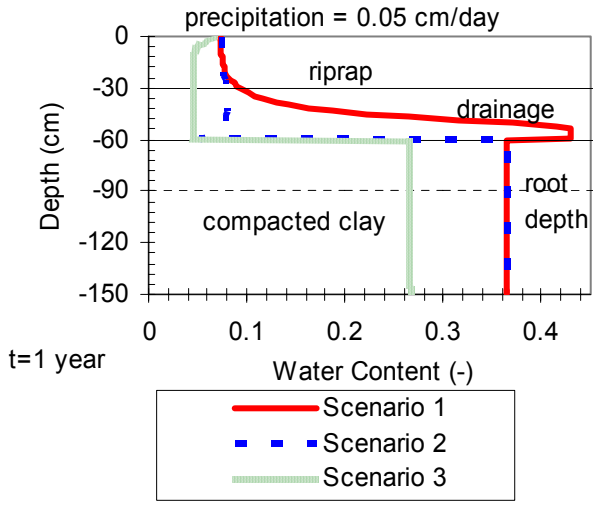

B.

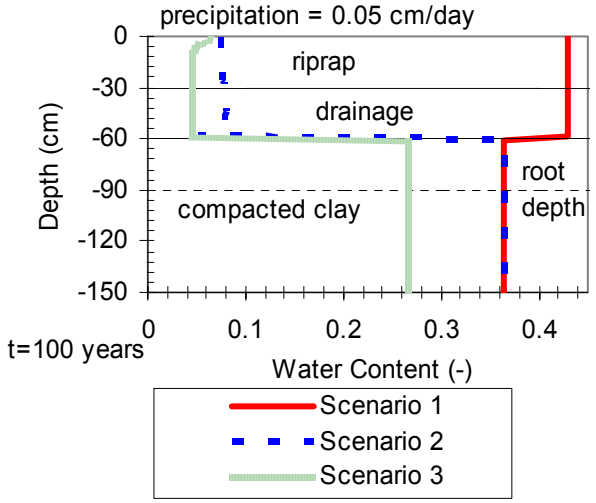

C.

Figure 22. The soil water content for the three Scenarios at A) 1 month, B) 1 year, and C) 100 years.

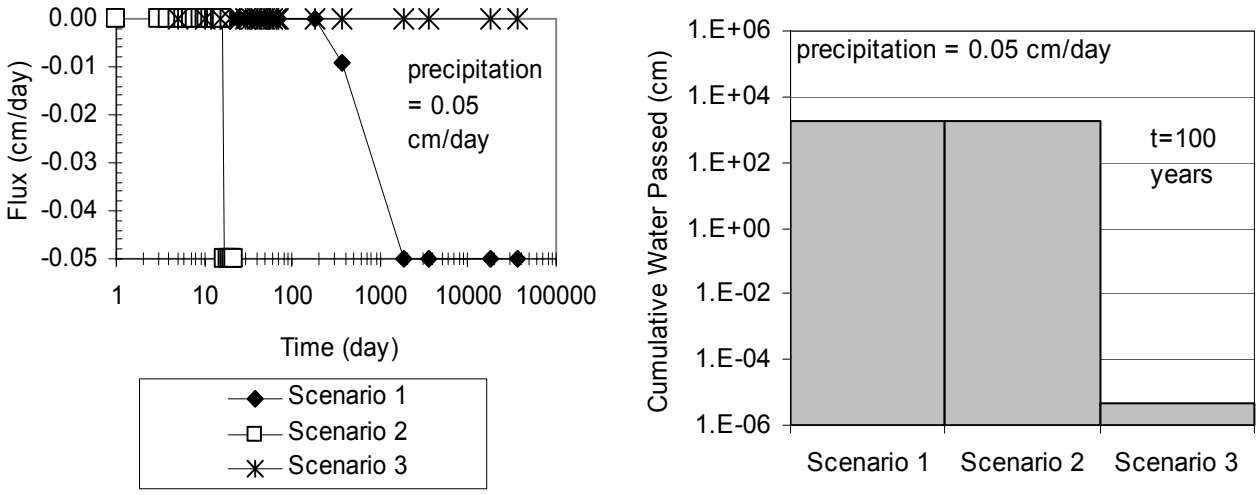

A. B.

Figure 23. The amount of water moving through the bottom of the soil profile A) as a function of time and B) after 100 years.

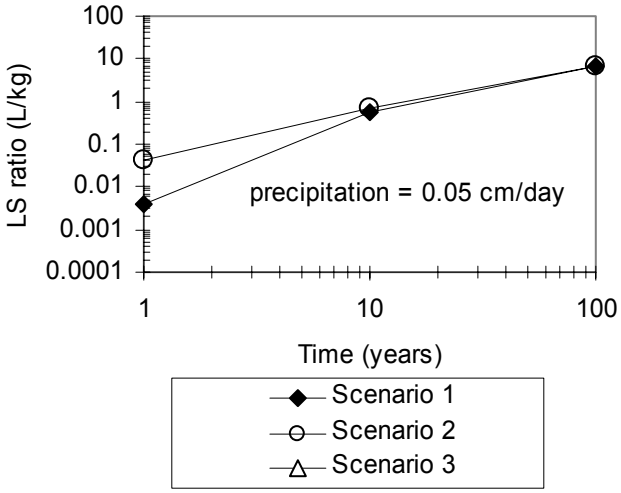

Figure 24. The Liquid to Solid (L/S) ratio as a function of time for the three Scenarios.

Conclusions

In the Burrell Site Study by Waugh and Smith (Waugh and Smith 1997), the landfill covers with plant intrusion exhibited an increased hydraulic conductivity. As predicted by HYDRUS-1D, the increased hydraulic conductivity allows more water to infiltrate through the landfill cover in the short term, especially before saturation. However, after 100 years, the amount of water flux is the same independent of hydraulic conductivity.

Once plant growth is established on the landfill cover, the plant's roots will take up excess water and prevent it from infiltrating the waste layer. It is even likely that the presence of plants will reduce the water content in the soil and the amount of water infiltrating the waste layer more than a landfill cover without plant growth design considerations.

CHAPTER V

WATER BALANCE ASSESSMENT FOR DIFFERENT LANDFILL COVERS

Introduction

Comparison studies of landfill covers performance are increasing as new problems and more regulations develop (Albright et al. 2002; Dwyer et al. 2000a). These comparison studies may evaluate the water infiltrating different landfill cover designs by comparing existing, regulated designs with alternative cover designs. Plant intrusion is a prime concern of closed disposal sites, and unintended vegetation growth has been documented at sites. A comparison of effect of root intrusion on the water balance for different landfill cover systems is still an area requiring study.

Objectives

The goal of the study presented in this chapter was to compare the performance of different landfill cover designs in the event of cover deterioration due to plant root intrusion. The specific objective was to compare the water balance of different cover designs when the cover is affected by tree intrusion and when the cover has been compromised by tree intrusion and the trees have been eliminated. The landfill cover performance was evaluated for both humid and arid sites.

Simulation Considerations

HYDRUS-1D was again used as a modeling tool for the water transport through the covers. Three different landfill cover designs were simulated using four different precipitation patterns. Three scenarios were considered; two considering water transport processes, and a third considering water transport, root growth, and root water uptake processes. Additionally, HYDRUS-1D will be used to predict water flux for covers in the Alternative Landfill Cover Demonstration (Dwyer et al. 2000a).

Landfill cover description

Three types of covers were selected for comparison: (i) the RCRA Subtitle D cover, (ii) the RCRA Subtitle C cover, and (iii) an evapotranspiration (ET) soil cover. The principle of the evapotranspiration cover is to allow vegetation growth to reduce soil water content, which contrasts with the RCRA's compacted clay as barrier layers. Details of these covers are given in the section on Landfill Cover Designs in Chapter 2, and a summary of the characteristics is given in Table 21.

The RCRA C landfill cover design (Figure 25 B) calls for a 60-cm native soil vegetation layer and a 30-cm drainage layer above the compacted clay layer (U.S. Environmental Protection Agency 1983b). The 60-cm compacted clay layer has a maximum hydraulic conductivity of $1x10^{-7}$ cm/sec, and is prescribed to be in contact with a low permeable geomembrane. As a conservative approach, the geomembrane was not included in these simulations. Silt loam, which is found in both Tennessee and Idaho, was selected to be the native vegetation soil in the simulation. The soil hydraulic parameters are listed in Table 22.

The RCRA D landfill cover (Figure 25 A) has a 15-cm upper layer of topsoil on top of a 45-cm compacted clay layer (U.S. Environmental Protection Agency 1983a). The compacted clay has a specified maximum hydraulic conductivity of $1x10^{-5}$ cm/sec. The RCRA D landfill cover was simulated with a 15-cm silt loam soil layer as the topsoil. The soil properties used for these layers are listed in Table 22.

The Evapotranspiration (ET) Landfill Cover (Figure 25 C) is not a prescriptive regulatory design and has no specifications to follow. The ET cover simulated was a 90-cm layer of a single soil, silt loam. The soil hydraulic properties for silt loam are in Table 22.

Table 21. Characteristics of the landfill covers evaluated

Cover type	Thickness (cm)	Number of layers	Description
RCRA Subtitle D	60	2	Top vegetation/soil layer – 15cm Compacted native soil – 45 cm
RCRA Subtitle C	150	3	Top vegetation/soil layer – 60 cm Sand drainage layer – 30 cm Compacted bentonite-amended soil – 60 cm
ET cover	90	1	Native soil layer – 90 cm

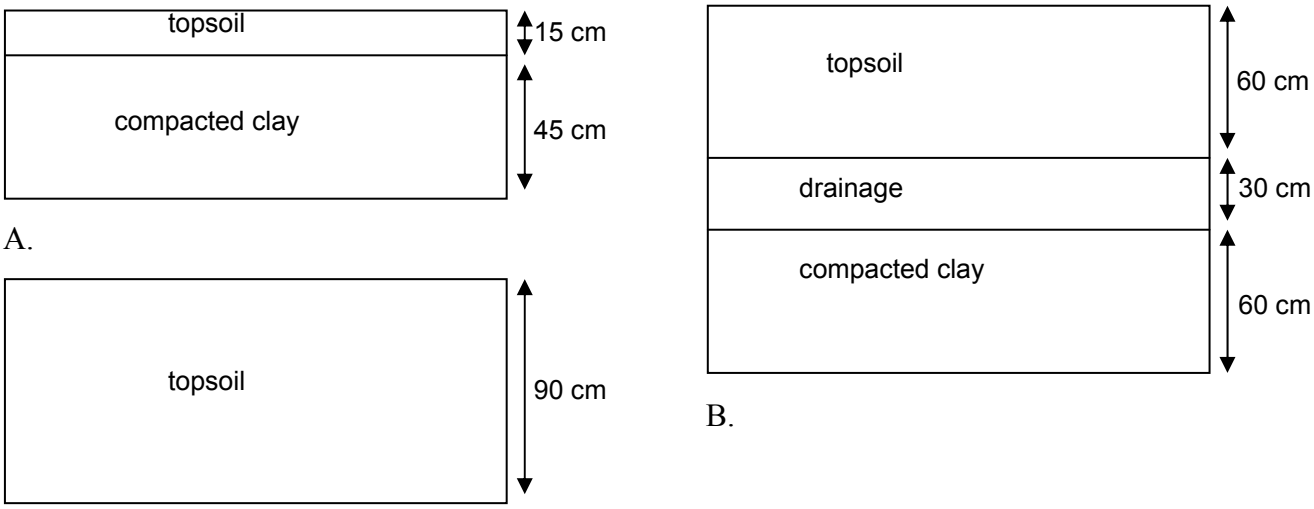

Figure 25. Schematic of the landfill covers evaluated. A) RCRA subtitle D, B) RCRA subtitle C, and C) the ET cover.

Table 22. Water Retention Parameters and Soil Summary.

Cover	Layer	Material	Θs (-)	Θr (-)	n (-)	α (cm-1)	Ks, cm/day (cm/sec)
RCRA D	Topsoil	Silt Loam[a]	0.45	0.067	1.41	0.02	10.8 ($1.25x10^{-4}$)
	Compacted Clay	Clay[b]	0.364	0.10	1.5240	0.0001	0.864 ($1x10^{-5}$)
RCRA C	Topsoil	Silt Loam[a]	0.45	0.067	1.41	0.02	10.8 ($1.25x10^{-4}$)
	Drainage	Sand[c]	0.43	0.045	2.68	0.145	712.8 ($8.25x10^{-3}$)
	Compacted Clay	Clay[b]	0.364	0.10	1.5240	0.0001	0.00864 ($1x10^{-7}$)
ET	Topsoil	Silt Loam[a]	0.45	0.067	1.41	0.02	10.8 ($1.25x10^{-4}$)

Sources: a) HYDRUS-1D catalogue, b) Waugh and Smith 1997, c) HYDRUS-1D catalogue.

Scenarios evaluated

For the RCRA C and RCRA D covers, three scenarios were evaluated. Scenario 1 assumed that the cover performed as designed over the entire period of the evaluation. Scenarios 2 and 3 assumed that the cover had tree with a root depth equal to the cover depth, which increased the saturated hydraulic conductivity of the compacted soil layer to 2.59 cm/day ($3x10^{-5}$ cm/sec), as seen in the site study in Burrell, PA (Waugh and Smith 1997). Scenario 2 considered that the tree had been eliminated, and Scenario 3 considered that the tree had been allowed to remain. The ET cover, which includes vegetation growth as part of the design, was simulated only with a tree consideration, and is included as both Scenarios 1 and 3 for comparison purposes. The period of evaluation was specified as 100 years.

Four precipitation conditions (2 generic cases and 2 actual daily precipitation data) were considered to capture the impact of extreme precipitation events: (A) a constant precipitation rate of 0.5 cm/day to represent the generic case of an humid climate region, (B) a constant precipitation rate of 0.05 cm/day to represent the generic case of an arid climate region, (C) actual daily precipitation data from Anderson County, Tennessee, where the Oak Ridge National Laboratory (ORNL) is located, and (D) actual precipitation data from Bonneville County, Idaho, where the Idaho National Engineering Laboratory (INEEL) is located. The labs at ORNL and INEL both contain buried waste landfills, and the two locations are representative of extreme climate regions. The actual precipitation data were daily values from August 2000 to July 2004 (NCDC 2005). This four-year string of data values was looped over 100 years. The daily precipitation data used for the simulations are presented in Figure 26 and in APPENDIX J.

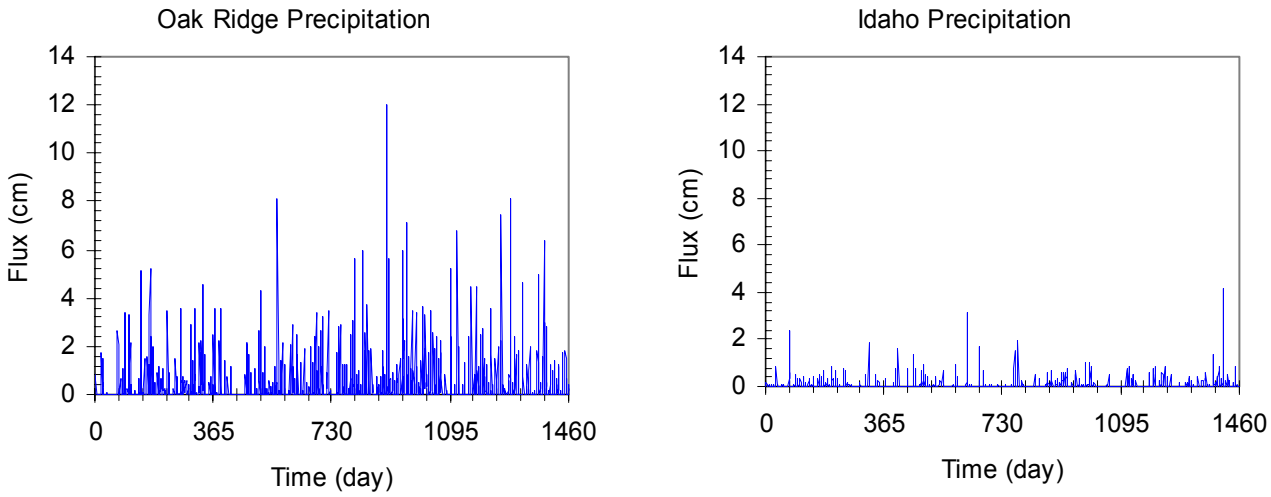

A. B.

Figure 26. Daily Precipitation Data for August 2000 to July 2004 for A) Oak Ridge and B) Idaho. (NCDC 2005)

Model setup

The van Genuchten-Mualem soil hydraulic model with the air-entry value of -2 cm option (See Equations [6], [7] in Chapter 3) was selected within HYDRUS-1D. For the simulations involving root water uptake, the Feddes equation was selected (See Equation [10] in Chapter 3). The deciduous fruit tree was selected as a generic tree representation, and the parameters for this tree, contained in the HYDRUS-1D catalogue, are given in APPENDIX J.

The upper boundary condition for Precipitation cases A and B was a constant flux. For Precipitation cases C and D, the upper boundary condition was selected as variable flux, using the daily precipitation values included in APPENDIX J. The lower boundary condition in all simulations was seepage face, the recommended condition for lysimeter representation (Šimunek et al. 1998).

The simulations in this study were conservative, as runoff and evaporation processes were not considered. The amount of water infiltrating the top of the landfill cover was assumed equal to the precipitation values.

The remaining details of the simulations' input parameters in HYDRUS-1D are included in APPENDIX J.

Simulation Results

The results of the simulations are presented as the water content in the landfill covers, the flux through the bottom of the landfill cover, and cumulative water passed after 100 years.

The water content profiles are given for each scenario at 1 year and at 100 years. For comparison purposes, the depth of each landfill was made to be dimensionless.

The flux through the bottom of the landfill cover is presented as a function of time. The flux is presented as a negative value, as the geometry of the cover is positive upward and negative with cover depth. The cumulative water passed through the bottom of the cover is compared for each cover in each scenario.

The liquid to solid (LS) ratio is an indication of the amount of water that is expected to contact the waste material over the estimated time period. The LS ratio here was calculated using Equation [15].

$$LS\left[\frac{\mathrm{V}}{\mathrm{M}}\right] = \frac{\text{amount infiltrated at time t}\left[\mathrm{L}\right]}{\rho_{fill}\left[\frac{\mathrm{M}}{\mathrm{V}}\right]\cdot \mathrm{H}_{fill}\left[\mathrm{L}\right]} \qquad [15]$$

where the density of the waste ρ was selected to 1.46 g/cm^3, and the depth of the waste H was chosen as 180 cm, selected from the values of a case study at the Burrell, PA UMT site (Waugh 1997).

Precipitation Case A: Constant Flux 0.5 cm/day

For Scenario 1, where the covers performed as designed, the RCRA C and RCRA D landfill covers were essentially saturated (topsoil θs= 0.45, drainage θs=0.43, clay θs=0.364) within one year, and there is no change in the soil moisture content between 1 year and 100 years (Figure 27 A, B). The Evapotranspiration cover, when performing as intended with vegetation growth, contained about 20% less water than the RCRA C and D covers (Figure 27 A, B). In the degraded Scenario 2 (which has no ET cover evaluated), the compacted clay layer is saturated by year one, but the sand drainage layer of RCRA C and the topsoil layers of the covers are unsaturated. This was attributed to the greater amount of water moving through the degraded clay layer. In Scenario 3, the impact of the tree can be seen in the reduction of soil moisture

content as compared with Scenarios 1 and 2 (Figure 27), about 4% for RCRA D and 10% for RCRA C.

The water flux through the bottom of the covers is displayed as a function of time in Figure 28 A, B, and C. The flux through the RCRA D cover reached equilibrium with the influx rate (0.5 cm/day) before the RCRA C cover did, but both were in equilibrium within 100 days (Figure 28 A). Comparing the RCRA C flux in Figure 28 A and B reveals that the degraded Scenario 2 allowed the water to infiltrate faster than in Scenario 1. The effect of the tree on the flux is evident in Figure 28 C, where there was virtually no flux through the bottom of the cover. The cumulative amount of water flux through the covers after 100 years is compiled in Figure 28 D. After 100 years, the volume of water for Scenarios 1 and 2 was not distinguishable (on the order of 10,000 cm), but Scenario 3 had significantly less water volume ($1x10^{-4}$ cm for RCRA C and 1 cm for RCRA D). The ET cover had negligible water flux over the simulation period.

The LS ratio is shown as a function of time in Figure 29. LS ratios after 10 years been observed at less than 2 L/kg , and it is thought that it may take 1000 years for a reduced-infiltration landfill to reach a LS ratio of 1 L/kg (Hjelmar et al. 2001; Johnson et al. 1998). Figure 29 A shows the LS ratio for Scenario 1; the ET cover's LS ratio was negligible and is not visible on the range. The tree in Scenario 3 reduced the LS ratio by at least six orders of magnitude (from 100 to less than $1x10^{-4}$) for the RCRA D cover, and at least four orders of magnitude (from 100 to $1x10^{-2}$) for the RCRA C landfill cover (Figure 29 B).

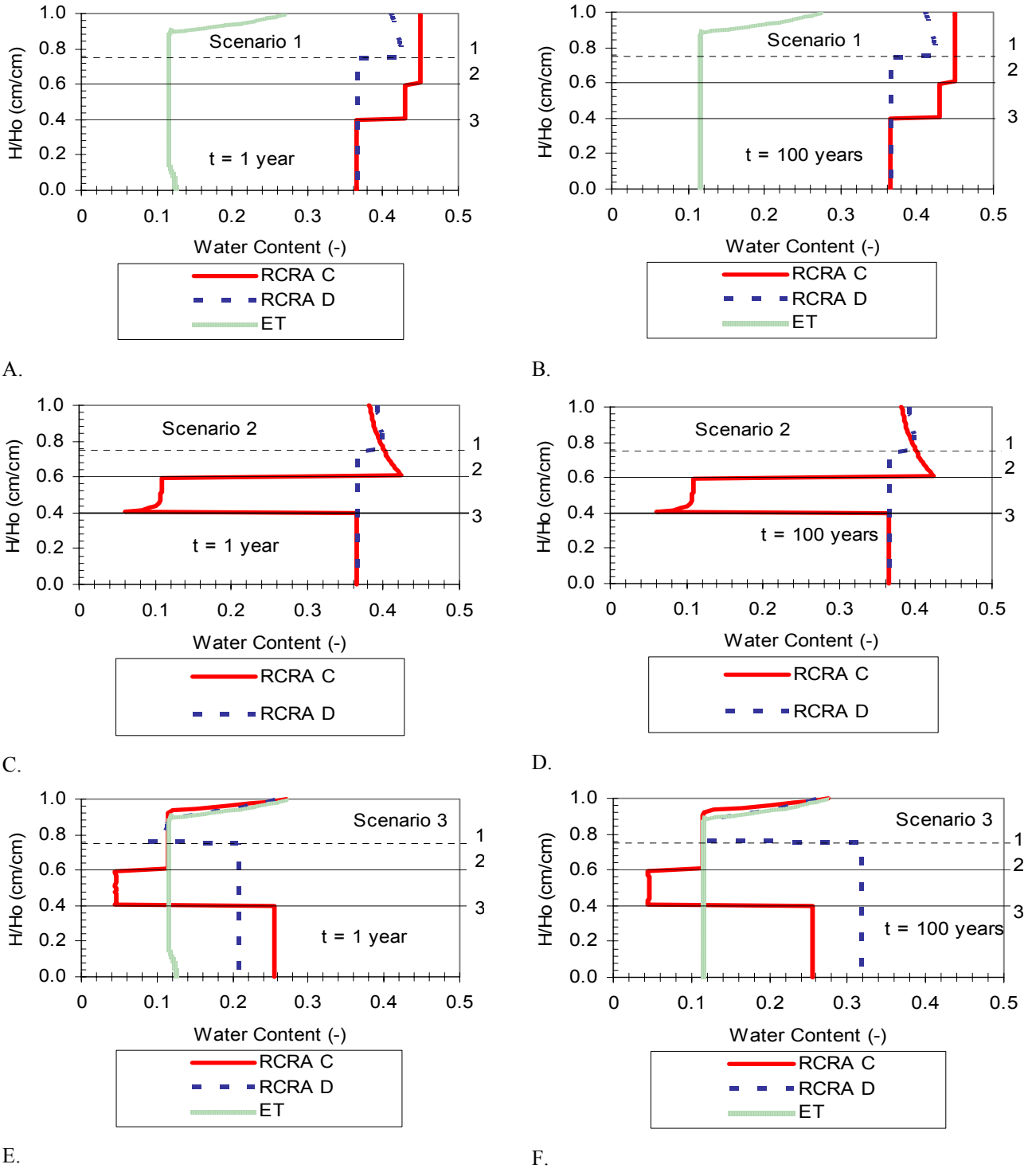

Figure 27. The Water Content as a function of cover depth (dimensionless H/H0) for Scenario 1 after A) 1 year and B) 100 years, for Scenario 2 after C) 1 year and D) 100 years, and Scenario 3 after E) 1 year and F) 100 years. The separate layers are defined by 1) the topsoil/compacted clay layer in RCRA D, 2) the topsoil/drainage layer in RCRA C, and 3) the drainage/compacted clay layer in RCRA C.

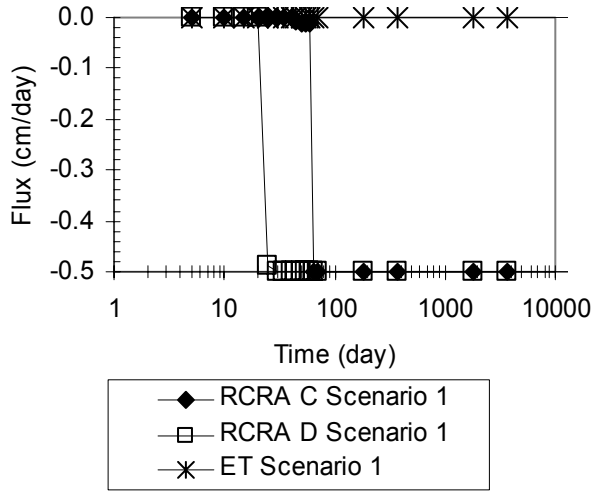

A.

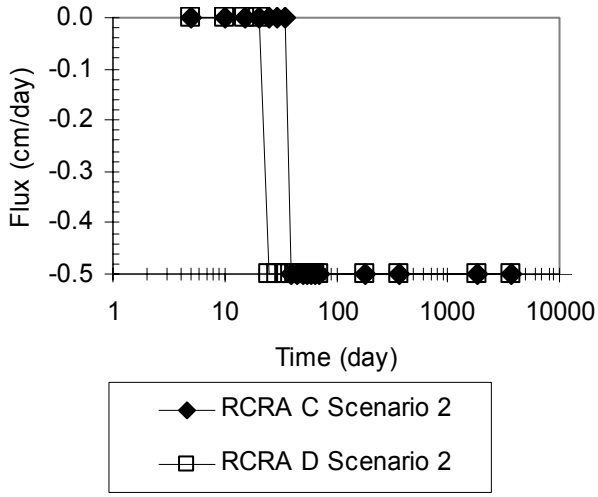

B.

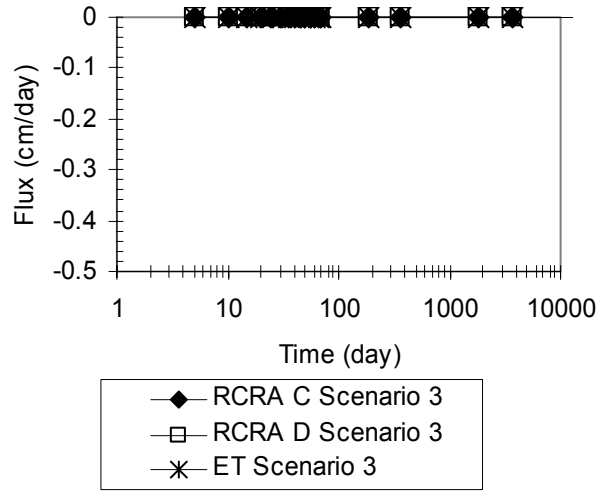

C.

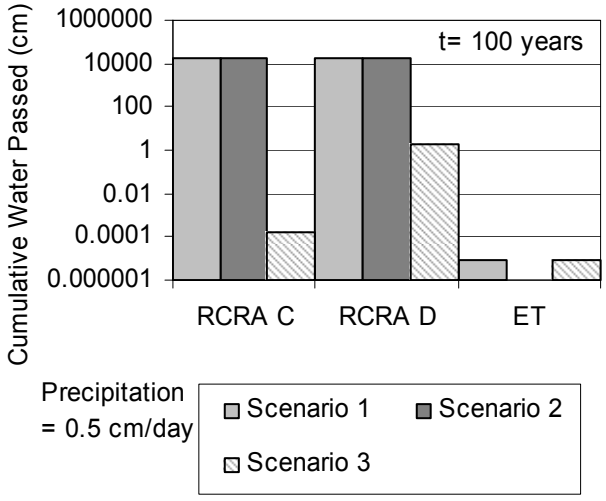

D.

Figure 28. Flux of water through the bottom of the landfill cover as a function of time for A) Scenario 1, B) Scenario 2, C) Scenario 3, and D) the cumulative water passed through the cover after 100 years.

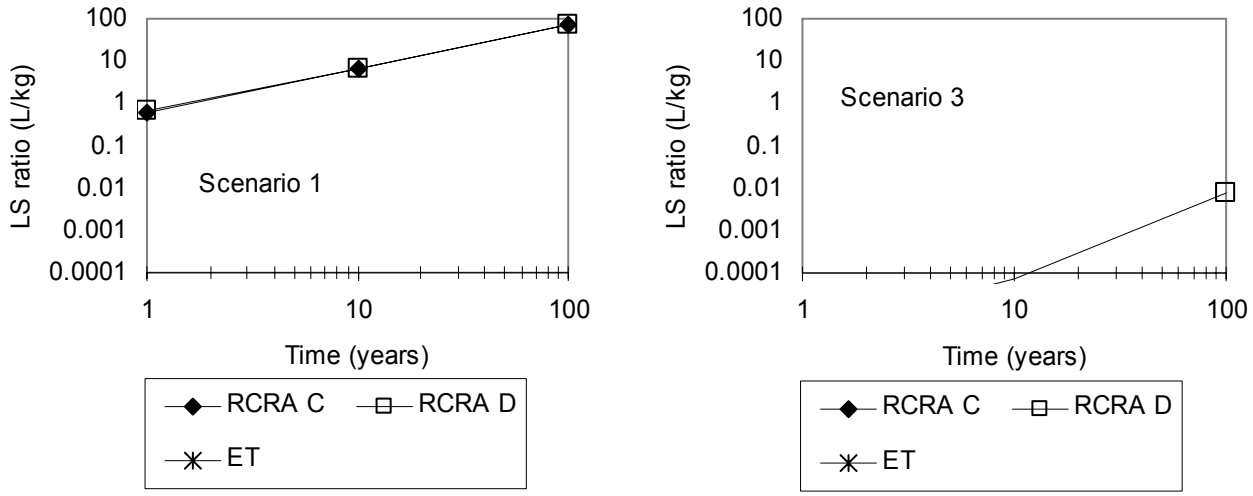

A. B.

Figure 29. The LS ratio for the covers as a function of time for A) Scenario 1 and B) Scenario 3.

Precipitation Case B: Constant Precipitation 0.05 cm/day

The soil water content profiles for the arid, constant Precipitation Case B are shown in Figure 30. The compacted clay layer was already saturated ($\theta s = 0.364$) by the first year for the RCRA C cover, although the sand drainage layer ($\theta s = 0.43$) was not; by 100 years, the entire soil profile was saturated and is similar to the profile of the greater Precipitation Case A after 100 years (Figure 30 A,B, Figure 27 B). In the degraded Scenario 2 the sand drainage layer of RCRA C was still unsaturated at year 100 (Figure 30 D), which was attributed to the greater amount of water moving through the degraded clay layer. In Scenario 3, the impact of the tree can be seen in the 4% and 10 % reduction of soil moisture content in the RCRA D and C covers as compared with Scenarios 1 and 2 (Figure 30).

The water flux through the bottom of the covers is displayed as a function of time in Figure 31 A, B, and C. The RCRA D cover preceded the RCRA C cover in reaching a flux rate equal to the influx precipitation rate (0.05 cm/day) in Scenario 1, but Scenario 2 revealed similar results for the RCRA C and RCRA D covers (Figure 31 A, B). The effect of the tree on the flux is evident in Figure 31 C, where there was virtually no flux through the bottom of the cover. The cumulative amount of water flux through the covers after 100 years is compiled in Figure 31 D.

After 100 years, the amount of water (about 1000 cm) for Scenarios 1 and 2 was not distinguishable for RCRA C and RCRA D covers (Figure 31 C, D). In Scenario 3, the amount of water was reduced to less than 1 cm for RCRA D and is negligible for RCRA C. As with Precipitation Case A, the ET cover showed essentially no water flux.

The LS ratio is shown as a function of time in Figure 32. The tree in Scenario 3 reduced the LS ratio from Scenario 1 by four orders of magnitude to less than 0.01 L/kg at 100 years for the RCRA C cover, and to negligible values for the RCRA D cover (Figure 32 B).

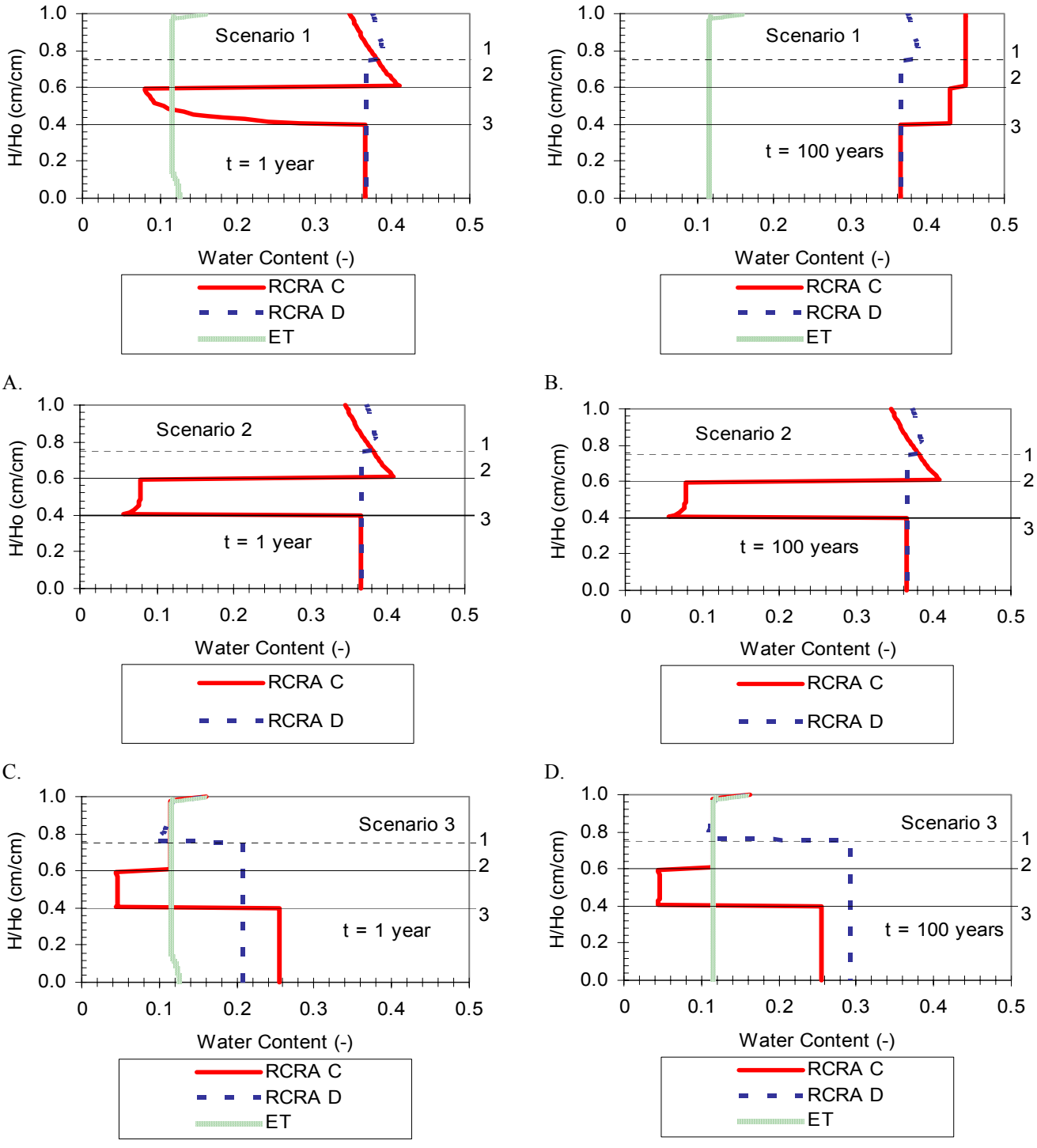

Figure 30. The Water Content as a function of cover depth (dimensionless H/H_0) for Scenario 1 after A) 1 year and B) 100 years, for Scenario 2 after C) 1 year and D) 100 years, and Scenario 3 after E) 1 year and F) 100 years. The separate layers are defined by 1) the topsoil/compacted clay layer in RCRA D, 2) the topsoil/drainage layer in RCRA C, and 3) the drainage/compacted clay layer in RCRA C.

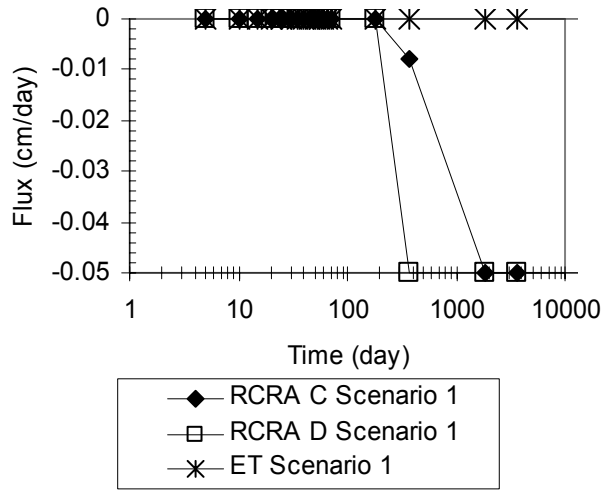

A.

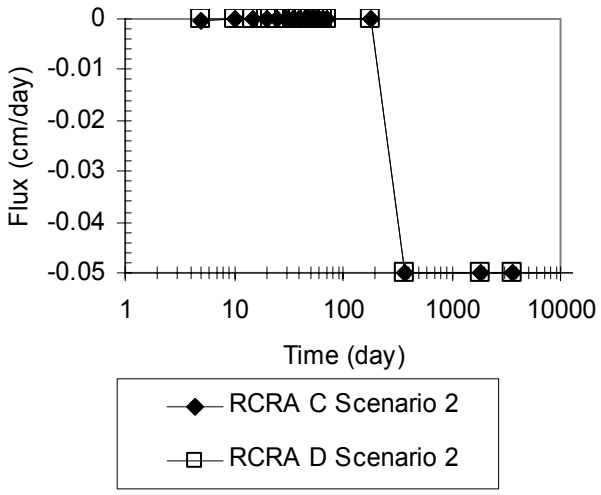

B.

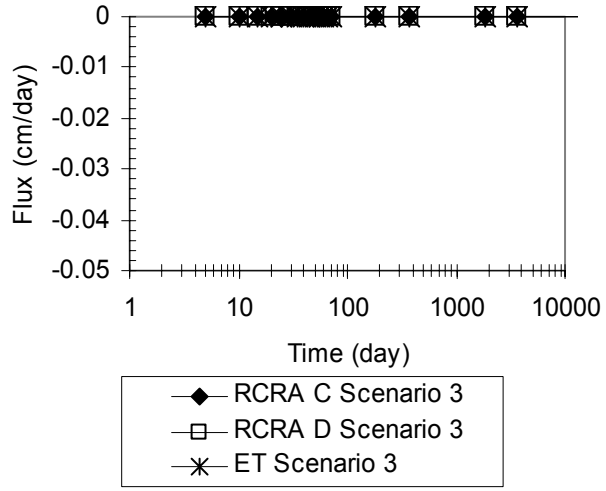

C.

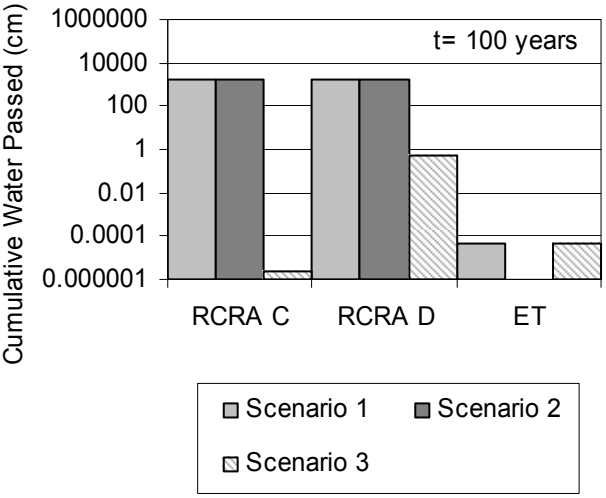

D.

Figure 31. Flux of water through the bottom of the landfill cover as a function of time for A) Scenario 1, B) Scenario 2, C) Scenario 3, and D) the cumulative water passed through the cover after 100 years.

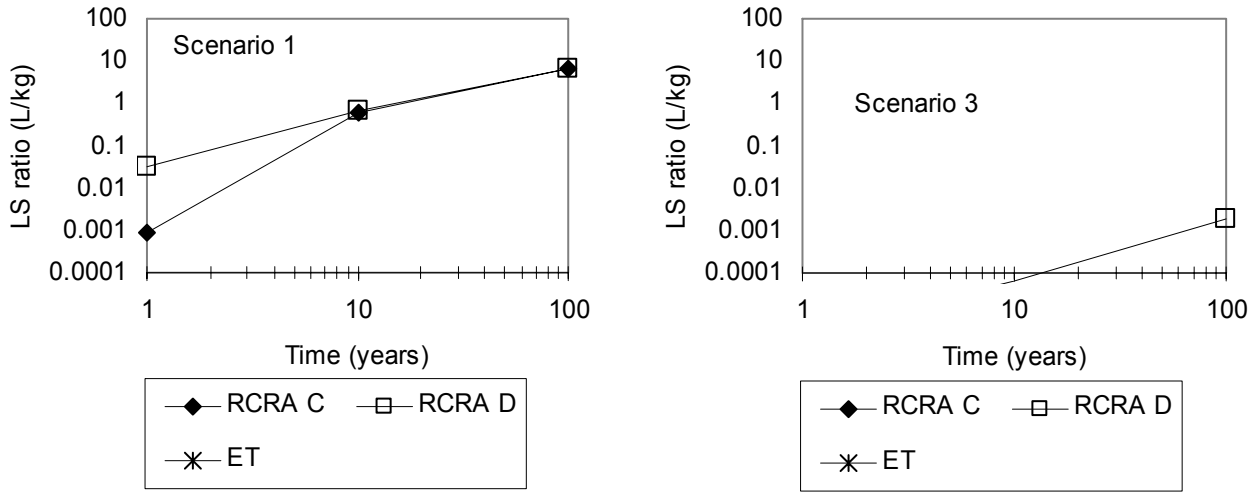

A. B.

Figure 32. The LS ratio for the covers as a function of time for A) Scenario 1 and B) Scenario 3.

Precipitation Case C: ORNL, Tennessee USA

Precipitation case C exhibits similar results for the soil moisture content as the Precipitation Case A where the constant flux was 0.5 cm/day. For Scenario 1, where the covers performed as designed, the RCRA C and RCRA D landfill covers were essentially saturated (topsoil θs= 0.45, drainage θs=0.43, clay θs=0.364) within one year, and there was no change in the soil moisture content between 1 year and 100 years (Figure 33 A, B). In the degraded Scenario 2, the compacted clay layer was saturated by year one for both RCRA covers, but the sand drainage layer of RCRA C and the topsoil layers of the covers were unsaturated. This was attributed to the greater amount of water moving through the degraded clay layer in Scenario 2. In Scenario 3, the impact of the tree can be seen in the reduction of soil moisture content as compared with Scenarios 1 and 2 (Figure 33). The moisture content in the RCRA C cover was reduced by about 10% and by about 4% in the RCRA D cover, as it was in the Precipitation Case A.

The water flux through the bottom of the covers is displayed as a function of time in Figure 34 A, B, and C, along with the varied precipitation values. The effect of the tree on the flux significant; there was virtually no flux through the bottom of the cover (Figure 34 C),

whereas in Scenario 1 the flux was very similar to the precipitation values (Figure 34 A, B) The cumulative amount of water passed through the covers after 100 years is compiled in Figure 34 D. After 100 years, the amount of water flux through the RCRA C and RCRA D covers for Scenarios 1 and 2 was about 10,000 cm. Scenario 3 showed a reduction of water of about 2 orders of magnitude (100 cm) for RCRA D and more than 6 orders of magnitude (>0.01 cm) for RCRA C. The ET cover had only negligible water flux.

The LS ratio is shown as a function of time in Figure 35. Figure 35 A is the LS ratio for Scenario 1. Figure 35 B shows that the tree reduced the LS ratio for the RCRA D cover by two orders of magnitude to approximately 1 L/kg after 100 years and to a negligible value for the RCRA C cover.

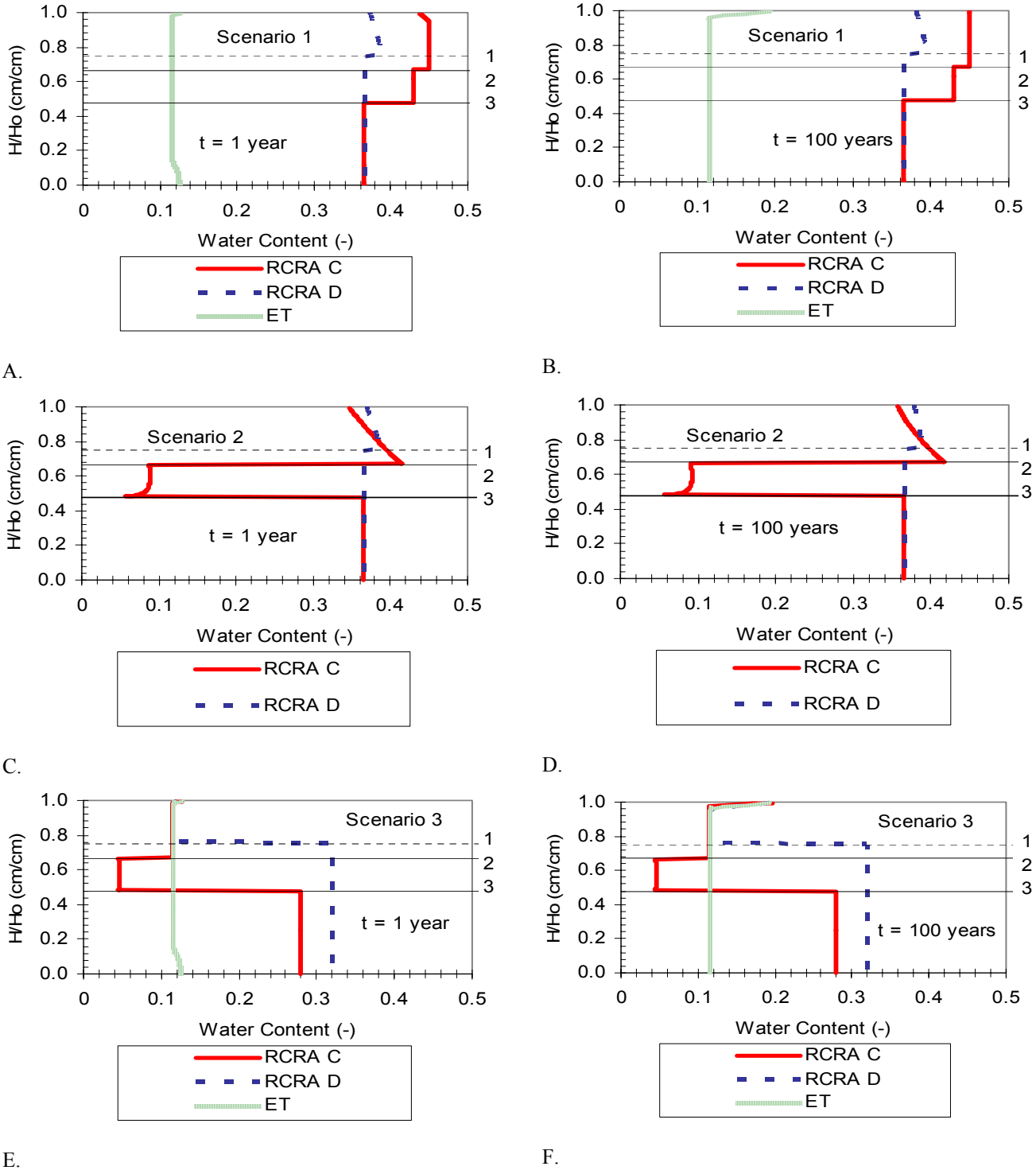

Figure 33. The Water Content as a function of cover depth (dimensionless H/H0) for Scenario 1 after A) 1 year and B) 100 years, for Scenario 2 after C) 1 year and D) 100 years, and Scenario 3 after E) 1 year and F) 100 years. The separate layers are defined by 1) the topsoil/compacted clay layer in RCRA D, 2) the topsoil/drainage layer in RCRA C, and 3) the drainage/compacted clay layer in RCRA C.

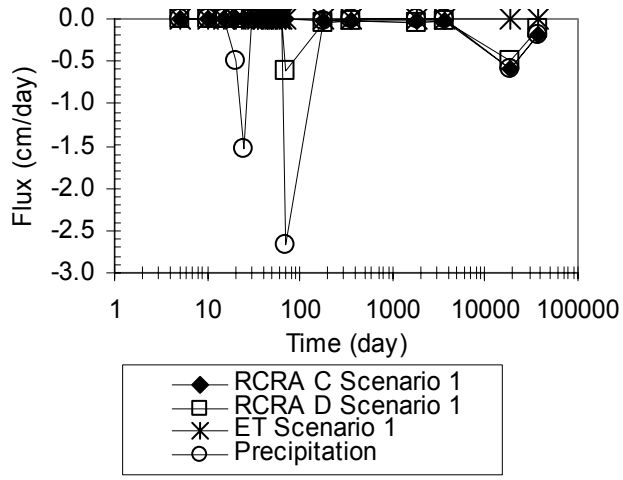

A.

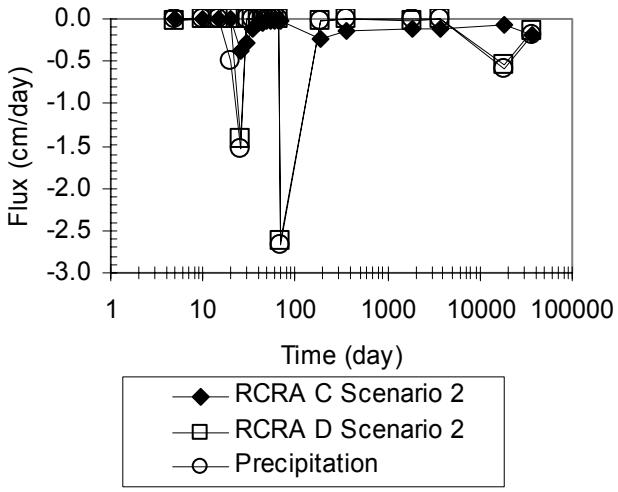

B.

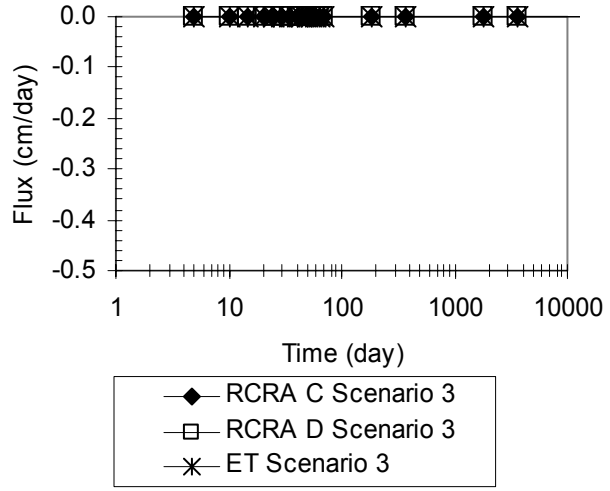

C.

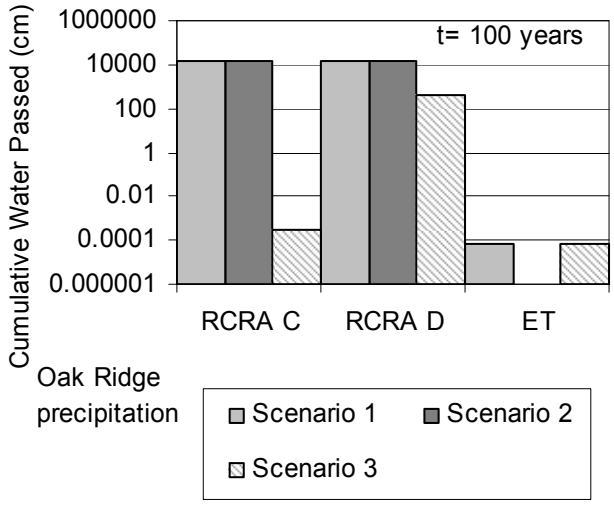

D.

Figure 34. Flux of water through the bottom of the landfill cover as a function of time for A) Scenario 1, B) Scenario 2, C) Scenario 3, and D) the cumulative water passed through the cover after 100 years.

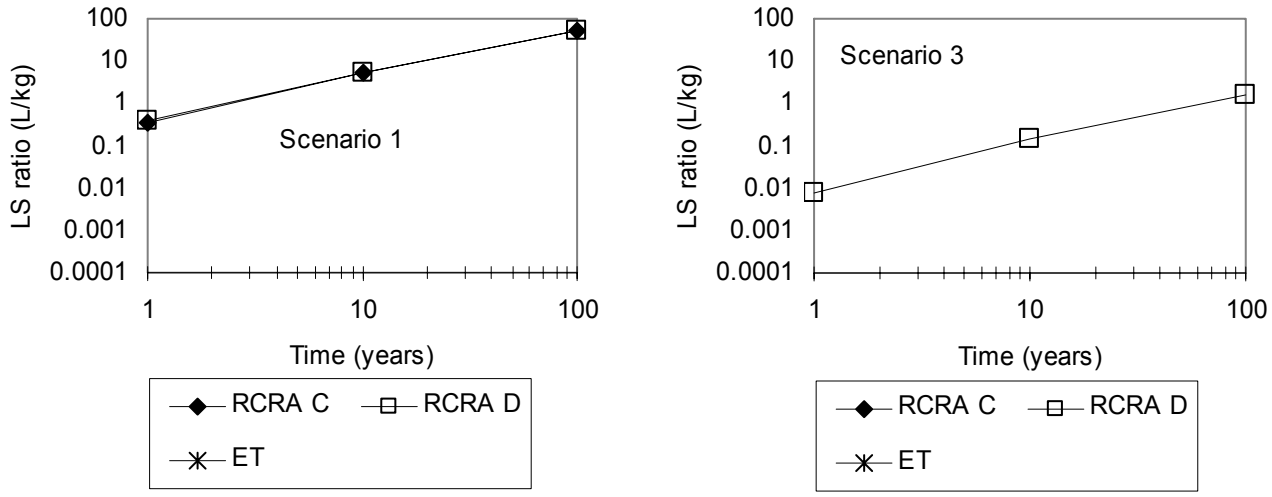

A. B.

Figure 35. The LS ratio for the covers as a function of time for A) Scenario 1 and B) Scenario 3.

Precipitation Case D: Idaho,USA

RCRA subtitle C simulations are not included in this Precipitation Case, as the software would not converge. The water content profiles for the RCRA D and ET covers (Figure 36) are similar to those in Precipitation Case B (Figure 27). For Scenario 1, the RCRA D landfill cover was essentially saturated (topsoil θs= 0.45, drainage θs=0.43, clay θs=0.364) within one year, and there was no change in the soil moisture content between 1 year and 100 years (Figure 36 A, B). The RCRA D cover also did not change for Scenario 2 from 1 to 100 years, and these results were similar to those in Precipitation Case B (Figure 27). The reduction of water content by 4% cover in Scenario 3 for the RCRA D cover was attributed to the root water uptake of the tree (Figure 36). Here, as with the other precipitation cases, the ET cover maintained less water content (0.12) in both Scenarios.

The flux of water through the bottom of the covers is displayed as a function of time in Figure 37 A, B, and C, along with the precipitation data. The pattern of precipitation and corresponding flux through the cover can be seen in Figure 37 A and B. The effect of the tree on the flux is evident in Figure 37 C, where there was virtually no flux through the bottom of the cover. The cumulative amount of water passed through the covers after 100 years is compiled in Figure 37 D. After 100 years, the amount of water for Scenarios 1 and 2 for RCRA D was about

1000 cm, but Scenario 3 had less than 10 cm after 100 years. The water through the ET cover was negligible.

The LS ratio is shown as a function of time in Figure 38. The LS ratio at 100 years is reduced from 10 L/kg to 0.01 L/kg when the tree is present on the RCRA D cover.

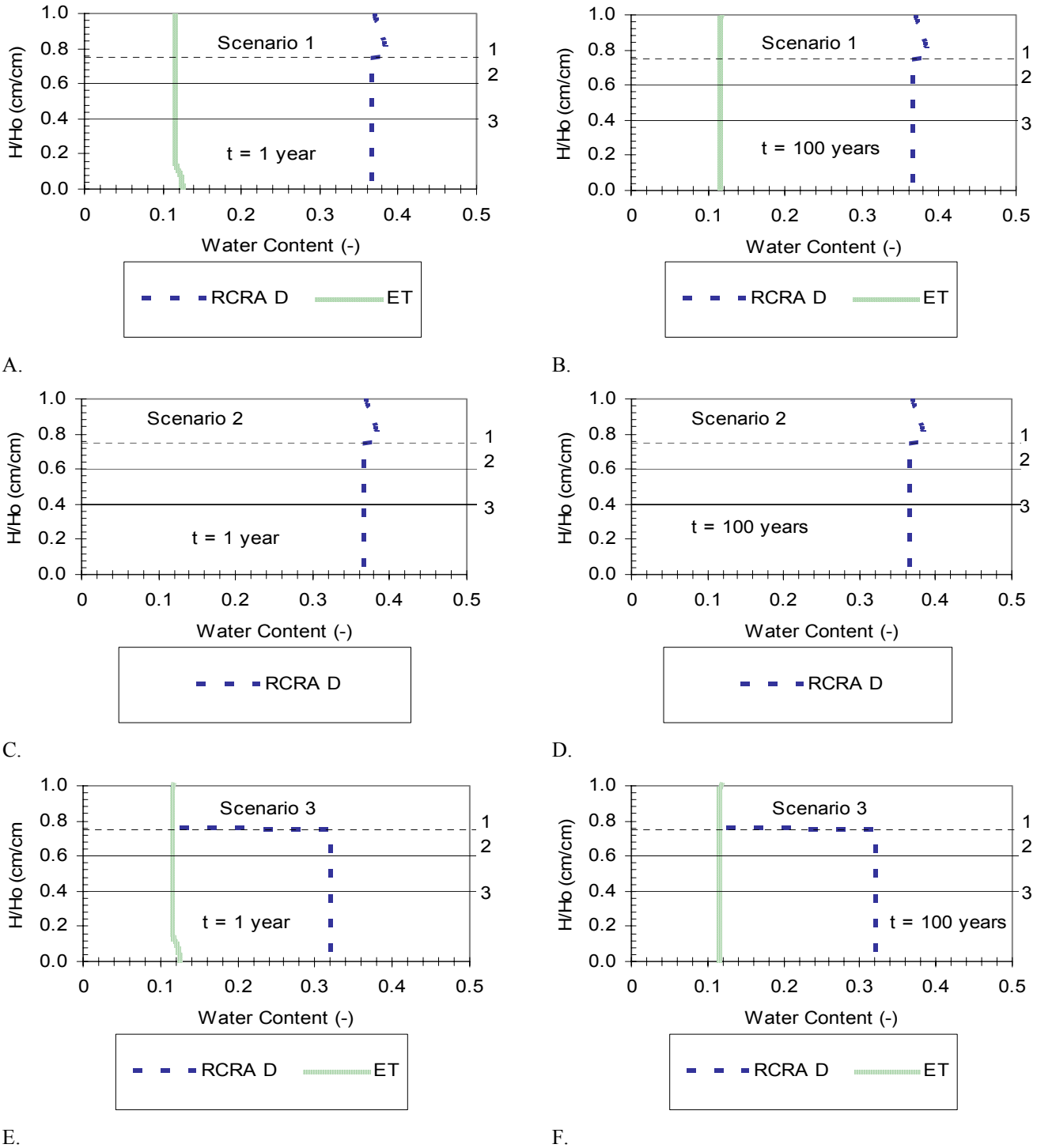

Figure 36. The Water Content as a function of cover depth (dimensionless H/H_0) for Scenario 1 after A) 1 year and B) 100 years, for Scenario 2 after C) 1 year and D) 100 years, and Scenario 3 after E) 1 year and F) 100 years. The separate layers are defined by 1) the topsoil/compacted clay layer in RCRA D, 2) the topsoil/drainage layer in RCRA C, and 3) the drainage/compacted clay layer in RCRA C.

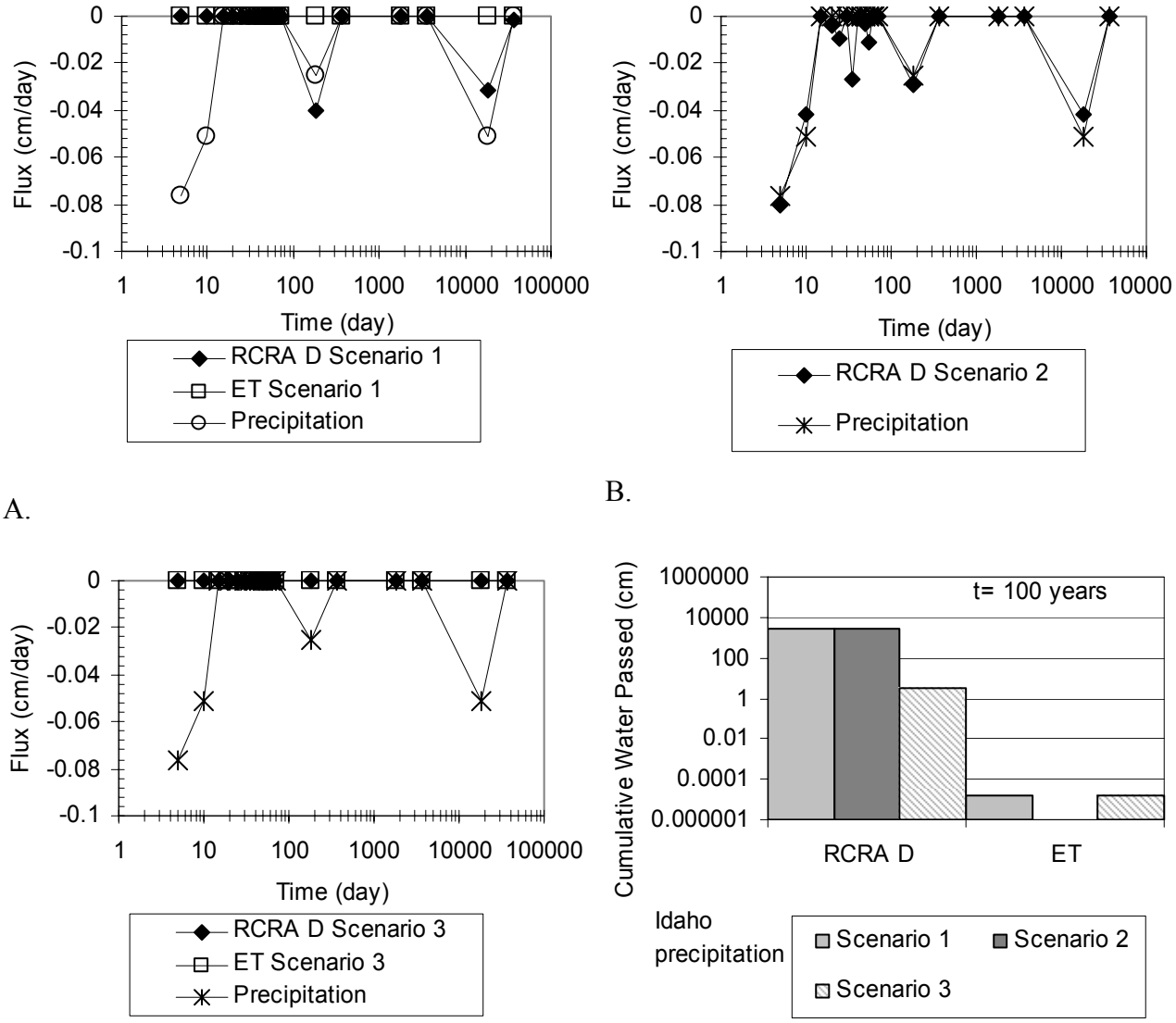

Figure 37. Flux of water through the bottom of the landfill cover as a function of time for A) Scenario 1, B) Scenario 2, C) Scenario 3, and the D) cumulative water passed through the cover after 100 years.

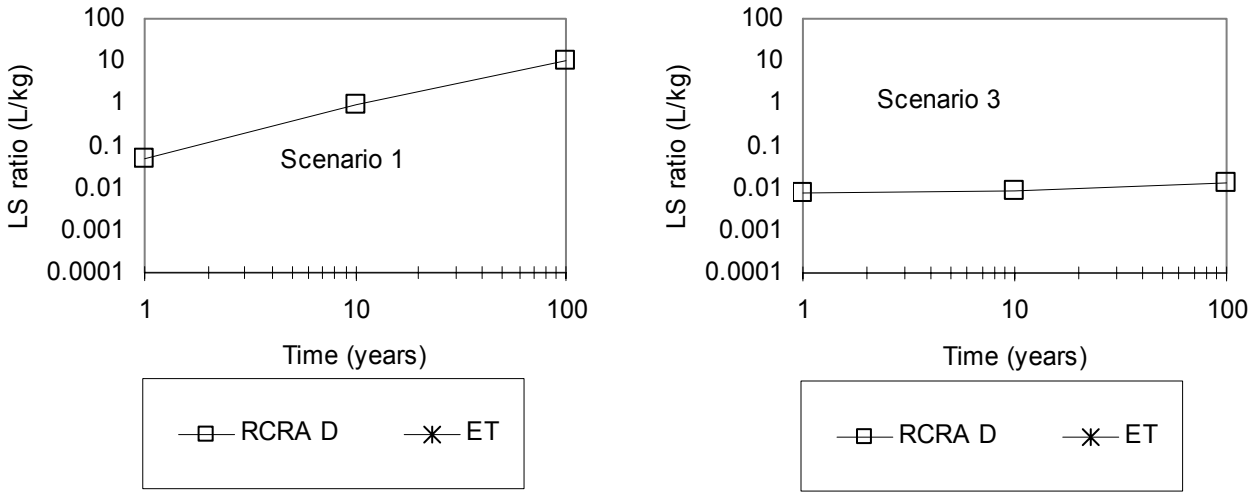

A. B.

Figure 38. The LS ratio for the covers as a function of time for A) Scenario 1 and B) Scenario 3.

ALCD Comparison

The Alternative Landfill Cover Demonstration (ALCD) measured the water flux through a variety of landfill covers, including RCRA C, RCRA D, and an ET cover (Dwyer et al. 2000a). The precipitation volume reported for 1998 was converted into a constant precipitation rate, and one year of this study was simulated in HYDRUS-1D for these covers. The total amount of water passed through the covers is compiled in Figure 39. The HYDRUS-1D model underestimated the flux through the bottom for all cases, and drastically underestimated for the ET and RCRA C covers.

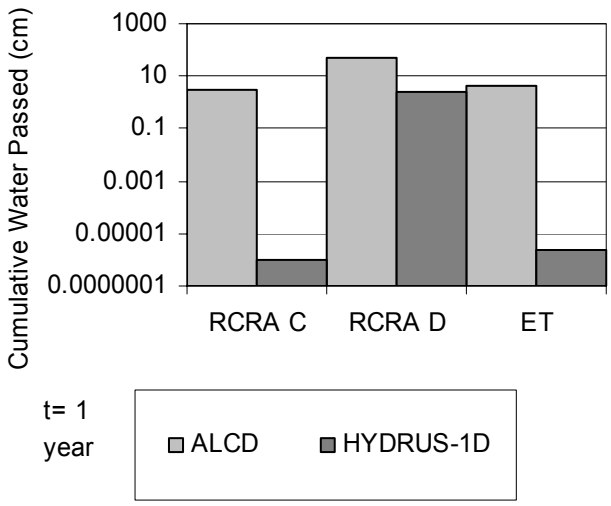

Figure 39. A comparison of water passed through the covers after one year as measured by the ALCD study and as predicted by HYDRUS-1D.

Conclusions

After 100 years, essentially all the water infiltrating a cover without vegetation growth will be transported through the entire cover in the HYDRUS-1D simulations. It has been seen that the landfill cover can behave as a reservoir, holding the water within the soil until it can pass through the cover (Johnson et al. 1998). This suggests that whether the cover were degraded or not degraded, the total amount of water infiltrating the top of the landfill cover will eventually infiltrate through the cover to the waste.

The presence of a tree, or perhaps other vegetation, provides an alternative outlet for excess soil water. The reduction of water in the landfill cover will reduce the water infiltrating through the cover, thereby also reducing the L/S ratio.

CHAPTER VII

CONCLUSIONS AND RECOMMENDATIONS

Landfill cover designs are susceptible to a wide range of physical, chemical, and biological factors. Some landfill covers are intended to inhibit deep-rooting vegetation, but studies suggest that such unintended vegetation is almost inevitable. There are multiple reasons to avoid vegetation growth on a landfill cover; vegetation attracts animals, and the roots of plants could penetrate the waste layer. The focus of this study was the roots' potential increase of hydraulic conductivity and subsequent effect on the water balance.

Once vegetation is established on a cover, the choice is either to allow the plant to grow or to eliminate it. Eliminating the vegetation at an early stage would prevent any further increase of the hydraulic conductivity. If the roots are already well established, however, they could actually aid the cover's performance by reducing the soil water content.

The water transport simulations in this study revealed that vegetation on a landfill cover should be allowed to remain.

The water movement through landfill covers was simulated using water transport, root growth, and root water uptake processes in the HYDRUS-1D software. A sensitivity analysis of HYDRUS-1D revealed that the saturated hydraulic conductivity parameter for the clay soil is influential on the water flux at the saturation threshold, where the flux rate changes sharply. The root water uptake process had the most significant impact and reduced the water flux through a soil layer to negligible amounts.

Simulations of the case study at the Burrell UMT site revealed that in the long term, the amount of water flux through the landfill cover will not be dependent on the hydraulic conductivity of the soil. Vegetation on the landfill cover reduced the water content of the cover and virtually eliminated water flux.

A comparison of different landfill covers without vegetation showed that after 100 years, the type of cover design did not affect the amount of water flux through the cover. For simulated RCRA C and RCRA D landfill covers, the water flux was reduced from 1000 or more cm to 1 cm or less after 100 years when vegetation was added to the landfill cover. Additionally, when a

tree was introduced to simulated RCRA C and RCRA D landfill cover, the LS ratio was reduced from 100 L/kg or more to 1 L/kg or less after 100 years.

In addition to the simulated RCRA C and RCRA D covers, an Evapotranspiration cover was simulated. As expected, the ET cover performed better than either RCRA cover. When a tree was added to the RCRA covers, the ET cover performed nearly as well as the RCRA C landfill cover and still better than the RCRA D landfill cover. The depth of the cover may be a factor in this result, as $d_{RCRA\ C} < d_{ET} < d_{RCRA\ D.}$ Based on these results, the best landfill cover would be a deep layer of soil with plenty of vegetation to reduce the water content.

The simulations in this study were conservative, as they did not account for alternative water paths such as evaporation and runoff. These water path processes may account for much water diversion in a landfill cover. Additional studies may be needed to evaluate these factors in a landfill cover performance comparison.

Recommendations for further study include the evaluation seasonal growing patterns of plant roots, preferential flow paths of water in soils (by two-dimensional modeling), and additional processes such as runoff and evaporation.

APPENDICES

APPENDIX A. HYDRUS-1D EQUATIONS.

Water Flow Equations

Darcy's equation for one dimensional saturated flow is:

$$J = -K_s\left(\frac{\partial H}{\partial x}\right) \qquad [16]$$

where J is fluid flux, K is the saturated hydraulic conductivity, x is the spatial coordinate (Šimunek et al. 1998; Warrick 2002). The Darcy equation modified for unsaturated flow is the Buckingham-Darcy equation:

$$J = -K_u\left(\frac{\partial h}{\partial x}+1\right) \qquad [17]$$

which is derived by defining the total head H as pressure head h and vertical spatial coordinate x. The unsaturated hydraulic conductivity K_u is a function of pressure head and/or of water content. Richards' equation for transient water flow is:

$$\frac{\partial \theta}{\partial t} = -\frac{\partial J}{\partial x} + S \qquad [18]$$

where θ is the volumetric water content, t is time, and S is the sink term, the volume water removed from a volume soil for unit time. The Buckingham equation coupled with Richards equation is therefore:

$$\frac{\partial \theta}{\partial t} = \frac{\partial}{\partial x}\left[K\left(\frac{\partial h}{\partial x}+1\right)\right] + S \qquad [19]$$

This equation for one-dimensional flow contains two dependent variables, pressure head h and water content θ (Warrick 2002). The form of the equation used by HYDRUS-1D is given as:

$$\frac{\partial \theta}{\partial t} = \frac{\partial}{\partial x}\left[K\left(\frac{\partial h}{\partial x}+\cos\alpha\right)\right] - S \qquad [20]$$

where α is the angle between flow direction and vertical axis. When the flow profile is completely vertical and α is equal to zero, the term cos α becomes one, as in the above equation.

Soil Hydraulic Properties Equations

The hydraulic conductivity K in the equation is given by

$$K(h,x) = K_s(x) K_r(h,x) \quad [21]$$

where K_s is the saturated hydraulic conductivity and K_r is the relative hydraulic conductivity (Šimunek et al. 1998).

Mualem gives the relative hydraulic conductivity K_r as:

$$K_r = \frac{K}{K_{sat}} = S_e^{\alpha} \quad [22]$$

The effective saturation is S_e is:

$$S_e = \frac{\theta - \theta_r}{\theta_s - \theta_r} \quad [23]$$

where θ is the water content, θ_r is the residual water content, and θ_s is the saturated water content (Mualem 1976).

The van Genuchten model for solving hydraulic conductivity as a function of water content is:

$$K_r(h) = S_e^{1/2}\left[1-\left(1-S_e^{1/m}\right)^m\right]^2 \quad [24]$$

$$m = 1 - 1/n \qquad n > 1 \quad [25]$$

where *l* is the pore connectivity parameter, and n is the pore size distribution index.

Multiplying this equation by K_{sat} gives the HYDRUS 1D form of van Genuchten:

$$K(h) = K_s S_e^l\left[1-\left(1-S_e^{1/m}\right)^m\right]^2 \quad [26]$$

(Šimunek et al. 1998; van Genuchten 1980). Mualem found the pore connectivity parameter *l* to be .5 on average for most soils (Mualem 1976).

Soil water content as a function of pressure head is given by van Genuchten as:

$$\theta(h) = \theta_r + \frac{\theta_s - \theta_r}{\left[1+(\alpha h)^n\right]^m} \quad [27]$$

In van Genuchten's study, $\alpha = 0.005$ cm^{-1}, n = 2, and m = 0.5, and h is positive (van Genuchten 1980).

HYDRUS-1D this is models this for the following conditions of pressure head h:

$$\theta(h) = \begin{cases} \theta_r + \dfrac{\theta_s - \theta_r}{\left[1 + |\alpha h|^n\right]^m} & h < 0 \\ \theta_s & h \geq 0 \end{cases} \quad [28]$$

(Mualem 1976; van Genuchten 1980).

Root Water Uptake Equations

HYDRUS-1D determines the sink term S in Richards' equation by

$$S(h) = \alpha(h) S_p \quad [29]$$

where S_p is the potential water uptake rate and α(h) is the root-water uptake water stress response function, 0≤α≤1 (Feddes et al. 1978). α(h) is the function given in Table 23 and Figure 40. Literature values exist for h1, h2, h3, and h4 for crops from Taylor and Ashcroft (Taylor and Ashcroft 1972).

Table 23. Root Water Uptake Stress Response Function

$0 \leq h \leq h1$	α = 0 close to saturation
$h1 < h < h2$	$\alpha = \dfrac{1}{h_1 - h_2}$, α is linear
$h2 \leq h \leq h3$	α =1, optimum range for α
$h3 < h \leq h4$	$\alpha = \dfrac{1}{h_3 - h_4}$, α is linear
$h4 < h$	α = 0 at the wilting point

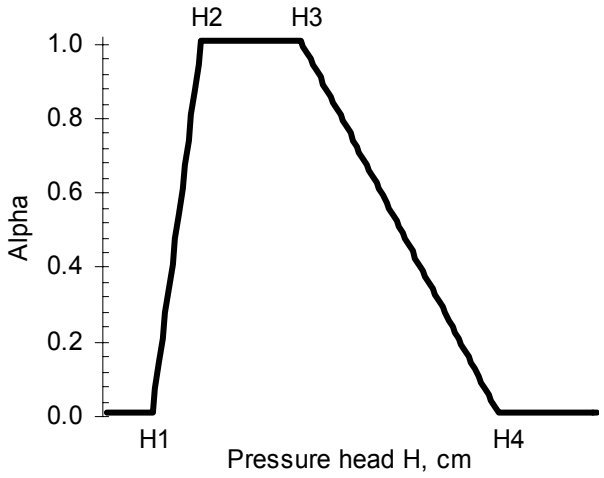

Figure 40 Root Water Uptake Stress Response Function

When the potential water uptake rate Sp is distributed evenly over the root zone, the equation

$$S_p = \frac{1}{L_R} T_p \qquad [30]$$

applies, where L_R is the depth of the root zone given by

$$L_R(t) = L_m f_r(t) \qquad [31]$$

L_m is the maximum rooting depth and $f_r(t)$ is the root growth coefficient given by the Verhulst-Pearl logistical growth equation,

$$f_r(t) = \frac{L_0}{L_0 + (L_m - L_0)e^{-rt}} \qquad [32]$$

where L_0 is the initial value of the rooting depth, r is the growth rate. The growth rate is calculated by HYDRUS-1D with either the assumption that the root growth depth reaches 50% of the maximum at the halfway point in the growing season, or by using a known root depth at a known time in the growing season (Šimunek and Suarez 1993).

T_p is the potential transpiration rate, set initially in HYDRUS-1D as 0.5 and 0.1 cm/day.

For non-uniform distribution of the potential water uptake rate,

$$S_p = b(x) T_p \qquad [33]$$

$$b(x) = \frac{b'(x)}{\int_{L_R} b'(x)\,dx} \quad [34]$$

$$\int_{L_R} b(x)\,dx = 1 \quad [35]$$

where b(x) is the normalized water uptake distribution, and b'(x) is the measured root distribution. Feddes expressed b(x) linearly with depth.

Solving with

$$b(x) = \frac{S_p}{T_p} \quad [36]$$

we find

$$\int_{L_R} S_p dx = T_p \quad [37]$$

$$S(h, h_\phi, x) = \alpha(h, h_\phi, x) b(x) T_p \quad [38]$$

$$T_a = \int_{L_R} S(h, h_\phi, x)\,dx = T_p \int_{L_R} a(h, h_\phi, x) b(x)\,dx \quad [39]$$

where Ta is the transpiration rate.

Boundary Conditions

System Independent

$$\left| \begin{array}{l} h(x,t) = h_0(t) \text{ at } x = 0 \text{ or } x = L \\ -K\left(\frac{\partial h}{\partial z} + \cos\alpha\right) = q_0(t) \text{ at } x = 0 \text{ or } x = L \\ \frac{\partial h}{\partial x} = 0 \text{ at } x = 0 \end{array} \right. \quad [40]$$

h_0 is the pressure head and q_0 is the soil water flux at the boundary.

System Dependent

Surface flux limits:

$$\left| -K\frac{\partial h}{\partial x} - K \right| \le E \qquad x = L \quad [41]$$

and $h_A \le h \le h_S \qquad x = L$ [42]

E is the maximum potential rate of infiltration, h_A is the minimum pressure head and h_S is the maximum pressure head at the soil surface.

Surface ponding: $$-K\left(\frac{\partial h}{\partial z}+\cos\alpha\right)=q_0(t)-\frac{dh}{dt} \text{ at } x=L \quad [43]$$

$$q_{drain}=\frac{8K_{hBot}D_{eq}h_{dr}+4K_{hTop}h_{dr}^2}{L_{dr}^2}+\frac{h_{dr}}{\gamma_{entr}} \quad [44]$$

q_{drain} is the drain discharge rate per surface area

K_{hTop} is the horizontal saturated hydraulic conductivity at the top of the system

K_{hBot} is the horizontal saturated hydraulic conductivity at the bottom of the system

h_{dr} is the watertable height above the drain

L_{dr} is the drain spacing

γ_{dr} is the entrance resistance

D_{eq} is the equivalent depth, a function of L_{dr} (Hooghoudt)

$$q_{drain}=\frac{4K_{hTop}h_{dr}^2}{L_{dr}^2}+\frac{h_{dr}}{\gamma_{entr}} \quad [45]$$

$$q_{drain}=\frac{K_v'}{D_v}+\frac{8\sum(KD)h_{dr}}{L_{dr}^2}\frac{\pi K_r' h_{dr}}{L_{dr}\ln\frac{a_{dr}D_r}{u}}+\frac{h_{dr}}{\gamma_{entr}} \quad [46]$$

K_v' is the saturated hydraulic conductivity in the layers with vertical flow

K_r' is the saturated hydraulic conductivity in the layers with vertical flow

D_v is the layer thickness with vertical flow

D_r is the layer thickness with radial flow

Space Time Discretization

The finite difference method is used to solve the equations:

Mass-lumped scheme:

$$\frac{\theta_i^{j+1,k+1}-\theta_i^{j}}{\Delta t}=\frac{1}{\Delta x}\left[K_{i+1/2}^{j+1,k+1}\frac{h_{i+1}^{j+1,k+1}-h_i^{j+1,k+1}}{\Delta x_i}-K_{i-1/2}^{j+1,k}\frac{h_i^{j+1,k+1}-h_{i-1}^{j+1,k+1}}{\Delta x_{i-1}}\right]+\frac{K_{i+1/2}^{j+1,k}-K_{i-1/2}^{j+1,k}}{\Delta x}-S_i^{j} \quad [47]$$

$$\Delta t=t^{j+1}-t^{j} \qquad \Delta x=\frac{x_{i+1}-x_{i-1}}{2}$$

$$\Delta x_i=x_{i+1}-x_i \qquad \Delta x_{i-1}=x_i-x_{i-1}$$

$$K_{i+1/2}^{j+1,k}=\frac{K_{i+1}^{j+1,k}+K_i^{j+1,k}}{2} \qquad K_{i-1/2}^{j+1,k}=\frac{K_i^{j+1,k}+K_{i-1}^{j+1,k}}{2}$$

Mass conservative method:

$$\frac{\theta_i^{j+1,k+1}-\theta_i^{j}}{\Delta t}=C_i^{j+1,k+1}\frac{h_i^{j+1,k+1}-h_i^{j+1,k}}{\Delta t}+\frac{\theta_i^{j+1,k}-\theta_i^{j}}{\Delta t} \quad [48]$$

C_i is the nodal value of the soil water capacity:

$$C_i^{j+1,k}=\left.\frac{d\theta}{dh}\right|^{j+1,k} \quad [49]$$

Matrix to be solved:

$$\left[P_w\right]^{j+1,k}\left\{h\right\}^{j+1,k+1}=\left\{F_w\right\} \quad [50]$$

$$\left[P_w\right]=\begin{vmatrix} d_1 & e_1 & 0 & & & & 0 \\ e_1 & d_2 & e_2 & 0 & & & 0 \\ 0 & e_2 & d_3 & e_3 & 0 & & 0 \\ & . & & . & & . & \\ & . & & . & & . & \\ 0 & & 0 & e_{N-3} & d_{N-2} & e_{N-2} & 0 \\ 0 & & & 0 & e_{N-2} & d_{N-1} & e_{N-1} \\ 0 & & & & 0 & e_{N-1} & d_N \end{vmatrix} \quad [51]$$

where d_i is defined by:

$$d_i=\frac{\Delta x}{\Delta t}C_i^{j+1,k}+\frac{K_{i+1}^{j+1,k}+K_i^{j+1,k}}{2\Delta x_i}+\frac{K_i^{j+1,k}+K_{i-1}^{j+1,k}}{2\Delta x_{i-1}} \quad [52]$$

e_i:

$$e_i = -\frac{K_{i+1}^{j+1,k} + K_i^{j+1,k}}{2\Delta x_i} \quad [53]$$

In the matrix $\{F_w\}$, f_i is defined by:

$$f = \frac{\Delta x}{\Delta t} C_i^{j+1,k} h_i^{j+1,k} - \frac{\Delta x}{\Delta t}\left(\theta_i^{j+1,k} - \theta_i^j\right)\frac{K_{i+1}^{j+1,k} + K_{i-1}^{j+1,k}}{2} - S_i^j \Delta x \quad [54]$$

Boundary Condition Flux Equations

$$q_1^{j+1} = -K_{1+1/2}^{j+1}\left[\frac{h_2^{j+1} - h_1^{j+1}}{\Delta x_i} + 1\right] \quad [55]$$

$$q_i^{j+1} = \frac{-K_{1+1/2}^{j+1}\left[\frac{h_{i+1}^{j+1} - h_i^{j+1}}{\Delta x_i} + 1\right]\Delta x_{i-1} - K_{i-1/2}^{j+1}\left[\frac{h_i^{j+1} - h_{i-1}^{j+1}}{\Delta x_{i-1}} + 1\right]\Delta x_i}{\Delta x_{i-1} + \Delta x_i} \quad [56]$$

$$q_N^{j+1} = -K_{N+1/2}^{j+1}\left[\frac{h_N^{j+1} - h_{N-1}^{j+1}}{\Delta x_{N-1}} + 1\right] - \frac{\Delta x_{N-1}}{2}\left[\frac{\theta_N^{j+1} - \theta_N^j}{\Delta t} + S_N^j\right] \quad [57]$$

Transpiration rate:

$$T_a = \sum_e \Delta x_i \frac{S_i + S_{i+1}}{2} \quad [58]$$

Graphical Editor in HYDRUS-1D

Technical details about the soil depths and soil moisture content is entered in the graphical editor of HYDRUS-1D.

Figure 41 A shows the soil material layers; this profile shows three different soil layers. Figure 41 B demonstrates how the nodes are placed. Up to ten nodes may be placed along the soil profile. Figure 41 C shows the profile of pressure head or of water content over the depth of the soil profile.

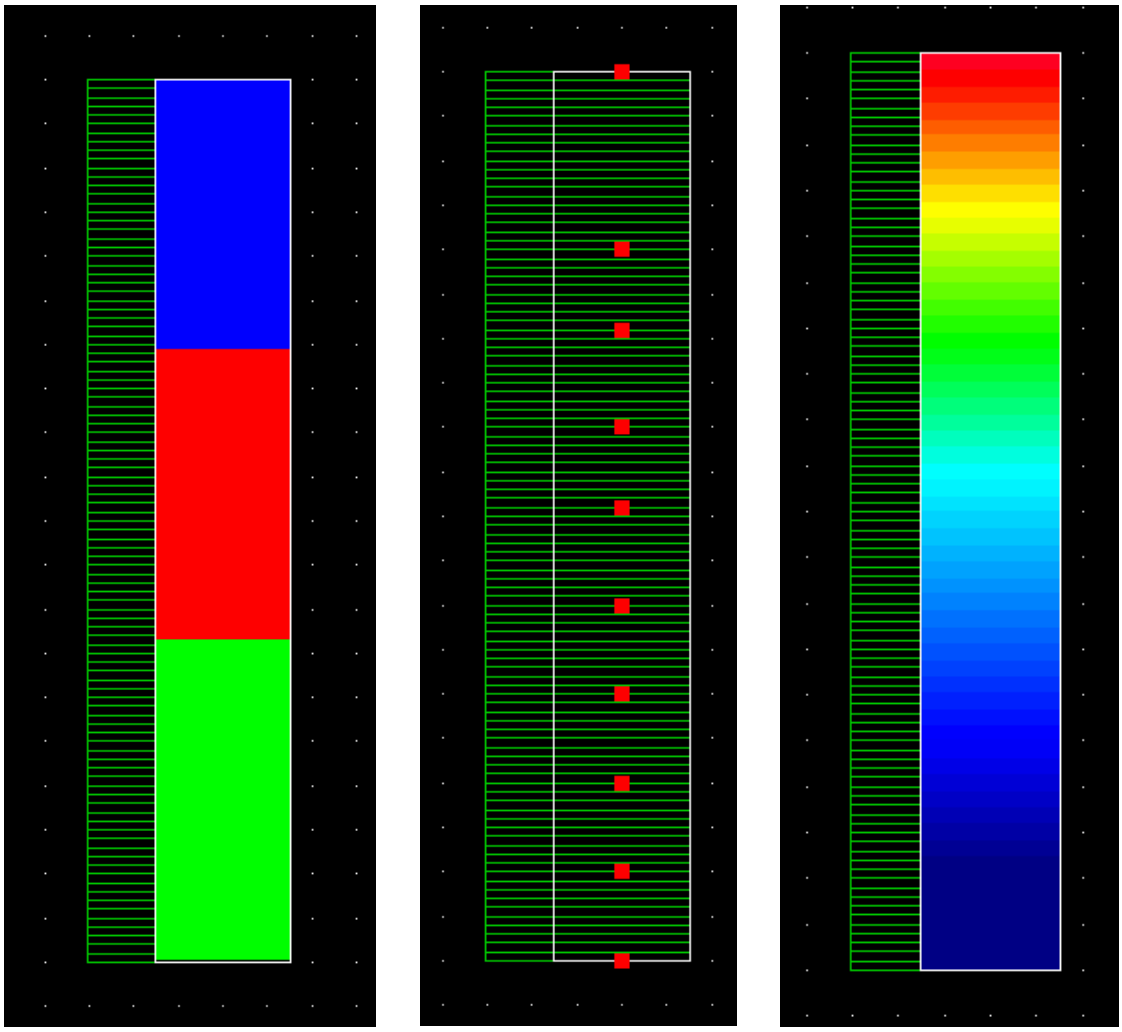

A. B. C.

Figure 41. Soil Profile Graphical Editor in HYDRUS-1D.

APPENDIX B. SENSITIVITY ANALYSIS CASES

Case	Ks 1	Ks 1 -25%	Ks 1 -25%	Ks 2	Ks 2 -25%	Ks +25%
Main Processes	Water Flow	Water Flow	Water Flow	Water Flow	Water Flow	Water Flow
Geometry						
Length Units	cm	cm	cm	cm	cm	cm
Number of Soil Materials	1	1	1	1	1	1
Number of Layers	1	1	1	1	1	1
Decline from Vertical Axis	1	1	1	1	1	1
Depth of Soil Profile	10	10	10	10	10	10
Time						
Time Units	day	day	day	day	day	day
Initial Time	0	0	0	0	0	0
Final Time	10	10	10	10	10	10
Initial Time Step	.01	.01	.01	.001	.001	.001
Minimum Time Step	.0001	.0001	.0001	1E-8	1E-8	1E-8
Maximum Time Step	1	1	1	1	1	1
Number of Time Variable Records	-	-	-	-	-	-
Iteration Criteria						
Maximum Number of Iterations	100	100	100	10000	10000	10000
Water Content Tolerance	.0001	.0001	.0001	.0001	.0001	.0001
Pressure Head Tolerance	.1	.1	.1	.1	.1	.1
Hydraulic Model						
van Genuchten-Mualem with air entry-value of -2 cm, no hysteresis						
Water Flow Parameters						
θr	0.068	0.068	0.068	0.068	0.068	0.068
θs	0.38	0.38	0.38	0.38	0.38	0.38
α	0.008	0.008	0.008	0.008	0.008	0.008
n	1.09	1.09	1.09	1.09	1.09	1.09
Ks	4.8	3.6	6.0	0.048	0.036	0.06
I	0.5	0.5	0.5	0.5	0.5	0.5
Boundary Condition						
Upper Boundary Condition	Constant Flux					
Lower Boundary Condition	Seepage Face					
Initial Condition	Water Content					
Constant Boundary Flux*	-0.5 (-0.05)	-0.5 (-0.05)	-0.5 (-0.05)	-0.5 (-0.05)	-0.5 (-0.05)	-0.5 (-0.05)
Graphical Editor						
Profile Discretization						
Number	101	101	101	101	101	101
Density	1	1	1	1	1	1
Material Distribution	1	1	1	1	1	1
Initial Condition, uniform	0.2	0.2	0.2	0.2	0.2	0.2
Subregions	1	1	1	1	1	1

*Precipitation Case A (Precipitation Case B)

Case	Ks 3	Ks 3 -25%	Ks 3 -25%	Grass	Tree
Main Processes	Water Flow	Water Flow	Water Flow	Water Flow Root Growth Root Water Uptake	Water Flow Root Growth Root Water Uptake
Geometry					
Length Units	cm	cm	cm	cm	cm
Number of Soil Materials	1	1	1	1	1
Number of Layers	1	1	1	1	1
Decline from Vertical Axis	1	1	1	1	1
Depth of Soil Profile	10	10	10	10	10
Time					
Time Units	day	day	day	day	day
Initial Time	0	0	0	0	0
Final Time	10	10	10	10	10
Initial Time Step	.01	.01	.01	.01	.01
Minimum Time Step	.0001	.0001	.0001	.0001	.0001
Maximum Time Step	1	1	1	1	1
Number of Time Variable Records	-	-	-	-	-
Iteration Criteria					
Maximum Number of Iterations	10000	10000	10000	10000	10000
Water Content Tolerance	.00001	.00001	.00001	.00001	.00001
Pressure Head Tolerance	.01	.01	.01	.01	.01
Hydraulic Model					
van Genuchten-Mualem with air entry-value of -2 cm, no hysteresis					
Water Flow Parameters					
θr	0.068	0.068	0.068	0.068	0.068
θs	0.38	0.38	0.38	0.38	0.38
α	0.008	0.008	0.008	0.008	0.008
n	1.09	1.09	1.09	1.09	1.09
Ks	480	360	600	4.8	4.8
I	0.5	0.5	0.5	0.5	0.5
Boundary Condition					
Upper Boundary Condition	Constant Flux				
Lower Boundary Condition	Seepage Face				
Initial Condition	Water Content				
Constant Boundary Flux*	-0.5 (-0.05)	-0.5 (-0.05)	-0.5 (-0.05)	-0.5 (-0.05)	-0.5 (-0.05)
Root Water Uptake				0.5	3.0
Root Water Uptake Model				Feddes, no solute stress	
Feddes Parameters				grass	Deciduous fruit
Root growth factors				50% after 50% growing time	
Initial root growth time				0	0
Harvest time				10	10
Initial root depth				1	1
Maximum root depth				10	10
Exponential Coefficient				0.105	0.105
Graphical Editor					
Profile Discretization					
Number	101	101	101	101	101
Density	1	1	1	1	1

Material Distribution	1	1	1	1	1
Initial Condition, uniform	0.2	0.2	0.2	0.2	0.2
Subregions	1	1	1	1	1

*Precipitation Case A (Precipitation Case B)

Case	Θ -25%	Θ +25%	Θr -25%	Θr +25%	Θs -25%	Θs +25%
Main Processes	Water Flow	Water Flow	Water Flow	Water Flow	Water Flow	Water Flow
Geometry						
Length Units	cm	cm	cm	cm	cm	cm
Number of Soil Materials	1	1	1	1	1	1
Number of Layers	1	1	1	1	1	1
Decline from Vertical Axis	1	1	1	1	1	1
Depth of Soil Profile	10	10	10	10	10	10
Time						
Time Units	day	day	day	day	day	day
Initial Time	0	0	0	0	0	0
Final Time	10	10	10	10	10	10
Initial Time Step	.01	.01	.01	.01	.01	.01
Minimum Time Step	.0001	.0001	.0001	.0001	.0001	.0001
Maximum Time Step	1	1	1	1	1	1
Number of Time Variable Records	-	-	-	-	-	-
Iteration Criteria						
Maximum Number of Iterations	10000	10000	100	100	100	100
Water Content Tolerance	.0001	.0001	.0001	.0001	.0001	.0001
Pressure Head Tolerance	.1	.1	.1	.1	.1	.1
Hydraulic Model						
van Genuchten-Mualem with air entry-value of -2 cm, no hysteresis						
Water Flow Parameters						
θr	0.068	0.068	0.051	0.085	0.068	0.068
θs	0.38	0.38	0.38	0.38	0.285	0.475
α	0.008	0.008	0.008	0.008	0.008	0.008
n	1.09	1.09	1.09	1.09	1.09	1.09
Ks	4.8	4.8	4.8	4.8	4.8	4.8
I	0.5	0.5	0.5	0.5	0.5	0.5
Boundary Condition						
Upper Boundary Condition	Constant Flux					
Lower Boundary Condition	Seepage Face					
Initial Condition	Water Content					
Constant Boundary Flux*	-0.5 (-0.05)	-0.5 (-0.05)	-0.5 (-0.05)	-0.5 (-0.05)	-0.5 (-0.05)	-0.5 (-0.05)
Graphical Editor						
Profile Discretization						
Number	101	101	101	101	101	101
Density	1	1	1	1	1	1
Material Distribution	1	1	1	1	1	1
Initial Condition, uniform	0.15	0.25	0.2	0.2	0.2	0.2
Subregions	1	1	1	1	1	1

*Precipitation Case A (Precipitation Case B)

Case	60 cm	Ks +25%	Ks -25%
Main Processes	Water Flow	Water Flow	Water Flow
Geometry			
Length Units	cm	cm	cm
Number of Soil Materials	1	1	1
Number of Layers	1	1	1
Decline from Vertical Axis	1	1	1
Depth of Soil Profile	60	60	60
Time			
Time Units	day	day	day
Initial Time	0	0	0
Final Time	30	30	30
Initial Time Step	$1e^{-5}$	$1e^{-5}$	$1e^{-5}$
Minimum Time Step	$1e^{-5}$	$1e^{-5}$	$1e^{-5}$
Maximum Time Step	0.1	0.1	0.1
Number of Time Variable Records	-	-	-
Iteration Criteria			
Maximum Number of Iterations	100	100	100
Water Content Tolerance	.0001	.0001	.0001
Pressure Head Tolerance	.1	.1	.1
Hydraulic Model			
van Genuchten-Mualem with air entry-value of -2 cm, no hysteresis			
Water Flow Parameters			
θr	0.068	0.068	0.068
θs	0.38	0.38	0.38
α	0.008	0.008	0.008
n	1.09	1.09	1.09
Ks	4.8	3.6	6.0
I	0.5	0.5	0.5
Boundary Condition			
Upper Boundary Condition	Constant Flux		
Lower Boundary Condition	Seepage Face		
Initial Condition	Water Content		
Constant Boundary Flux*	-0.5	-0.5	-0.5
Graphical Editor			
Profile Discretization			
Number	101	101	101
Density	1	1	1
Material Distribution	1	1	1
Initial Condition, uniform	0.2	0.2	0.2
Subregions	1	1	1

APPENDIX C. BURRELL CASES.

Case	Scenario 1	Scenario 2	Scenario 3
Main Processes	Water Flow	Water Flow	Water Flow Root Growth Root Water Uptake
Geometry			
Length Units	cm	cm	cm
Number of Soil Materials	3	3	3
Number of Layers	3	3	3
Decline from Vertical Axis	1	1	1
Depth of Soil Profile	150	150	150
Time			
Time Units	day	day	day
Initial Time	0	0	0
Final Time	36500	36500	36500
Initial Time Step	.001	.001	.001
Minimum Time Step	1E-7	1E-7	1E-7
Maximum Time Step	1	1	1
Number of Time Variable Records	-	-	-
Iteration Criteria			
Maximum Number of Iterations	10000	10000	10000
Water Content Tolerance	.0001	.0001	.0001
Pressure Head Tolerance	.1	.1	.1
Hydraulic Model			
van Genuchten-Mualem with air entry-value of -2 cm, no hysteresis			
Water Flow Parameters			
Layer 1			
θr	0.045	0.045	0.045
θs	0.43	0.43	0.43
α	0.145	0.145	0.145
n	2.68	2.68	2.68
Ks	1400	1400	1400
I	0.5	0.5	0.5
Layer 2			
θr	0.045	0.045	0.045
θs	0.43	0.43	0.43
α	0.145	0.145	0.145
n	2.68	2.68	2.68
Ks	700	700	700
I	0.5	0.5	0.5
Layer 3			
θr	0.1	0.1	0.1
θs	0.364	0.364	0.364
α	0.0001	0.0001	0.0001
n	1.524	1.524	1.524
Ks	0.00864	2.592	2.592
I	0.5	0.5	0.5
Boundary Condition			
Upper Boundary Condition	Constant Flux		

Lower Boundary Condition	Seepage Face		
Initial Condition	Water Content		
Constant Boundary Flux*	-0.5 (-0.05)	-0.5 (-0.05)	-0.5 (-0.05)
Root Water Uptake			3.0
Root Water Uptake Model			Feddes, no solute stress
Feddes Parameters			Deciduous fruit
Root growth factors			50% after 50% growing time
Initial root growth time			0
Harvest time			36500
Initial root depth			80
Maximum root depth			90
Exponential Coefficient			0.105
Graphical Editor			
Profile Discretization			
Number	101	101	101
Density (upper, lower)	(0.5,1)	(0.5,1)	(0.5,1)
Material Distribution			
1	0-30	0-30	0-30
2	30-60	30-60	30-60
3	60-150	60-150	60-150
Initial Condition, uniform	0.2	0.2	0.2
Subregion			
1	0-30	0-30	0-30
2	30-60	30-60	30-60
3	60-150	60-150	60-150

*Precipitation Case A (Precipitation Case B)

APPENDIX D. RCRA C CONSTANT FLUX.

Case	Scenario 1	Scenario 2	Scenario 3
Main Processes	Water Flow	Water Flow	Water Flow Root Growth Root Water Uptake
Geometry			
Length Units	cm	cm	cm
Number of Soil Materials	3	3	3
Number of Layers	3	3	3
Decline from Vertical Axis	1	1	1
Depth of Soil Profile	150	150	150
Time			
Time Units	day	day	day
Initial Time	0	0	0
Final Time	36500	36500	36500
Initial Time Step	.001	.001	.001
Minimum Time Step	1E-7	1E-7	1E-7
Maximum Time Step	1	1	1
Number of Time Variable Records	-	-	-
Iteration Criteria			
Maximum Number of Iterations	10000	10000	10000
Water Content Tolerance	.00001	.00001	.00001
Pressure Head Tolerance	.01	.01	.01
Hydraulic Model			
van Genuchten-Mualem with air entry-value of -2 cm, no hysteresis			
Water Flow Parameters			
Layer 1			
θr	0.067	0.067	0.067
θs	0.45	0.45	0.45
α	0.02	0.02	0.02
n	1.41	1.41	1.41
Ks	10.8	10.8	10.8
I	0.5	0.5	0.5
Layer 2			
θr	0.045	0.045	0.045
θs	0.43	0.43	0.43
α	0.145	0.145	0.145
n	2.68	2.68	2.68
Ks	712.8	712.8	712.8
I	0.5	0.5	0.5
Layer 3			
θr	0.1	0.1	0.1
θs	0.364	0.364	0.364
α	0.0001	0.0001	0.0001
n	1.524	1.524	1.524
Ks	0.00864	2.592	2.592
I	0.5	0.5	0.5
Boundary Condition			
Upper Boundary Condition	Constant Flux		

Lower Boundary Condition	Seepage Face		
Initial Condition	Water Content		
Constant Boundary Flux*	-0.5 (-0.05)	-0.5 (-0.05)	-0.5 (-0.05)
Root Water Uptake			3.0
Root Water Uptake Model			Feddes, no solute stress
Feddes Parameters			Deciduous fruit
Root growth factors			50% after 50% growing time
Initial root growth time			0
Harvest time			36500
Initial root depth			80
Maximum root depth			90
Exponential Coefficient			0.105
Graphical Editor			
Profile Discretization			
Number	101	101	101
Density (upper, lower)	(0.5,1)	(0.5,1)	(0.5,1)
Material Distribution			
1	0-60	0-60	0-60
2	60-90	60-90	60-90
3	90-150	90-150	90-150
Initial Condition, uniform	0.2	0.2	0.2
Subregion			
1	0-60	0-60	0-60
2	60-90	60-90	60-90
3	90-150	90-150	90-150

*Precipitation Case A (Precipitation Case B)

APPENDIX E. RCRA C DAILY PRECIPITATION DATA.

Case	Scenario 1	Scenario 2	Scenario 3
Main Processes	Water Flow	Water Flow	Water Flow Root Growth Root Water Uptake
Geometry			
Length Units	cm	cm	cm
Number of Soil Materials	3	3	3
Number of Layers	3	3	3
Decline from Vertical Axis	1	1	1
Depth of Soil Profile	150	150	150
Time			
Time Units	day	day	day
Initial Time	0	0	0
Final Time	36500	36500	36500
Initial Time Step	.001	.001	.001
Minimum Time Step	1E-13	1E-9	1E-7
Maximum Time Step	1	1	1
Number of Time Variable Records	36500	36500	36500
Iteration Criteria			
Maximum Number of Iterations	10000	10000	10000
Water Content Tolerance	.0001	.0001	.0001
Pressure Head Tolerance	.1	.1	.1
Hydraulic Model			
van Genuchten-Mualem with air entry-value of -2 cm, no hysteresis			
Water Flow Parameters			
Layer 1			
θr	0.067	0.067	0.067
θs	0.45	0.45	0.45
α	0.02	0.02	0.02
n	1.41	1.41	1.41
Ks	10.8	10.8	10.8
I	0.5	0.5	0.5
Layer 2			
θr	0.045	0.045	0.045
θs	0.43	0.43	0.43
α	0.145	0.145	0.145
n	2.68	2.68	2.68
Ks	712.8	712.8	712.8
I	0.5	0.5	0.5
Layer 3			
θr	0.1	0.1	0.1
θs	0.364	0.364	0.364
α	0.0001	0.0001	0.0001
n	1.524	1.524	1.524
Ks	0.00864	2.592	2.592
I	0.5	0.5	0.5
Boundary Condition			
Upper Boundary Condition	Variable Pressure Head / Flux		

Lower Boundary Condition	Seepage Face		
Initial Condition	Water Content		
Time Variable Boundary Conditions			
* see APPENDIX J for Precipitation Data			
Root Water Uptake Model			Feddes, no solute stress
Feddes Parameters			Deciduous fruit
Root growth factors			50% after 50% growing time
Initial root growth time			0
Harvest time			36500
Initial root depth			80
Maximum root depth			90
Exponential Coefficient			0.105
Graphical Editor			
Profile Discretization			
Number	401	251	201
Density (upper, lower)	(0.5,1)	(0.5,1)	(0.5,1)
Material Distribution			
1	0-60	0-60	0-60
2	60-90	60-90	60-90
3	90-150	90-150	90-150
Initial Condition, uniform	0.2	0.2	0.2
Subregion			
1	0-60	0-60	0-60
2	60-90	60-90	60-90
3	90-150	90-150	90-150

APPENDIX F. RCRA D CONSTANT FLUX.

Case	Scenario 1	Scenario 2	Scenario 3
Main Processes	Water Flow	Water Flow	Water Flow Root Growth Root Water Uptake
Geometry			
Length Units	cm	cm	cm
Number of Soil Materials	2	2	2
Number of Layers	2	2	2
Decline from Vertical Axis	1	1	1
Depth of Soil Profile	60	60	60
Time			
Time Units	day	day	day
Initial Time	0	0	0
Final Time	36500	36500	36500
Initial Time Step	.01	.01	.01
Minimum Time Step	1E-5	1E-5	1E-5
Maximum Time Step	1	1	1
Number of Time Variable Records	36500	36500	36500
Iteration Criteria			
Maximum Number of Iterations	10000	10000	10000
Water Content Tolerance	.0001	.0001	.0001
Pressure Head Tolerance	.1	.1	.1
Hydraulic Model			
van Genuchten-Mualem with air entry-value of -2 cm, no hysteresis			
Water Flow Parameters			
Layer 1			
θr	0.067	0.067	0.067
θs	0.45	0.45	0.45
α	0.02	0.02	0.02
n	1.41	1.41	1.41
Ks	10.8	10.8	10.8
I	0.5	0.5	0.5
Layer 2			
θr	0.1	0.1	0.1
θs	0.364	0.364	0.364
α	0.0001	0.0001	0.0001
n	1.524	1.524	1.524
Ks	0.864	2.592	2.592
I	0.5	0.5	0.5
Boundary Condition			
Upper Boundary Condition	Constant Flux		
Lower Boundary Condition	Seepage Face		
Initial Condition	Water Content		
Constant Boundary Flux*	-0.5 (-0.05)	-0.5 (-0.05)	-0.5 (-0.05)
Root Water Uptake Model			Feddes, no solute stress
Feddes Parameters			Deciduous fruit
Root growth factors			50% after 50% growing time
Initial root growth time			0

Harvest time			36500
Initial root depth			50
Maximum root depth			60
Exponential Coefficient			0.105
Graphical Editor			
Profile Discretization			
Number	101	101	101
Density (upper, lower)	(0.5,1)	(0.5,1)	(0.5,1)
Material Distribution			
1	0-15	0-15	0-15
2	15-60	15-60	15-60
Initial Condition, uniform	0.2	0.2	0.2
Subregion			
1	0-15	0-15	0-15
2	15-60	15-60	15-60

*Precipitation Case A (Precipitation Case B)

APPENDIX G. RCRA D DAILY PRECIPITATION DATA.

Case	Scenario 1	Scenario 2	Scenario 3
Main Processes	Water Flow	Water Flow	Water Flow Root Growth Root Water Uptake
Geometry			
Length Units	cm	cm	cm
Number of Soil Materials	2	2	2
Number of Layers	2	2	2
Decline from Vertical Axis	1	1	1
Depth of Soil Profile	60	60	60
Time			
Time Units	day	day	day
Initial Time	0	0	0
Final Time	36500	36500	36500
Initial Time Step	.01	.01	.01
Minimum Time Step	1E-5	1E-5	1E-5
Maximum Time Step	1	1	1
Number of Time Variable Records	-	-	-
Iteration Criteria			
Maximum Number of Iterations	10000	10000	10000
Water Content Tolerance	.0001	.0001	.0001
Pressure Head Tolerance	.1	.1	.1
Hydraulic Model			
van Genuchten-Mualem with air entry-value of -2 cm, no hysteresis			
Water Flow Parameters			
Layer 1			
θr	0.067	0.067	0.067
θs	0.45	0.45	0.45
α	0.02	0.02	0.02
n	1.41	1.41	1.41
Ks	10.8	10.8	10.8
I	0.5	0.5	0.5
Layer 2			
θr	0.1	0.1	0.1
θs	0.364	0.364	0.364
α	0.0001	0.0001	0.0001
n	1.524	1.524	1.524
Ks	0.864	2.592	2.592
I	0.5	0.5	0.5
Boundary Condition			
Upper Boundary Condition	Variable Pressure Head / Flux		
Lower Boundary Condition	Seepage Face		
Initial Condition	Water Content		
Time Variable Boundary Conditions			
* see APPENDIX J for Precipitation Data			
Root Water Uptake			3.0
Root Water Uptake Model			Feddes, no solute stress
Feddes Parameters			Deciduous fruit

Root growth factors			50% after 50% growing time
Initial root growth time			0
Harvest time			36500
Initial root depth			50
Maximum root depth			60
Exponential Coefficient			0.105
Graphical Editor			
Profile Discretization			
Number	101	101	101
Density (upper, lower)	(0.5,1)	(0.5,1)	(0.5,1)
Material Distribution			
1	0-15	0-15	0-15
2	15-60	15-60	15-60
Initial Condition, uniform	0.2	0.2	0.2
Subregion			
1	0-15	0-15	0-15
2	15-60	15-60	15-60

APPENDIX H. ET CONSTANT FLUX.

Case	Scenario 1	Scenario 2	Scenario 3
Main Processes	Water Flow	Water Flow	Water Flow Root Growth Root Water Uptake
Geometry			
Length Units	cm	cm	cm
Number of Soil Materials	3	3	3
Number of Layers	3	3	3
Decline from Vertical Axis	1	1	1
Depth of Soil Profile	150	150	150
Time			
Time Units	day	day	day
Initial Time	0	0	0
Final Time	36500	36500	36500
Initial Time Step	.001	.001	.001
Minimum Time Step	1E-7	1E-7	1E-7
Maximum Time Step	1	1	1
Number of Time Variable Records	-	-	-
Iteration Criteria			
Maximum Number of Iterations	10000	10000	10000
Water Content Tolerance	.0001	.0001	.0001
Pressure Head Tolerance	.1	.1	.1
Hydraulic Model			
van Genuchten-Mualem with air entry-value of -2 cm, no hysteresis			
Water Flow Parameters			
Layer 1			
θr	0.045	0.045	0.045
θs	0.43	0.43	0.43
α	0.145	0.145	0.145
n	2.68	2.68	2.68
Ks	1400	1400	1400
I	0.5	0.5	0.5
Layer 2			
θr	0.045	0.045	0.045
θs	0.43	0.43	0.43
α	0.145	0.145	0.145
n	2.68	2.68	2.68
Ks	700	700	700
I	0.5	0.5	0.5
Layer 3			
θr	0.1	0.1	0.1
θs	0.364	0.364	0.364
α	0.0001	0.0001	0.0001
n	1.524	1.524	1.524
Ks	0.00864	2.592	2.592
I	0.5	0.5	0.5
Boundary Condition			
Upper Boundary Condition	Constant Flux		

Lower Boundary Condition	Seepage Face		
Initial Condition	Water Content		
Constant Boundary Flux	-0.5 (-0.05)	-0.5 (-0.05)	-0.5 (-0.05)
Root Water Uptake			3.0
Root Water Uptake Model			Feddes, no solute stress
Feddes Parameters			Deciduous fruit
Root growth factors			50% after 50% growing time
Initial root growth time			0
Harvest time			36500
Initial root depth			80
Maximum root depth			90
Exponential Coefficient			0.105
Graphical Editor			
Profile Discretization			
Number	101	101	101
Density (upper, lower)	(0.5,1)	(0.5,1)	(0.5,1)
Material Distribution			
1	0-30	0-30	0-30
2	30-60	30-60	30-60
3	60-150	60-150	60-150
Initial Condition, uniform	0.2	0.2	0.2
Subregion			
1	0-30	0-30	0-30
2	30-60	30-60	30-60
3	60-150	60-150	60-150

*Precipitation Case A (Precipitation Case B)

APPENDIX I. ET DAILY PRECIPITATION DATA

Case	Scenario 1	Scenario 2	Scenario 3
Main Processes	Water Flow	Water Flow	Water Flow Root Growth Root Water Uptake
Geometry			
Length Units	cm	cm	cm
Number of Soil Materials	3	3	3
Number of Layers	3	3	3
Decline from Vertical Axis	1	1	1
Depth of Soil Profile	150	150	150
Time			
Time Units	day	day	day
Initial Time	0	0	0
Final Time	36500	36500	36500
Initial Time Step	.001	.001	.001
Minimum Time Step	1E-7	1E-7	1E-7
Maximum Time Step	1	1	1
Number of Time Variable Records	-	-	-
Iteration Criteria			
Maximum Number of Iterations	10000	10000	10000
Water Content Tolerance	.0001	.0001	.0001
Pressure Head Tolerance	.1	.1	.1
Hydraulic Model			
van Genuchten-Mualem with air entry-value of -2 cm, no hysteresis			
Water Flow Parameters			
Layer 1			
θr	0.045	0.045	0.045
θs	0.43	0.43	0.43
α	0.145	0.145	0.145
n	2.68	2.68	2.68
Ks	1400	1400	1400
I	0.5	0.5	0.5
Layer 2			
θr	0.045	0.045	0.045
θs	0.43	0.43	0.43
α	0.145	0.145	0.145
n	2.68	2.68	2.68
Ks	700	700	700
I	0.5	0.5	0.5
Layer 3			
θr	0.1	0.1	0.1
θs	0.364	0.364	0.364
α	0.0001	0.0001	0.0001
n	1.524	1.524	1.524
Ks	0.00864	2.592	2.592
I	0.5	0.5	0.5
Boundary Condition			
Upper Boundary Condition	Variable Pressure Head/Flux		

Lower Boundary Condition	Seepage Face		
Initial Condition	Water Content		
Time Variable Boundary Conditions			
* see APPENDIX J for Precipitation Data			
Root Water Uptake			3.0
Root Water Uptake Model			Feddes, no solute stress
Feddes Parameters			Deciduous fruit
Root growth factors			50% after 50% growing time
Initial root growth time			0
Harvest time			36500
Initial root depth			80
Maximum root depth			90
Exponential Coefficient			0.105
Graphical Editor			
Profile Discretization			
Number	101	101	101
Density (upper, lower)	(0.5,1)	(0.5,1)	(0.5,1)
Material Distribution			
1	0-30	0-30	0-30
2	30-60	30-60	30-60
3	60-150	60-150	60-150
Initial Condition, uniform	0.2	0.2	0.2
Subregion			
1	0-30	0-30	0-30
2	30-60	30-60	30-60
3	60-150	60-150	60-150

APPENDIX J. PRECIPITATION DATA

Precipitation Data in centimeters.

Month	Day	Year	Idaho Precipitation	Oak Ridge Precipitation	Year	Idaho Precipitation	Oak Ridge Precipitation
9	1	2000	0.3048	0	2001	0	2.4892
9	2	2000	0.8382	0.0762	2001	0	0
9	3	2000	0	0.7874	2001	0	1.8034
9	4	2000	0	0.0254	2001	0	3.556
9	5	2000	0	0	2001	0	0
9	6	2000	0.1016	0	2001	0.762	0
9	7	2000	0	0	2001	0	0
9	8	2000	0	0	2001	0	0
9	9	2000	0	0	2001	0	0
9	10	2000	0	0	2001	0	0.0762
9	11	2000	0	0	2001	0	0
9	12	2000	0	0	2001	0	0
9	13	2000	0	0	2001	1.5748	0
9	14	2000	0	0	2001	0	0
9	15	2000	0	0	2001	0	0
9	16	2000	0	0	2001	0	0
9	17	2000	0.0762	0	2001	0	0
9	18	2000	0	0	2001	0	0
9	19	2000	0	0	2001	0	0
9	20	2000	0	0	2001	0	2.2098
9	21	2000	0.0762	1.778	2001	0	0
9	22	2000	0.0254	0	2001	0	0
9	23	2000	0.0508	0.4572	2001	0	0
9	24	2000	0	0.3048	2001	0	3.5814
9	25	2000	0	1.524	2001	0	0.4318
9	26	2000	0	1.4732	2001	0	0
9	27	2000	0	0	2001	0	0
9	28	2000	0	0	2001	0	0
9	29	2000	0	0	2001	0	0
9	30	2000	0	0	2001	0	0
10	1	2000	0	0	2001	0	0
10	2	2000	0	0	2001	0	0
10	3	2000	0	0	2001	0	0
10	4	2000	0	0	2001	0	0
10	5	2000	0	0	2001	0	0
10	6	2000	0	0	2001	0	1.3716
10	7	2000	0	0.0508	2001	0	0
10	8	2000	0	0	2001	0	0
10	9	2000	0	0	2001	0	0
10	10	2000	0.3048	0	2001	0	0
10	11	2000	0.5588	0	2001	0.7366	0
10	12	2000	0.3048	0	2001	0	0.0762
10	13	2000	2.3622	0	2001	0	0.1524
10	14	2000	0.2032	0	2001	0	0.7112

Month	Day	Year	Idaho Precipitation	Oak Ridge Precipitation	Year	Idaho Precipitation	Oak Ridge Precipitation
10	15	2000	0.127	0	2001	0	0
10	16	2000	0	0	2001	0	0
10	17	2000	0	0	2001	0	0
10	18	2000	0	0	2001	0	0
10	19	2000	0	0	2001	0	0
10	20	2000	0	0	2001	0	0
10	21	2000	0	0	2001	0	0
10	22	2000	0	0	2001	0	0
10	23	2000	0	0	2001	0	0
10	24	2000	0	0	2001	0	0
10	25	2000	0.0254	0	2001	0	1.143
10	26	2000	0	0	2001	0	0
10	27	2000	0.0762	0	2001	0	0
10	28	2000	0	0	2001	0	0
10	29	2000	0.0762	0	2001	0	0
10	30	2000	0.254	0	2001	0	0
10	31	2000	0.5334	0	2001	1.397	0
11	1	2000	0	0	2001	0	0
11	2	2000	0	0	2001	0	0
11	3	2000	0	0	2001	0	0
11	4	2000	0	0	2001	0	0
11	5	2000	0.3302	0	2001	0	0
11	6	2000	0.1016	0	2001	0.7874	0
11	7	2000	0	0.2286	2001	0.4826	0
11	8	2000	0.1778	1.524	2001	0	0
11	9	2000	0.0762	2.667	2001	0	0
11	10	2000	0	2.032	2001	0	0
11	11	2000	0	0	2001	0	0
11	12	2000	0.0508	0	2001	0	0
11	13	2000	0	0	2001	0	0
11	14	2000	0.0508	0.0508	2001	0	0
11	15	2000	0.3302	0	2001	0	0
11	16	2000	0.1778	0	2001	0	0
11	17	2000	0.0254	0.635	2001	0	0
11	18	2000	0	0	2001	0.127	0
11	19	2000	0	0	2001	0	0
11	20	2000	0	0	2001	0	0
11	21	2000	0	0	2001	0.1778	0
11	22	2000	0	0	2001	0.635	0
11	23	2000	0	0	2001	0.1778	0
11	24	2000	0.127	0	2001	0	0
11	25	2000	0	1.0922	2001	0.7112	0
11	26	2000	0.2286	0.0508	2001	0.254	0
11	27	2000	0.4318	0	2001	0	0
11	28	2000	0	0	2001	0	0
11	29	2000	0	0.1016	2001	0.9144	0
11	30	2000	0.2032	0	2001	0.0762	0

Month	Day	Year	Idaho Precipitation	Oak Ridge Precipitation	Year	Idaho Precipitation	Oak Ridge Precipitation
12	1	2000	0	0	2001	0.1524	0
12	2	2000	0	0	2001	0.4826	0
12	3	2000	0	3.3782	2001	0.2794	0
12	4	2000	0	0	2001	0.0254	0
12	5	2000	0	0	2001	0.4572	0
12	6	2000	0	0	2001	0.4826	0
12	7	2000	0	0	2001	0	0.127
12	8	2000	0	0	2001	0	0.762
12	9	2000	0.0762	0	2001	0	0.8128
12	10	2000	0.127	0.254	2001	0	0.0762
12	11	2000	0.2794	0	2001	0.127	2.1336
12	12	2000	0	0.0762	2001	0.0508	0
12	13	2000	0.1524	0	2001	0.3556	1.4986
12	14	2000	0.3048	3.3274	2001	0.4318	2.032
12	15	2000	0.2032	0.0254	2001	0	0
12	16	2000	0	1.016	2001	0	0
12	17	2000	0.127	2.1844	2001	0.127	0
12	18	2000	0	0	2001	0	1.6764
12	19	2000	0	0.381	2001	0.1016	0
12	20	2000	0	0	2001	0	0
12	21	2000	0	0.0254	2001	0	0
12	22	2000	0.0254	0	2001	0	0
12	23	2000	0.0508	0	2001	0	0.381
12	24	2000	0.4318	0	2001	0	0.9144
12	25	2000	0.3048	0	2001	0	0
12	26	2000	0	0	2001	0	0
12	27	2000	0	0	2001	0	0
12	28	2000	0	0	2001	0.1016	0
12	29	2000	0	0	2001	0	0
12	30	2000	0	0	2001	0	0
12	31	2000	0	0	2001	0	0
1	1	2001	0	0	2002	0	0
1	2	2001	0	0.127	2002	0	0
1	3	2001	0	0	2002	0.1016	0
1	4	2001	0	0	2002	0.4318	0
1	5	2001	0	0	2002	0	0
1	6	2001	0	0	2002	0.0762	1.0922
1	7	2001	0	0	2002	0.3048	0.254
1	8	2001	0	0.0254	2002	0	0
1	9	2001	0	0	2002	0	0
1	10	2001	0.3048	0	2002	0	0
1	11	2001	0	0	2002	0	0.254
1	12	2001	0.508	0.635	2002	0	0
1	13	2001	0	0	2002	0	0
1	14	2001	0.254	0.1016	2002	0	0

Month	Day	Year	Idaho Precipitation	Oak Ridge Precipitation	Year	Idaho Precipitation	Oak Ridge Precipitation
1	15	2001	0.0254	0	2002	0.0254	0
1	16	2001	0	0	2002	0.0762	0
1	17	2001	0.0254	0	2002	0.1016	0
1	18	2001	0.0254	0.508	2002	0.254	0.635
1	19	2001	0.0508	5.1054	2002	0.1016	2.6416
1	20	2001	0.4318	1.7018	2002	0.0762	2.4638
1	21	2001	0	0.0254	2002	0.254	0.5842
1	22	2001	0	0.0254	2002	0.1524	0
1	23	2001	0	0	2002	0.0254	3.7846
1	24	2001	0	0	2002	0	4.318
1	25	2001	0.7112	0	2002	0	3.9878
1	26	2001	0.127	0	2002	0	0
1	27	2001	0	0.0508	2002	0.0508	0
1	28	2001	0.0254	0	2002	0.6858	0
1	29	2001	0.0508	0	2002	0.0254	0
1	30	2001	0.0254	1.524	2002	0.0254	0
1	31	2001	0.0254	0	2002	0.0254	0
2	1	2001	0	0	2002	0.0508	0.9144
2	2	2001	0	0	2002	0	0
2	3	2001	0	0	2002	0	0
2	4	2001	0.1778	0	2002	0	0.2286
2	5	2001	0	0	2002	0	0
2	6	2001	0.3302	0	2002	0	0
2	7	2001	0.0254	0	2002	0	2.0066
2	8	2001	0	0	2002	0	0.762
2	9	2001	0	0	2002	0	0
2	10	2001	0	1.5748	2002	0	0
2	11	2001	0.0508	0	2002	0	0.2286
2	12	2001	0.0508	1.27	2002	0	0
2	13	2001	0.0254	0.0762	2002	0	0
2	14	2001	0	0.127	2002	0	0
2	15	2001	0.0254	2.5908	2002	0	0
2	16	2001	0	3.3274	2002	0	0.0508
2	17	2001	0	5.207	2002	0	0
2	18	2001	0	0	2002	0	0
2	19	2001	0	0	2002	0.0254	0
2	20	2001	0.8636	0	2002	0.0254	0.3048
2	21	2001	0	0.0254	2002	0	0.6096
2	22	2001	0.2794	2.3876	2002	0	0
2	23	2001	0.3302	0.0762	2002	0	0
2	24	2001	0.254	0	2002	0	0
2	25	2001	0.2794	2.0066	2002	0	0
2	26	2001	0	0.254	2002	0	0.3048
2	27	2001	0	0	2002	0	0.0762
2	28	2001	0	0	2002	0.0508	0

Month	Day	Year	Idaho Precipitation	Oak Ridge Precipitation	Year	Idaho Precipitation	Oak Ridge Precipitation
3	1	2001	0	0	2002	0	0
3	2	2001	0	0.0254	2002	0	0.2032
3	3	2001	0.6604	0	2002	0	0.508
3	4	2001	0	0.1524	2002	0	0
3	5	2001	0	0.508	2002	0	0
3	6	2001	0	0.0508	2002	0.0254	0
3	7	2001	0	0	2002	0.9652	0
3	8	2001	0	0	2002	0.4318	0
3	9	2001	0.3048	0	2002	0	0
3	10	2001	0.0762	0	2002	0	1.143
3	11	2001	0	0	2002	0.0254	0
3	12	2001	0	0	2002	0.0254	0.508
3	13	2001	0	0.889	2002	0.4064	0.254
3	14	2001	0	0	2002	0	0.0508
3	15	2001	0	0.635	2002	0	0
3	16	2001	0.0762	1.1938	2002	0	2.4384
3	17	2001	0	0.0508	2002	0.0254	3.6322
3	18	2001	0	0	2002	0	8.0772
3	19	2001	0	0	2002	0	1.27
3	20	2001	0	0.254	2002	0	0
3	21	2001	0	0.6604	2002	0	0.2032
3	22	2001	0	0.1524	2002	0	0
3	23	2001	0	0	2002	0	0
3	24	2001	0	0	2002	0	0
3	25	2001	0	0	2002	0	0
3	26	2001	0	0	2002	0	0
3	27	2001	0	0	2002	0	1.397
3	28	2001	0.7366	0	2002	0	0
3	29	2001	0.0254	0	2002	0	0
3	30	2001	0	1.0414	2002	0	0.254
3	31	2001	0	0.127	2002	0	2.159
4	1	2001	0	0.254	2002	0	1.9812
4	2	2001	0.6858	0	2002	0	0
4	3	2001	0	0.127	2002	0	0
4	4	2001	0.0254	0	2002	0	0
4	5	2001	0	0	2002	0	0
4	6	2001	0	0	2002	0	0
4	7	2001	0.1524	0	2002	0	0
4	8	2001	0.1524	0	2002	0	0
4	9	2001	0	0	2002	0	1.27
4	10	2001	0	0	2002	0	0.635
4	11	2001	0	0	2002	0.0508	0
4	12	2001	0.0762	0	2002	0.1524	0
4	13	2001	0.0508	3.5052	2002	0	0
4	14	2001	0.0762	0.0508	2002	0.2286	0

Month	Day	Year	Idaho Precipitation	Oak Ridge Precipitation	Year	Idaho Precipitation	Oak Ridge Precipitation
4	15	2001	0	0.0254	2002	1.778	0
4	16	2001	0	0.9144	2002	3.175	0
4	17	2001	0	0	2002	0.0254	0
4	18	2001	0	0	2002	0	0
4	19	2001	0.0508	0	2002	0.0508	0
4	20	2001	0.0254	0	2002	0	0
4	21	2001	0	0	2002	0	0
4	22	2001	0	0	2002	0.1016	0.127
4	23	2001	0	0	2002	0	0
4	24	2001	0	0	2002	0	0
4	25	2001	0	0	2002	0	2.032
4	26	2001	0	0	2002	0	0
4	27	2001	0	0	2002	0.0762	0
4	28	2001	0	0	2002	0	0.0254
4	29	2001	0	0	2002	0	0.0254
4	30	2001	0	0	2002	0	0
5	1	2001	0	0.254	2002	0	2.8702
5	2	2001	0	0	2002	0	0.0508
5	3	2001	0	0	2002	0	1.143
5	4	2001	0	0	2002	0	0.3302
5	5	2001	0	0	2002	0	0.0762
5	6	2001	0	0	2002	0	0
5	7	2001	0	1.524	2002	0	0
5	8	2001	0	0.1778	2002	0	0.2286
5	9	2001	0	0.254	2002	0	0.254
5	10	2001	0	0	2002	0	0.254
5	11	2001	0	0	2002	0	0.635
5	12	2001	0	0.762	2002	0	0
5	13	2001	0	0.1016	2002	0	0
5	14	2001	0	0	2002	0	2.4892
5	15	2001	0	0	2002	0	0
5	16	2001	0.1778	0	2002	0	0
5	17	2001	0	0	2002	0	0
5	18	2001	0	0	2002	0	1.651
5	19	2001	0.0508	0	2002	0	0
5	20	2001	0	0.0508	2002	0	0
5	21	2001	0	0	2002	1.7272	0
5	22	2001	0	3.556	2002	1.016	0
5	23	2001	0	0.508	2002	0.1016	0
5	24	2001	0	0.5588	2002	0.0254	0
5	25	2001	0	0.1524	2002	0	0
5	26	2001	0	0	2002	0	0
5	27	2001	0	0.127	2002	0	0.8636
5	28	2001	0	0.7366	2002	0	1.3208
5	29	2001	0	0.0762	2002	0	0
5	30	2001	0	0	2002	0	0
5	31	2001	0	0	2002	0	0

Month	Day	Year	Idaho Precipitation	Oak Ridge Precipitation	Year	Idaho Precipitation	Oak Ridge Precipitation
6	1	2001	0	0.508	2002	0.0508	0
6	2	2001	0	0.508	2002	0.7112	0
6	3	2001	0	0.5588	2002	0.4572	0
6	4	2001	0.5334	0.2794	2002	0.1524	0
6	5	2001	0.127	0.0508	2002	0	0.127
6	6	2001	0	0.0508	2002	0	0
6	7	2001	0	0.254	2002	0	1.9304
6	8	2001	0	0.5842	2002	0.1016	0
6	9	2001	0	0.0254	2002	0	0
6	10	2001	0	0	2002	0	0
6	11	2001	0	0	2002	0	0
6	12	2001	0	0	2002	0	0
6	13	2001	0	0	2002	0	0
6	14	2001	1.8288	0.2286	2002	0	0.254
6	15	2001	0	0.381	2002	0.0254	0.508
6	16	2001	0	0.0762	2002	0	0
6	17	2001	0	0	2002	0	0
6	18	2001	0	0	2002	0	0
6	19	2001	0	0	2002	0	0
6	20	2001	0	0	2002	0	0
6	21	2001	0	0	2002	0.0508	0
6	22	2001	0	1.6764	2002	0	0
6	23	2001	0	2.8956	2002	0	0
6	24	2001	0	0	2002	0	0.3048
6	25	2001	0	0	2002	0	0
6	26	2001	0	0.127	2002	0.127	0
6	27	2001	0	0	2002	0	0
6	28	2001	0	0.2032	2002	0	1.9812
6	29	2001	0	0.254	2002	0	0
6	30	2001	0	1.4478	2002	0	0
7	1	2001	0	0	2002	0	0
7	2	2001	0	0.381	2002	0	0
7	3	2001	0	0	2002	0	0
7	4	2001	0	0.8382	2002	0	1.3208
7	5	2001	0	0.5588	2002	0	0
7	6	2001	0.4826	3.556	2002	0	0.1016
7	7	2001	0	0	2002	0.0254	0
7	8	2001	0	0	2002	0	0
7	9	2001	0	0.0508	2002	0	0
7	10	2001	0.1778	0.0254	2002	0	0
7	11	2001	0	0	2002	0	2.413
7	12	2001	0	0	2002	0	0
7	13	2001	0	0	2002	0	1.1938
7	14	2001	0.2286	0	2002	0	3.3782
7	15	2001	0.2032	0	2002	0	0
7	16	2001	0	0	2002	0.0762	0

Month	Day	Year	Idaho Precipitation	Oak Ridge Precipitation	Year	Idaho Precipitation	Oak Ridge Precipitation
7	17	2001	0	0	2002	0	0
7	18	2001	0	0.3302	2002	0	0
7	19	2001	0	0.0508	2002	0.0508	1.016
7	20	2001	0	2.159	2002	0	0
7	21	2001	0	0.4318	2002	0	0.2794
7	22	2001	0	1.7526	2002	0.0254	0
7	23	2001	0	0.1016	2002	0	0
7	24	2001	0	0	2002	0	1.9558
7	25	2001	0	0.1524	2002	0	0
7	26	2001	0	2.2352	2002	0	0
7	27	2001	0	0.127	2002	0	0
7	28	2001	0	2.921	2002	0	0
7	29	2001	0	4.572	2002	0	2.6416
7	30	2001	0	2.032	2002	0	0.9906
7	31	2001	0	0	2002	0	1.143
8	1	2001	0	0	2002	0	0
8	2	2001	0	0	2002	0	0
8	3	2001	0.3302	0	2002	0	0.4318
8	4	2001	0	1.6256	2002	0	0
8	5	2001	0.0762	0	2002	0	3.2004
8	6	2001	0	0	2002	0	0
8	7	2001	0	0	2002	0	0
8	8	2001	0	0	2002	0.0508	0
8	9	2001	0	0	2002	0	0
8	10	2001	0	0	2002	0	0
8	11	2001	0	0	2002	0	0
8	12	2001	0	0	2002	0	0
8	13	2001	0.0254	0.0254	2002	0	0
8	14	2001	0	0	2002	0	0
8	15	2001	0	0	2002	0	0
8	16	2001	0.0254	0	2002	0	0
8	17	2001	0	0	2002	0	0.9144
8	18	2001	0	0	2002	0	0.254
8	19	2001	0	0	2002	0	0.5842
8	20	2001	0	0.508	2002	0	3.4798
8	21	2001	0	0	2002	0	0
8	22	2001	0	0	2002	0	0
8	23	2001	0	0	2002	0	0
8	24	2001	0	0	2002	0	0
8	25	2001	0	0.762	2002	0	0
8	26	2001	0	0	2002	0	0.2032
8	27	2001	0	0	2002	0.0508	0
8	28	2001	0	0.381	2002	0	0
8	29	2001	0	0	2002	0	0
8	30	2001	0	0	2002	0	0
8	31	2001	0.1524	0	2002	0	0

Month	Day	Year	Idaho Precipitation	Oak Ridge Precipitation	Year	Idaho Precipitation	Oak Ridge Precipitation
9	1	2002	0	0	2003	0	2.413
9	2	2002	0	0	2003	0	0
9	3	2002	0	0	2003	0	0
9	4	2002	0	0	2003	0	5.207
9	5	2002	0.127	0	2003	0.3048	0
9	6	2002	0.762	0	2003	0	0
9	7	2002	1.524	0	2003	0	0
9	8	2002	0	0	2003	0.4826	0.0254
9	9	2002	0	0	2003	0.1524	0
9	10	2002	0	0	2003	0.508	0
9	11	2002	0	0	2003	0	0
9	12	2002	0	0	2003	0	0
9	13	2002	0	0	2003	0	0
9	14	2002	0	0.9652	2003	0	0
9	15	2002	0	1.7526	2003	0	0.4318
9	16	2002	0	0	2003	0	0
9	17	2002	0.127	0	2003	0.2286	0
9	18	2002	1.9558	0.1016	2003	0	0
9	19	2002	0	0	2003	0	0
9	20	2002	0	0	2003	0	0
9	21	2002	0	2.6162	2003	0	0
9	22	2002	0	2.794	2003	0	1.0922
9	23	2002	0	2.6924	2003	0	6.7818
9	24	2002	0	0	2003	0	0
9	25	2002	0	0	2003	0	0
9	26	2002	0	2.921	2003	0	0
9	27	2002	0	1.9558	2003	0	0.0254
9	28	2002	0	0.381	2003	0	1.9812
9	29	2002	0	0	2003	0	0
9	30	2002	0.0762	0	2003	0	0
10	1	2002	0.254	0	2003	0	0
10	2	2002	0	0	2003	0	0
10	3	2002	0.0508	0	2003	0	0
10	4	2002	0.1016	0	2003	0	0
10	5	2002	0	1.27	2003	0	0
10	6	2002	0	0	2003	0	0
10	7	2002	0	0.3302	2003	0	0
10	8	2002	0	0	2003	0	0
10	9	2002	0	0	2003	0	0
10	10	2002	0	0.2032	2003	0	0.0254
10	11	2002	0	1.27	2003	0	0.381
10	12	2002	0	0.3048	2003	0	0
10	13	2002	0	0	2003	0	0
10	14	2002	0	0	2003	0	0.0254

Month	Day	Year	Idaho Precipitation	Oak Ridge Precipitation	Year	Idaho Precipitation	Oak Ridge Precipitation
10	15	2002	0	0	2003	0	1.3462
10	16	2002	0	1.2192	2003	0	0
10	17	2002	0	0	2003	0	0
10	18	2002	0	0	2003	0	0
10	19	2002	0	0	2003	0	0
10	20	2002	0	0	2003	0	0
10	21	2002	0	0.0508	2003	0	0
10	22	2002	0	0	2003	0	0
10	23	2002	0	0	2003	0	0
10	24	2002	0	0.254	2003	0	0
10	25	2002	0	0	2003	0	0
10	26	2002	0	0.6858	2003	0	0
10	27	2002	0	0.0254	2003	0	2.3876
10	28	2002	0	0.254	2003	0	0.0508
10	29	2002	0	2.4384	2003	0.5588	0
10	30	2002	0	2.5146	2003	0	0
10	31	2002	0	0	2003	0	0
11	1	2002	0	0	2003	0	0
11	2	2002	0	0	2003	0	0
11	3	2002	0	0.127	2003	0	0
11	4	2002	0	0.381	2003	0	0
11	5	2002	0	0.3302	2003	0	0.381
11	6	2002	0	3.0988	2003	0	4.4704
11	7	2002	0	0	2003	0	0.3048
11	8	2002	0.5334	0	2003	0	0
11	9	2002	0.2032	0	2003	0.762	0
11	10	2002	0.1524	1.6002	2003	0.0254	0
11	11	2002	0	5.6642	2003	0	0
11	12	2002	0	0.0762	2003	0	0
11	13	2002	0	0	2003	0.4064	0.8128
11	14	2002	0	0	2003	0.8382	0
11	15	2002	0	0	2003	0.0508	0.127
11	16	2002	0	0.8128	2003	0.508	0.5842
11	17	2002	0	0.508	2003	0.2286	0.7112
11	18	2002	0	0	2003	0	0
11	19	2002	0	0.381	2003	0	4.4704
11	20	2002	0	0	2003	0	0.4826
11	21	2002	0	0.9652	2003	0.0254	0
11	22	2002	0	0	2003	0	0
11	23	2002	0.2794	0	2003	0	0
11	24	2002	0.3302	0	2003	0	1.016
11	25	2002	0	0.1778	2003	0	0.3048
11	26	2002	0	0	2003	0	0
11	27	2002	0	0.381	2003	0	0
11	28	2002	0	0	2003	0	1.143
11	29	2002	0	0	2003	0.254	0.4318
11	30	2002	0	0	2003	0	0

Month	Day	Year	Idaho Precipitation	Oak Ridge Precipitation	Year	Idaho Precipitation	Oak Ridge Precipitation
12	1	2002	0	0	2003	0.0762	0
12	2	2002	0	0	2003	0	0
12	3	2002	0	0.0254	2003	0	0.254
12	4	2002	0	0.4572	2003	0	2.5146
12	5	2002	0	5.969	2003	0.2286	0.2286
12	6	2002	0	0	2003	0.5588	0
12	7	2002	0	0	2003	0.508	0
12	8	2002	0	0	2003	0.0762	0
12	9	2002	0	0	2003	0	0
12	10	2002	0.0762	0.127	2003	0.0762	2.7178
12	11	2002	0	1.8288	2003	0.254	0
12	12	2002	0	0.0254	2003	0	0
12	13	2002	0	0.508	2003	0.889	0.2286
12	14	2002	0	2.54	2003	0.1016	1.4986
12	15	2002	0.1778	0	2003	0	0
12	16	2002	0.2286	0	2003	0	0.762
12	17	2002	0.5842	0	2003	0	0.3048
12	18	2002	0.2032	0	2003	0	0.1524
12	19	2002	0	0	2003	0	0.2032
12	20	2002	0.2032	3.7338	2003	0	0.0508
12	21	2002	0.0762	0	2003	0.4572	0
12	22	2002	0.0762	0	2003	0	0
12	23	2002	0	0	2003	0	1.2192
12	24	2002	0	1.8288	2003	0	0.0762
12	25	2002	0	1.0668	2003	0	0
12	26	2002	0	0	2003	0	0
12	27	2002	0.254	0	2003	0	0
12	28	2002	0	0	2003	0	0
12	29	2002	0.0508	0	2003	0	0.508
12	30	2002	0	0	2003	0	0.127
12	31	2002	0.7112	0	2003	0	0
1	1	2003	0.2794	1.9304	2004	0.4826	0
1	2	2003	0	0.0762	2004	0	0.1778
1	3	2003	0.0254	0.381	2004	0	0
1	4	2003	0	0	2004	0	0.381
1	5	2003	0.0254	0	2004	0	3.556
1	6	2003	0	0.0254	2004	0	1.6256
1	7	2003	0	0	2004	0	0
1	8	2003	0	0	2004	0	0
1	9	2003	0	0	2004	0	0.381
1	10	2003	0.2286	0	2004	0	0
1	11	2003	0.1016	0	2004	0	0
1	12	2003	0.0508	0	2004	0	0
1	13	2003	0.0508	0	2004	0	0
1	14	2003	0.0762	0	2004	0	0

Month	Day	Year	Idaho Precipitation	Oak Ridge Precipitation	Year	Idaho Precipitation	Oak Ridge Precipitation
1	15	2003	0.3302	0	2004	0	0
1	16	2003	0	0	2004	0	0
1	17	2003	0	0.762	2004	0	0
1	18	2003	0	0	2004	0	1.524
1	19	2003	0	0.254	2004	0	0.508
1	20	2003	0	0	2004	0	0
1	21	2003	0	0.381	2004	0	0
1	22	2003	0.0254	0.1016	2004	0	0
1	23	2003	0.1778	0.381	2004	0	0
1	24	2003	0	0	2004	0	0
1	25	2003	0	0	2004	0	0.4826
1	26	2003	0	0	2004	0	1.9812
1	27	2003	0.1778	0.0254	2004	0	0.3048
1	28	2003	0.5842	0	2004	0	0
1	29	2003	0	0.762	2004	0	0
1	30	2003	0.0508	0.4318	2004	0.1778	0
1	31	2003	0	0	2004	0	0
2	1	2003	0.2286	0.0762	2004	0	0
2	2	2003	0.2794	0	2004	0	0
2	3	2003	0	0	2004	0	2.2352
2	4	2003	0.635	1.8034	2004	0	0
2	5	2003	0	0	2004	0	0.127
2	6	2003	0	0	2004	0	7.493
2	7	2003	0	1.143	2004	0	0.5842
2	8	2003	0.635	0	2004	0	0.0508
2	9	2003	0.0254	0	2004	0	0
2	10	2003	0	0.8382	2004	0	0
2	11	2003	0	0	2004	0	0
2	12	2003	0	0	2004	0	0.381
2	13	2003	0.3302	0	2004	0	0
2	14	2003	0.4318	0	2004	0	0
2	15	2003	0.0508	4.064	2004	0	0.0508
2	16	2003	0.7366	11.9888	2004	0	0.254
2	17	2003	0	2.7178	2004	0.1524	0
2	18	2003	0.0762	0.1778	2004	0.1778	0.127
2	19	2003	0	0	2004	0	0
2	20	2003	0	0.3556	2004	0	0
2	21	2003	0.0254	0.1016	2004	0	0
2	22	2003	0.0254	5.6134	2004	0	0
2	23	2003	0	1.3208	2004	0	0
2	24	2003	0	0	2004	0.1524	0
2	25	2003	0	0	2004	0	0.1778
2	26	2003	0	0.5842	2004	0.4318	0.3048
2	27	2003	0	0.6858	2004	0	0.5842
2	28	2003	0	0.5588	2004	0.3048	0
2	29				2004	0	0

Month	Day	Year	Idaho Precipitation	Oak Ridge Precipitation	Year	Idaho Precipitation	Oak Ridge Precipitation
3	1	2003	0	0	2004	0	0
3	2	2003	0	0	2004	0	0.8128
3	3	2003	0	0	2004	0.0762	0.635
3	4	2003	0.1778	0	2004	0.2286	0.0508
3	5	2003	0	0.1778	2004	0	0
3	6	2003	0	0.889	2004	0	8.1534
3	7	2003	0	0	2004	0	0
3	8	2003	0	0	2004	0	0
3	9	2003	0	0	2004	0	0
3	10	2003	0	0	2004	0.0508	0.508
3	11	2003	0	0	2004	0	0
3	12	2003	0	0	2004	0	0
3	13	2003	0	0	2004	0	0
3	14	2003	0.508	0.5842	2004	0	0
3	15	2003	0.0254	0.0254	2004	0	0.254
3	16	2003	0.6858	0	2004	0	2.3622
3	17	2003	0	0	2004	0	0.1778
3	18	2003	0.0254	0.635	2004	0	1.4986
3	19	2003	0	0.508	2004	0	0
3	20	2003	0	1.27	2004	0	0
3	21	2003	0	0.1524	2004	0	1.6764
3	22	2003	0	0	2004	0	0
3	23	2003	0.0762	0	2004	0	0
3	24	2003	0	0	2004	0	0
3	25	2003	0	0	2004	0	0
3	26	2003	0.3302	0	2004	0.4318	0
3	27	2003	0	0	2004	0	0
3	28	2003	0	0	2004	0	0
3	29	2003	0	0.7874	2004	0	0
3	30	2003	0	1.4732	2004	0	1.8034
3	31	2003	0	0	2004	0	0.127
4	1	2003	0	0	2004	0.0254	0.0254
4	2	2003	0.0762	0	2004	0	0
4	3	2003	0.1016	0	2004	0	0
4	4	2003	0.0508	0	2004	0	0
4	5	2003	0	0.762	2004	0	0
4	6	2003	0	0	2004	0	0
4	7	2003	0.0762	5.969	2004	0.2794	0
4	8	2003	0	0.0762	2004	0.2286	0
4	9	2003	0	3.175	2004	0.254	0
4	10	2003	0	1.524	2004	0	0
4	11	2003	0	2.2606	2004	0	0.0254
4	12	2003	0	0	2004	0	1.016
4	13	2003	0	0	2004	0	4.6228
4	14	2003	0.0254	0	2004	0	0.7112

Month	Day	Year	Idaho Precipitation	Oak Ridge Precipitation	Year	Idaho Precipitation	Oak Ridge Precipitation
4	15	2003	1.016	0	2004	0	0
4	16	2003	0	0	2004	0	0
4	17	2003	0.1016	0	2004	0.381	0
4	18	2003	0	7.1374	2004	0.3048	0
4	19	2003	0	0	2004	0.254	0
4	20	2003	0	0	2004	0.5588	0
4	21	2003	0	0.8636	2004	0	0
4	22	2003	0.1016	0	2004	0	0.254
4	23	2003	0.1016	0	2004	0	0
4	24	2003	0	0	2004	0.127	0.3048
4	25	2003	0.0762	0	2004	0	0
4	26	2003	0.9906	1.5748	2004	0	1.27
4	27	2003	0	0	2004	0	0.127
4	28	2003	0.2794	0	2004	0	0
4	29	2003	0.7112	0	2004	0.0762	0
4	30	2003	0	0.5842	2004	0	0
5	1	2003	0.0254	0	2004	0	0.127
5	2	2003	0	0.0508	2004	0	1.016
5	3	2003	0.8636	1.0414	2004	0	1.9558
5	4	2003	0	0	2004	0	0
5	5	2003	0.127	1.143	2004	0	0
5	6	2003	0	3.4798	2004	0	0
5	7	2003	0	2.3368	2004	0	0
5	8	2003	0	0.4826	2004	0	0
5	9	2003	0	0	2004	0	0
5	10	2003	0	0	2004	0	0
5	11	2003	0.2032	0.9906	2004	0.254	0
5	12	2003	0.127	0.381	2004	1.397	0
5	13	2003	0	0	2004	0.2032	0
5	14	2003	0	0	2004	0.0508	0.0762
5	15	2003	0	0	2004	0.0762	0
5	16	2003	0	0.127	2004	0.1778	0
5	17	2003	0	1.0922	2004	0.0762	0
5	18	2003	0	3.3782	2004	0	0
5	19	2003	0	0.7366	2004	0	0.127
5	20	2003	0	0.1016	2004	0.0254	0.1524
5	21	2003	0	1.1684	2004	0	0
5	22	2003	0	0.635	2004	0.2286	0
5	23	2003	0	0	2004	0.4064	0
5	24	2003	0	0	2004	0.0254	0
5	25	2003	0	0	2004	0.1524	0
5	26	2003	0	0.4826	2004	0.1524	0.127
5	27	2003	0	0	2004	0.3302	1.8288
5	28	2003	0	0	2004	0.7112	1.2954
5	29	2003	0	0.3048	2004	0.8636	0.127
5	30	2003	0	0	2004	0	0
5	31	2003	0	0.2286	2004	0	4.9784

Month	Day	Year	Idaho Precipitation	Oak Ridge Precipitation	Year	Idaho Precipitation	Oak Ridge Precipitation
6	1	2003	0	0	2004	0	0.0508
6	2	2003	0	0	2004	0	0
6	3	2003	0	0.254	2004	0.127	0.2286
6	4	2003	0	1.3716	2004	0.3556	0.4572
6	5	2003	0	0	2004	0	0
6	6	2003	0	0	2004	0	0
6	7	2003	0	3.683	2004	0	0
6	8	2003	0	3.1242	2004	0	0
6	9	2003	0	0.0762	2004	0.2032	0
6	10	2003	0	0	2004	4.1656	0
6	11	2003	0	0	2004	0.1778	0
6	12	2003	0	1.9304	2004	0	0
6	13	2003	0	0.5588	2004	0	1.5748
6	14	2003	0	0.2794	2004	0	0.0508
6	15	2003	0	0.508	2004	0	6.35
6	16	2003	0	0.2286	2004	0	0.6858
6	17	2003	0	3.302	2004	0	0
6	18	2003	0.0508	0.3556	2004	0	3.0226
6	19	2003	0	0.8636	2004	0	0.0762
6	20	2003	0	0	2004	0.254	0.0254
6	21	2003	0.1016	0	2004	0	0
6	22	2003	0	0	2004	0	0
6	23	2003	0	0	2004	0	0.5334
6	24	2003	0.5334	0	2004	0	0.3302
6	25	2003	0	0	2004	0	0.4572
6	26	2003	0	0	2004	0	2.8194
6	27	2003	0	1.7272	2004	0.508	0
6	28	2003	0	0.2032	2004	0	0
6	29	2003	0	0	2004	0.2286	0.1778
6	30	2003	0	0.127	2004	0	0
7	1	2003	0	0.8128	2004	0	0
7	2	2003	0	3.5052	2004	0	0
7	3	2003	0	0.0508	2004	0	0
7	4	2003	0	0	2004	0	0.381
7	5	2003	0	0	2004	0	1.27
7	6	2003	0	0	2004	0	1.0414
7	7	2003	0	0.1016	2004	0	0.254
7	8	2003	0	0	2004	0	0
7	9	2003	0	0	2004	0	0
7	10	2003	0	1.2192	2004	0	0
7	11	2003	0	2.54	2004	0	0
7	12	2003	0	0	2004	0	1.016
7	13	2003	0	0.4318	2004	0.2032	0.9652
7	14	2003	0	0	2004	0	0.1778
7	15	2003	0	0	2004	0	0
7	16	2003	0	1.9304	2004	0	0

Month	Day	Year	Idaho Precipitation	Oak Ridge Precipitation	Year	Idaho Precipitation	Oak Ridge Precipitation
7	17	2003	0	0.6858	2004	0	0
7	18	2003	0	0	2004	0.8636	1.397
7	19	2003	0	0	2004	0.127	0
7	20	2003	0	0	2004	0	0
7	21	2003	0	0	2004	0	0
7	22	2003	0	1.0668	2004	0.127	0
7	23	2003	0	2.4384	2004	0	0.4064
7	24	2003	0	0	2004	0	0
7	25	2003	0	0	2004	0	0
7	26	2003	0	0	2004	0	0.254
7	27	2003	0	0	2004	0	0.6858
7	28	2003	0	0	2004	0	0.2286
7	29	2003	0	1.4986	2004	0	0
7	30	2003	0	0	2004	0	1.1938
7	31	2003	0	0.9144	2004	0	0.127
8	1	2003	0	1.7272	2004	0	1.2192
8	2	2003	0	1.7272	2004	0	0
8	3	2003	0	0.0508	2004	0.2032	0
8	4	2003	0	2.2352	2004	0.0762	0
8	5	2003	0	0.6604	2004	0.0762	0
8	6	2003	0	0	2004	0	0.1778
8	7	2003	0	0	2004	0	0
8	8	2003	0	0	2004	0	0
8	9	2003	0	0	2004	0	0
8	10	2003	0	0	2004	0.0508	0
8	11	2003	0	0	2004	0	0
8	12	2003	0	0.0254	2004	0	0.381
8	13	2003	0	0	2004	0	1.7018
8	14	2003	0	0	2004	0	0
8	15	2003	0	0	2004	0	0
8	16	2003	0	0	2004	0	0
8	17	2003	0.127	0.8128	2004	0	0
8	18	2003	0.762	0	2004	0.1016	0
8	19	2003	0	0	2004	0	0
8	20	2003	0	0	2004	0	0
8	21	2003	0	0.1778	2004	0	1.8034
8	22	2003	0.2794	0	2004	0	1.524
8	23	2003	0.7112	0	2004	0	0
8	24	2003	0	0	2004	0.0508	0
8	25	2003	0.4826	0	2004	0	0.635
8	26	2003	0.8382	0	2004	0	0
8	27	2003	0.0762	0	2004	0	0
8	28	2003	0	0	2004	0	0.0254
8	29	2003	0	0	2004	0	0.381
8	30	2003	0	0	2004	0	0.127
8	31	2003	0	0	2004	0	0.254

REFERENCES

(2005). "Register of Ecological Models." http://eco.wiz.uni-kassel.de.

Albright, W. H., Gee, G. W., Wilson, G. V., and Fayer, M. J. (2002). "Alternative Cover Assessment Project Phase 1 Report." *41183*, Desert Research Insitute.

Al-Yaqout, A. F., and Hamoda, M. F. (2003). "Evaluation of landfill leachate in arid climate-a case study." *Environment International*, 29, 593-600.

Bengtsson, L., Bendz, D., Hogland, W., Rosqvist, H., and Akesson, M. (1994). "Water balance for landfills of different age." *Journal of Hydrology*, 158, 203-217.

Blackman, J., William C. (2001). *Basic Hazardous Waste Management, 3rd Edition*, Lewis Publishers, Boca Raton.

Caldwell, J. A., and Reith, C. C. (1993). *Principles and Practice of Waste Encapsulation*, Lewis Publishers, Boca Raton.

Carsel, R. F., and Parrish, R. S. (1988). "Developing Joint Probability Distributions of Soil Water Retention Characteristics." *Water Resources Research*, 24(5), 755(15).

Daniel, D. E. "Surface Barriers: Problems, Solutions, and Future Needs." *Thirty-Third Hanford Symposium on Health and the Environment*, Pasco, Washington, 441-487.

Dwyer, S. F., Reavis, B. A., and Newman, G. (2000a). "Alternative Landfill Cover Demonstration, FY2000 Annual Data Report." *SAND2000-2427*, Sandia National Laboratories, Albuquerque, NM.

Dwyer, S. F., Wolters, G. L., and Newman, G. (2000b). "FY97-99 Vegetation Analysis of ALCD Soil Amended Landfill Cover Plots." Sandia National Laboratories, Albuquerque, NM.

Feddes, R. A., Kowalik, P. J., and Zaradny, H. (1978). *Simulation of field water use and crop yield*, Pudoc, Wageningen.

Hjelmar, O., van der Sloot, H. A., Guyonnet, D., Rietra, R. P. J. J., Brun, A., and Hall, D. "Development of acceptance criteria for landfilling of waste." *8th Waste Management and Landfill Symposium*, 711-721.

Ho, C. K., Arnold, B. W., Cochran, J. R., Taira, R. Y., and Pelton, M. A. (2004). "A probabilistic model and software tool for evaluating the long-term performance of landfill covers." *Environmental Modeling and Software*, 19, 63-88.

INEEL. (2001). "Technical Baseline for the Long-Term Stewardship National Program." *INEEL/Ext-01-01133, 2001*, Idaho National Engineering and Envrionmental Laboratory, Idaho Falls.

Interstate Technology & Regulatory Council. (2003). "Technology Overview Using Case Studies of Alternative Landfill Technologies and Associated Regulatory Topics." Alternative Landfill Technologies Team.

Johnson, C. A., Richner, G. A., Vitvar, T., Schittli, N., and Eberhard, M. (1998). "Hydrological and Geochemical factors affecting leachate composition in municipal solid waste incenerator bottom ash. Part I: The hydrology of Landfill Lostorf, Switzerland." *Journal of Contaminant Hydrology*, 33, 361-376.

Johnson, C. A., Schaap, M. G., and Abbaspour, K. C. (2001). "Model comparison of flow through a municipal solid waste incinerator ash landfill." *Journal of Hydrology*, 243, 55-72.

Khire, M. V., Benson, C. H., and Bosscher, P. J. (1997). "Water Balance Modeling of Earthen Final Covers." *Journal of Geotechnical and Geoenvironmental Engineering*, 744-754.

Kostelnik, K. M., Clarke, J. H., Harbour, J. L., Sanchez, F., and Parker, F. L. (2004). "A Sustainable Environmental Protection System for the Management of Residual Contaminants."

Kumthekar, U., Chiou, J. D., Prochaska, M., and Benson, C. H. "Development of a Long-Term Monitoring System to Evaluate Cover System Performance." *Waste Management 2002 Conference Proceedings. HLW, LLW, Mixed, Hazardous Wastes and Environmental Restoration - Working Towards a Cleaner Environment*, Tucson, AZ.

Landeen, D. S. "The Influence of Small-Mammal Burrowing Activity on Water Storage at the Hanford Site." *Thirty-Third Hanford Symposium on Health and the Environment*, Pasco, Washington, 523-543.

Leoni, G. L. M., Soares, A. M. d. S., and Fernandes, H. M. (2004). "Computational modelling of final covers for uranium mill tailings impoundments." *Journal of Hazardous Materials*, 110, 139-149.

Ludwig, C., Johnson, C. A., Kappeli, M., Ulrich, A., and Riediker, S. (2000). "Hydrological and geochemical factors controlling the leaching of cemented MSWI air pollution control residues: A lysimeter field study." *Journal of Contaminant Hydrology*, 42, 253-272.

Miller, C. J., and Lee, J. Y. (1999). "Response of Landfill Clay Liners to Extended Periods of Freezing." *Engineering Geology*, 51, 291-302.

Mualem, Y. (1976). "A New Model for Predicting the Hydraulic Conductivity of Unsaturated Porous Media." *Water Resources Research*, 12(3), 513(10).

NCDC. (2005). "http://www.ncdc.noaa.gov/oa/ncdc.html." NOAA.

Pruess, K., Oldenburg, C., and Moridis, G. (1999). "TOUGH2 User's Guide, Version 2.0." *Lawrence Berkeley National Laboratory Report LBNL-43134*, University of California, Berkeley.

Qian, X., Koerner, R. M., and Gray, D. H. (2002). *Geotechnical Aspects of Landfill Design and Construction*, Prentice Hall, Upper Saddle River, NJ.

Scanlon, B. R., Christman, M., Reedy, R. C., Porro, I., Simunek, J., and Flerchinga, G. N. (2002). "Intercode Comparisons for Simulating Water Balance of Surficial Sediments in Semiarid Regions." *Water Resources Research*, 38(12).

Šimunek, J., Šejna, M., and van Genuchten, M. T. (1998). "The HYDRUS-1D Software Package for Simulating the One-Dimensional Movement of Water, Heat, and Multiple Solutes in Variably-Saturated Media." U.S. Salinity Laboratory, Riverside, California.

Simunek, J. (2004). "HYDRUS-2D Forums." http://www.pc-progress.cz/_forum/topic.asp?TOPIC_ID=267.

Šimunek, J., and Suarez, D. L. (1993). "Modeling of Carbon Dioxide Transport and Production in Soil, 1." *Water Resources Research*, 29(2), 487(10).

Smith, E. D., Luxmoore, R. J., and Suter II, G. W. (1997). "Natural Physical and Biological Processes Comprise the Long-Term Performance of Compacted Soil Caps." Barrier Technologies for Environmental Management, National Academy Press, Washington, D.C., D-61-D-70.

Suter, G. W. I., Luxmoore, R. J., and Smith, E. D. (1993). "Compacted Soil Barriers at Abandoned Landfill Sites are Likely to Fail in the Long Term." *Journal of Environmental Quality*, 22(2), 217-226.

Suter II, G. W., Luxmoore, R. J., and Smith, E. D. (1993). "Compacted Soil Barriers at Abandoned Landfill Sites are Likely to Fail in the Long Term." *Journal of Environmental Quality*, 22(2), 217-226.

Taylor, S. A., and Ashcroft, G. L. (1972). *Physical Edaphology*, W. H. Freeman, San Francisco.

U.S. Department of Energy. (1997). "Linking Legacies: Connecting the Cold War Nuclear Weapons Production Processes to Their Environmental Consequences." *DOE/EM-0319*, U.S. Department of Energy, Office of Environmental Management, Washington, DC.

U.S. DOE. (1990a). "1990 Annual Prelicensing Inspection of Burrell Uranium Mill Tailings Vicinity Property, Burrell, Pennsylvania." *DOE/ID/12584-83*, U.S. Department of Energy Grand Junction Office, Grand Junction.

U.S. DOE. (1990b). "1990 Annual Prelicensing Inspection of Canonsburg Uranium Mill Tailings Disposal Site, Canonsburg, Pennsylvania." *DOE/ID/12584-84*, U.S. Department of Energy Grand Junction Office, Grand Junction.

U.S. DOE. (1992). "1992 Annual Prelicensing Inspection of the Shiprock, New Mexico, UMTRA Project Disposal Site." *DOE/ID/12584-137*, U.S. Department of Energy Grand Junction Office, Grand Junction.

U.S. DOE. (1993). "1992 Annual Prelicensing Inspection of the Canonsburg, Pennsylvania, UMTRA Project Disposal Site." *DOE/ID/12584-147*, U.S. Department of Energy Grand Junction Office, Grand Junction.

U.S. Environmental Protection Agency. (1983a). "Criteria for Municipal Solid Waste Landfills." 40 CFR 258, Washington, D.C.

U.S. Environmental Protection Agency. (1983b). "Standards for Owners and Operators of Hazardous Waste Treatment, Storage, and Disposal Facilites." 40 CFR 264, Washington, D.C.

van Genuchten, M. T. (1980). "A Closed-Form Equation for Predicting the Hydraulic Conductivity of Unsaturated Soils." *Soil Science Society of American Journal*, 44, 892-898.

Warrick, A. W. (2002). *Soil Physics Companion*, CRC, Boca Raton.

Waugh, W. J. "Ecology of Uranium Mill Tailings Covers." *Landfill Capping in the Semi-Arid West: Problems, Perspectives, and Solutions*, Jackson Lake Lodge, Grand Teton National Park, 199-212.

Waugh, W. J. "Monitoring the long-term performance of uranium mill tailings covers." *WM'99 Conference*, Tuscon, AZ.

Waugh, W. J., and Smith, G. M. (1997). "Effects of Root Intrusion at the Burrell, Pennsylvania, Uranium Mill Tailings Disposal Site." *GJO-97-5-TAR GJO-LTSM-4*, U.S. Department of Energy, Grand Junction.